

Transmission Line Parameter Estimation using Synchrophasor Data

by

Prashanth Kumar Mansani

A Thesis Presented in Partial Fulfillment
of the Requirement for the Degree
Master of Science

Approved Nov 2018 by the
Graduate Supervisory Committee:

Anamitra Pal, Chair

Keith E. Holbert

Daniel Tylavsky

ARIZONA STATE UNIVERSITY

December 2018

ABSTRACT

Transmission line parameters play an important role in state estimation, dynamic line rating, and fault analysis. Because of this, several methods have been proposed in the literature for line parameter estimation, especially using synchrophasor data. However, success of most prior research has been demonstrated using purely synthetic data. A synthetic dataset does not have the problems encountered with real data, such as invariance of measurements and realistic field noise. Therefore, the algorithms developed using synthetic datasets may not be as effective when used in practice. On the other hand, the true values of the line parameters are unknown and therefore the algorithms cannot be directly implemented on real data. A multi-stage test procedure is developed in this work to circumvent this problem.

In this thesis, two popular algorithms, namely, moving-window total least squares (MWTLS) and recursive Kalman filter (RKF) are applied on real data in multiple stages. In the first stage, the algorithms are tested on a purely synthetic dataset. This is followed by testing done on pseudo-synthetic datasets generated using real PMU data. In the final stage, the algorithms are implemented on the real PMU data obtained from a local utility. The results show that in the context of the given problem, RKF has better performance than MWTLS. Furthermore, to improve the performance of RKF on real data, ASPEN data are used to calculate the initial estimates. The estimation results show that the RKF algorithm can reliably estimate the sequence impedances, using ASPEN data as a starting condition. The estimation procedure is repeated over different time periods and the corresponding results are presented.

Finally, the significance of data drop-outs and its impact on the use of parameter estimates for real-time power system applications, such as state estimation and dynamic line rating, is discussed. To address the problem (of data drop-outs), an auto regressive integrated moving average (ARIMA) model is implemented. The ability of this model to predict the variations in sequence impedances is demonstrated.

ACKNOWLEDGMENTS

I would like to offer my special thanks to my advisor, Dr. Anamitra Pal for the guidance during my thesis and for giving me an opportunity to conduct research. I would also like to express gratitude towards my committee members Dr. Daniel Tylavsky and Dr. Keith E. Holbert for their valuable time and inputs.

In addition, I would also like to express my gratitude to the financial support provided by Salt River Project (SRP) for the research work done in this thesis. Especially, I want to acknowledge the valuable inputs provided by Matthew Rhodes & Brian Keel.

Finally, yet importantly, I would like to thank my family & friends for their support and encouragement.

TABLE OF CONTENTS

	Page
LIST OF TABLES.....	vi
LIST OF FIGURES.....	vii
CHAPTER	
1. INTRODUCTION.....	1
1.1. Transmission Line Equivalent Circuits.....	1
1.2. Conventional Line Parameter Estimation (Model-based).....	3
1.3. Measurement-based Transmission Line Parameter Estimation	4
1.4. Motivation and Objective	7
1.5. Thesis Overview	8
2. MATHEMATICAL FORMULATION.....	9
2.1. Symmetrical Formulation	11
2.2. Unsymmetrical Formulation	12
3. ALGORITHMS.....	14
3.1. Moving Window Total Least Squares Method.....	15
3.2. Recursive Kalman Filter Method.....	16
4. TRANSMISSION LINE PARAMETER ESTIMATION	18
4.1. Data Pre-Processing.....	18
4.1.1. File Conversion	18

CHAPTER	Page
4.1.2. Data Synchronization	18
4.1.3. Data Cleaning	19
4.1.4. Estimation of Complex Voltages and Currents.....	19
4.2. Test Procedure	20
4.3. Line Parameter Estimation Using Synthetic Data.....	21
4.3.1. Sensitivity analysis	24
4.4. Line Parameter Estimation Using Pseudo-Synthetic Data.....	25
4.5. Implementation on the Real System	29
4.5.1. Time Series Analysis of Sequence Impedances.....	34
5. LINE PARAMETER ESTIMATION DURING DATA-DROPOUTS.....	39
5.1. Overview of ARIMA.....	40
5.2. Application of ARIMA Models	42
6. CONCLUSION & FUTURE SCOPE.....	45
6.1. Conclusion	45
6.2. Future Scope	46
REFERENCES	48
APPENDIX A	54
APPENDIX B.....	63
APPENDIX C.....	72

LIST OF TABLES

Table	Page
4.1. Simulation Results on Synthetic Data.....	23
4.2. Condition Number of Regression Matrix.....	28
5.1. Results of ARIMA Model.....	43

LIST OF FIGURES

Figure	Page
1.1. Positive Sequence Small Length Transmission Line Model.....	2
1.2. Positive Sequence Medium Length Transmission Line Model.....	2
1.3. Positive Sequence Long Length Transmission Line Model.....	2
1.4. Pmu Installations Across North America [19]	5
2.1. Transmission Line Pi Model.....	9
3.1. Recursive Kalman Filter	17
4.1. Three-Stage Test Procedure for Algorithm Validation	21
4.2. Noise in Voltage vs Percentage of Error.....	24
4.3. Noise in Current vs Percentage of Error	25
4.4. Noise in Current vs Percentage of Error	26
4.5. Noise in Voltage vs Percentage of Error.....	26
4.6. Variation of The Voltage of 500 Kv Transmission Line.....	27
4.7. Recursive Kalman Filter with Initial Estimates Calculated from Aspen.....	29
4.8. Estimated Three-Phase Resistance Using Symmetrical Formulation	30
4.9. Estimated Three-Phase Resistance Using Unsymmetrical Formulation	30
4.10. Estimated Three-Phase Reactance Using Symmetrical Formulation	31
4.11. Estimated Three-Phase Reactance Using Unsymmetrical Formulation.....	31
4.12. Estimated Zero-Sequence Resistance Using Symmetrical Formulation	32
4.13. Estimated Zero-Sequence Resistance Using Unsymmetrical Formulation.....	32
4.14. Estimated Zero-Sequence Reactance Using Symmetrical Formulation.....	33

Figure	Page
4.15. Estimated Zero-Sequence Reactance Using Unsymmetrical Formulation.....	33
4.16. Estimated Zero-Sequence Resistance Using Symmetrical Formulation	34
4.17. Estimated Zero-Sequence Resistance Using Unsymmetrical Formulation.....	35
4.18. Estimated Zero-Sequence Reactance Using Symmetrical Formulation.....	35
4.19. Estimated Zero-Sequence Reactance Using Unsymmetrical Formulation.....	36
4.20. Estimated Positive-Sequence Resistance Using Symmetrical Formulation.....	36
4.21. Estimated Positive-Sequence Resistance Using Unsymmetrical Formulation.....	37
4.22. Estimated Positive-Sequence Reactance Using Symmetrical Formulation	37
4.23. Estimated Positive-Sequence Reactance Using Unsymmetrical Formulation	38
5.1. Voltage Magnitude of a 500 Kv Transmission Line for 24 Hours.....	40
5.2. Observed and Forecasted Zero-Sequence Resistance Using Arima Model; Outliers are Highlighted by Red Ovals	43
5.3. Observed and Forecasted Zero-Sequence Reactance Using Arima Model; Outliers are Highlighted by Red Ovals	44

CHAPTER 1

INTRODUCTION

The demand for electricity is expected to grow with time due to the advancements made in electric vehicle technologies, and increasing number of new businesses [1]-[2]. This rising demand, coupled with increasing renewable penetration, is increasing the stress on the power system. Therefore, the need for robust techniques for state estimation, dynamic line rating (DLR), and stability assessment is essential now more than ever. Accurate modeling of transmission lines in general, and sequence impedances, in particular, play a crucial role in all these analyses.

1.1. Transmission Line Equivalent Circuits

Depending on its length, a transmission line can be represented by three types of equivalent circuits as described below [3]:

1. Short line (0-50 miles)
2. Medium line (50-150 miles)
3. Long line (150 miles or more)

A short length transmission line is represented by a series resistance and reactance as shown in Figure 1.1. Shunt capacitance is usually neglected in the short line model. In the medium line model (Figure 1.2), the line resistance and reactance are assumed to be concentrated in the middle. The total capacitive effect between the transmission line and the earth is divided between the two-shunt branches, one at the beginning and the other at the

end. A long transmission line is modeled as a cascade of medium line segments as shown in Figure 1.3.

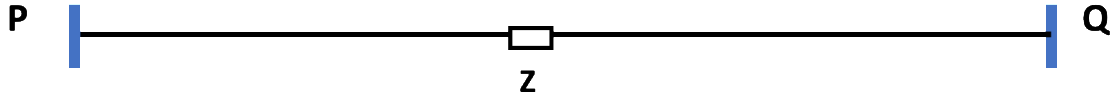


Figure 1.1. Positive sequence small length transmission line model

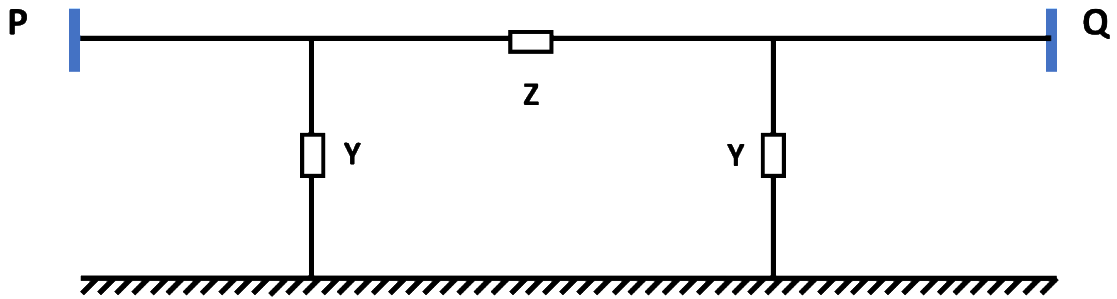


Figure 1.2. Positive sequence medium length transmission line model

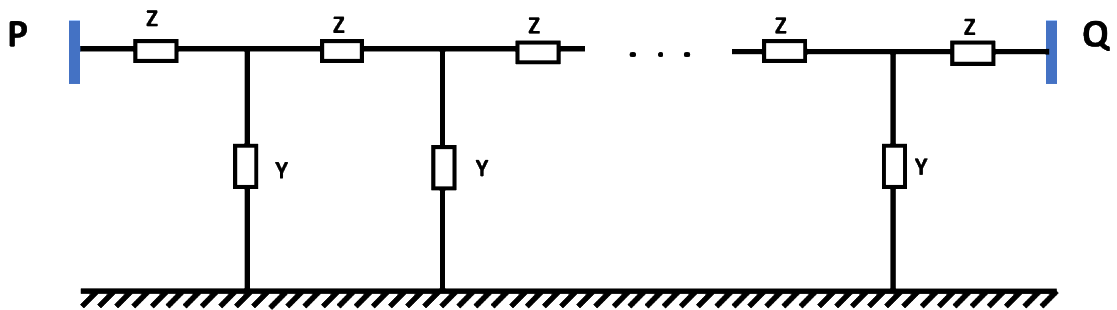


Figure 1.3. Positive sequence long length transmission line model

1.2. Conventional Line Parameter Estimation (Model-based)

Traditionally, line parameters, viz. resistance, admittance/capacitance, and inductance/reactance were estimated using the geometry of the conductors and Carson's formula [4]-[5]. The dc resistance of the transmission line at temperature T is given by,

$$R_{dc,T} = \frac{\rho_T * l}{A} \quad (1.1)$$

where ρ_T represents the resistivity of the conductor at temperature T , l is the length of the conductor and A is the cross-sectional area. For an ac transmission line, the resistance is usually higher because of skin effect and proximity effect.

The inductance of the transmission line can be calculated by calculating the flux linkages. Inductance of composite conductor with unequal spacing is given by

$$L = 2 \times 10^{-7} \ln \frac{D_{xy}}{D_{yy}} \text{ H/m per conductor} \quad (1.2)$$

where D_{xy} is the GMD (Geometric Mean Distance) and D_{xx} is the GMR (Geometric Mean Radius). GMD and GMR are calculated using the radius of the conductor and distance between the conductors.

The capacitance of the line can be computed by calculating the electric field of the conductor. The capacitance of the composite conductor with unequal spacing is given by

$$C = \frac{2\pi\epsilon}{\ln\left(\frac{D_{eq}}{D_{sc}}\right)} \quad (1.3)$$

$$D_{eq} = \sqrt[3]{D_{ab} D_{bc} D_{ca}} \quad (1.4)$$

$$D_{sc} = \sqrt[n]{rd^{n-1}} \text{ (for } n \text{ bundled conductor, } n \in \{2, 3\} \text{)} \quad (1.5)$$

where D_{ab}, D_{bc}, D_{ca} are the distance between the phase conductors, r is the radius of the conductor, and d is the bundle spacing.

However, the accuracy of the conventional approach for line parameter estimation decreases over time, as it does not account for age, usage, operating conditions, and other factors.

1.3. Measurement-based Transmission Line Parameter Estimation

An alternative approach for estimating the line parameters is by using voltage and current measurements taken at the opposite ends of the transmission lines. The development of phasor measurement units (PMUs) in the mid-1980s facilitated the measurement of highly accurate time-stamped voltage and current phasors [6]. A PMU typically outputs at the rate of 30 observations per second and the time-stamped data can be used for a variety of applications [7]-[18]. According to North American SynchroPhasor Initiative (NASPI) [19], over 2,800 networked PMUs are installed across North America as shown in Figure 1.4. The widespread installation of PMUs in recent years has renewed interest in the development of online methods for parameter estimation [20]-[27]. A brief overview of these methods is provided below.

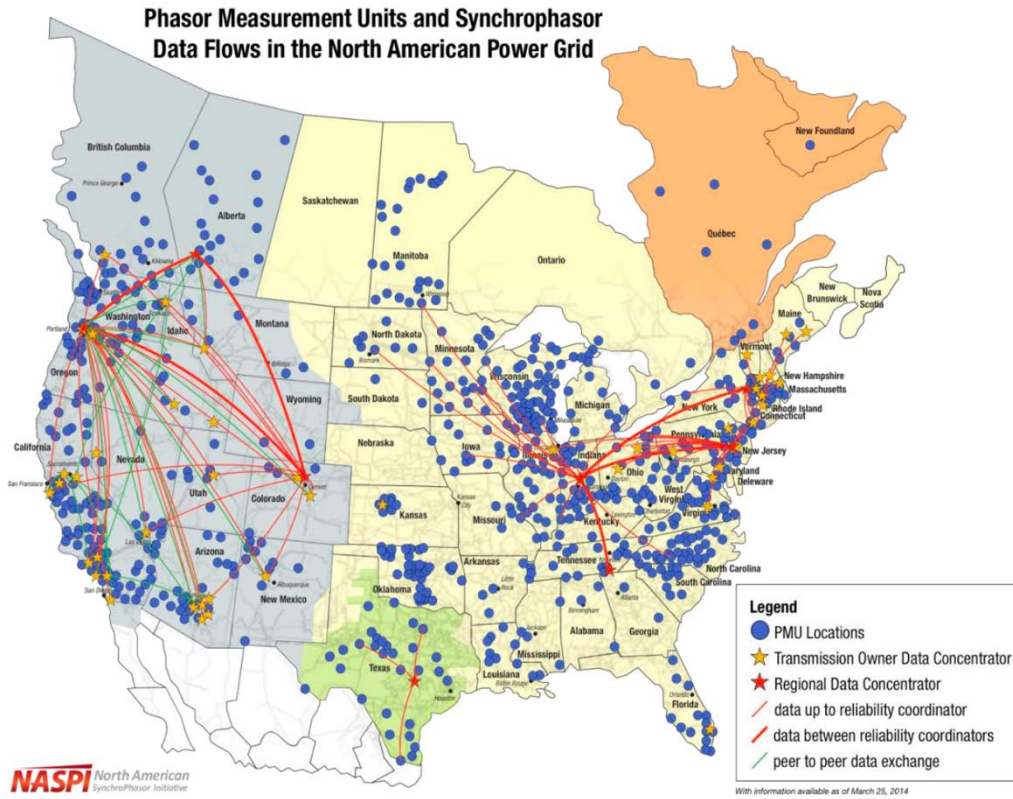


Figure 1.4. PMU installations across North America [19]

In [20], the authors proposed a new algorithm for online parameter estimation of untransposed parallel lines using a distributed line model and least squares method. Although the authors validated the proposed algorithm with EMTP simulations, practical considerations such as PMU measurement errors were not modeled in that work. In [21], modal components of the characteristic impedance and propagation constants were found using Clarke's transformation and the authors tested their algorithms using EMTP simulation data. However, the transmission lines were assumed to be transposed which may not be true in general.

Parameters of the double circuit transmission line were estimated in [22]. The method used voltage measurements from both sides and current measurements from one side to determine the parameters of a fully transposed double circuit transmission line. However, the method required one of the double circuit lines to be de-energized to estimate the zero-sequence impedance, which may not be always possible in practice. In [23], the parameters of the untransposed transmission line were calculated using equivalent pi and distributed line models. The methods were tested using MATLAB simulations and it was concluded that pi model could estimate parameters with three different states that have zero sequence component as input. On the other hand, distributed line model could estimate parameters with two different states but required the ratio of zero-sequence voltage to positive sequence voltage to be larger compared to the equivalent pi model. However, measurement errors were ignored in that work.

A framework for the estimation of positive sequence impedance was proposed in [24], which also minimized the effect of measurement errors. In [25] zero sequence impedance of the untransposed transmission line was estimated using line voltages, currents, active and reactive powers measured by the PMU. However, PMU errors were not considered in that work. The authors in [26] proposed a new method to estimate line parameters and measurements simultaneously, yet the proposed method required the voltage transformer, current transformer and PMU installed at one end of the transmission line to be pre-calibrated. Least squares method was examined in [27], to estimate the parameters of transposed and untransposed lines using ATP simulations. However, the method did not account for errors in the regression matrix.

Since PMU measurements are obtained in real-time, the developed online methods can track the variation of parameters with time. Traditionally, the line regression model used for parameter estimation is shown in (1.6).

$$\mathbf{Z} = \mathbf{H} * \boldsymbol{\theta} + \boldsymbol{\epsilon} \quad (1.6)$$

In (1.6), \mathbf{Z} is the data matrix, \mathbf{H} is the regression matrix, $\boldsymbol{\theta}$ represents the parameters to be estimated, and $\boldsymbol{\epsilon}$ represents the error. The data matrix, as well as regression matrix, are calculated using PMU measurements. Although PMUs are more accurate (than SCADA), their measurements do contain a noise component that is introduced by the instrumentation channels, including the PMUs themselves. Therefore, errors in the data matrix, as well as the regression matrix, must be accounted for, to estimate the parameters accurately. Two prior publications [28]-[29] that accounted for errors in both the matrices are analyzed in this work. In [28], online estimation of positive sequence line parameters of a 500 kV line using a moving window total least squares (MWTLS) approach was proposed. In [29], recursive Kalman filter (RKF) was used to estimate the three-phase line parameters using synthetic data.

1.4. Motivation and Objective

Most of the prior work has focused on positive sequence line parameter estimation, which often ignores the problems encountered in the real systems (which are three phase). Similarly, most studies tested their results using synthetic data, which might not capture many of the challenges encountered with real data. Therefore, there is a genuine need to study the *three-phase parameter estimation problem with real data*. The main objective of

this thesis is to address this knowledge gap by using real PMU data to study the line parameter estimation problem. The problem of online line parameter estimation is investigated using a total least square, and a Kalman filter-based formulation, employing PMU data obtained from a local utility.

1.5. Thesis Overview

The rest of the thesis is structured as follows. Mathematical formulation of the employed regression model is presented in Chapter 2. Chapter 3 reviews the estimation algorithms, namely, RKF and MWTLS. Chapter 4 presents the parameter estimation results. Chapter 5 discusses parameter estimation during data dropouts. The conclusions and future scope are provided in Chapter 6.

CHAPTER 2

MATHEMATICAL FORMULATION

Most of the transmission lines of the local utility that provided the PMU data were within 150 miles, and therefore, a medium length transmission line was chosen for this work. A three-phase medium length transmission line can be represented by an equivalent pi-circuit as shown in Figure 2.1.

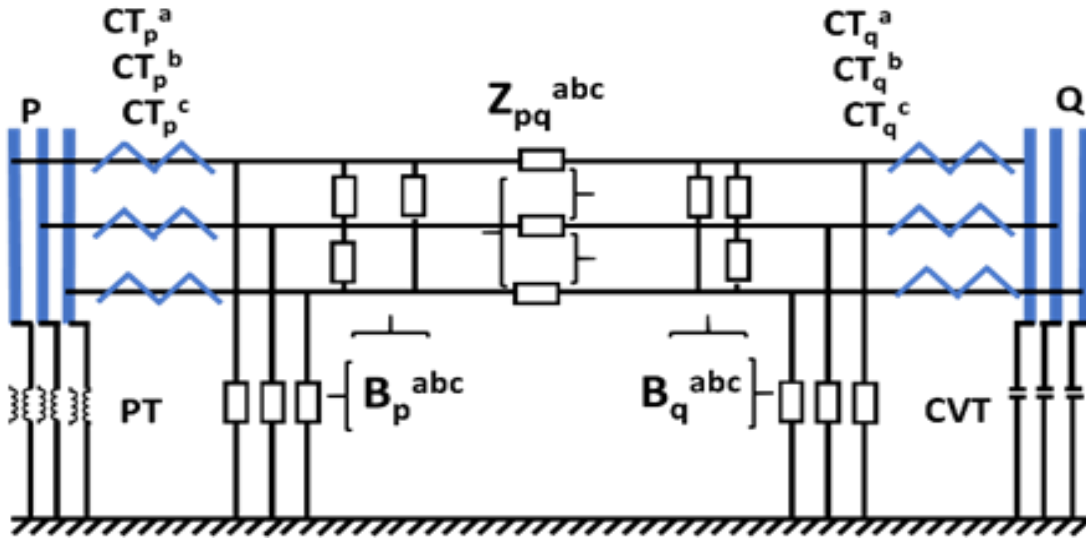


Figure 2.1. Transmission line pi model

The transmission line is assumed to have PMUs installed at both ends. It may also be symmetrical or unsymmetrical. The (self and mutual) series impedances of the three-phase transmission line is given by,

$$\mathbf{Z}_{pq}^{abc} = \begin{bmatrix} Z_{pq}^a & Z_{pq}^{ab} & Z_{pq}^{ac} \\ Z_{pq}^{ba} & Z_{pq}^b & Z_{pq}^{bc} \\ Z_{pq}^{ca} & Z_{pq}^{cb} & Z_{pq}^c \end{bmatrix} = [\mathbf{Y}_{pq}^{abc}]^{-1} \quad (2.1)$$

The impedance matrix contains 18 unknowns (9 real + 9 imaginary). Similarly, the shunt susceptances on either side of the transmission line are given by

$$\mathbf{B}_p^{abc} = j \begin{bmatrix} B_p^a + B_p^{ab} + B_p^{ac} & -B_p^{ab} & -B_p^{ac} \\ -B_p^{ba} & B_p^b + B_p^{ba} + B_p^{bc} & -B_p^{bc} \\ -B_p^{ca} & -B_p^{cb} & B_p^c + B_p^{ca} + B_p^{cb} \end{bmatrix} \quad (2.2)$$

$$\mathbf{B}_q^{abc} = j \begin{bmatrix} B_q^a + B_q^{ab} + B_q^{ac} & -B_q^{ab} & -B_q^{ac} \\ -B_q^{ba} & B_q^b + B_q^{ba} + B_q^{bc} & -B_q^{bc} \\ -B_q^{ca} & -B_q^{cb} & B_q^c + B_q^{ca} + B_q^{cb} \end{bmatrix} \quad (2.3)$$

The two susceptance matrices consist of a total 18 unknowns (9 unknowns each). The unknown parameters can be calculated by solving KCL and KVL equations. The equations (in matrix form) are given in (2.4) and (2.5) below.

$$\mathbf{I}_{pq}^{abc} + \mathbf{I}_{qp}^{abc} = \mathbf{B}_p^{abc} * \mathbf{V}_p^{abc} + \mathbf{B}_q^{abc} * \mathbf{V}_q^{abc} \quad (2.4)$$

$$\mathbf{V}_p^{abc} - \mathbf{V}_q^{abc} = \mathbf{Z}_{pq}^{abc} * \mathbf{I}_{pq}^{abc} \quad (2.5)$$

$$\text{In (2.4), and (2.5), } \mathbf{I}_{pq}^{abc} = \begin{bmatrix} I_{pq}^a \\ I_{pq}^b \\ I_{pq}^c \end{bmatrix}, \mathbf{I}_{qp}^{abc} = \begin{bmatrix} I_{qp}^a \\ I_{qp}^b \\ I_{qp}^c \end{bmatrix}, \mathbf{V}_p^{abc} = \begin{bmatrix} V_{pq}^a \\ V_{pq}^b \\ V_{pq}^c \end{bmatrix}, \mathbf{V}_q^{abc} = \begin{bmatrix} V_{qp}^a \\ V_{qp}^b \\ V_{qp}^c \end{bmatrix}$$

The KCL, KVL equations given in (2.4), and (2.5) can be rewritten in the form of a regression model to estimate the parameters. Accordingly, (2.4) and (2.5) can be rewritten as,

$$\mathbf{Z}_{sh} = \mathbf{H}_{sh} \times \mathbf{j}\boldsymbol{\theta}_{sh} \quad (2.6)$$

$$\mathbf{Z}_{se} = \mathbf{H}_{se} \times \boldsymbol{\theta}_{se} \quad (2.7)$$

The matrices described in (2.6)-(2.7) depend on the parameters described by (2.1)-(2.3). The parametric matrices can be symmetrical or unsymmetrical. Therefore, two types of formulations arise, namely,

Symmetrical formulation

Unsymmetrical formulation

2.1. Symmetrical Formulation

In the symmetrical formulation, it is assumed that the impedance and susceptance matrices are symmetric. The resulting matrices for the regression model described by (2.6) are given by

$$\mathbf{Z}_{sh} = \begin{bmatrix} I_{pq}^a + I_{qp}^a \\ I_{pq}^b + I_{qp}^b \\ I_{pq}^c + I_{qp}^c \end{bmatrix} \quad (2.8)$$

$$\mathbf{H}_{sh} = \begin{bmatrix} V_p^a & 0 & 0 & V_p^{ab} & 0 & V_p^{ac} & V_q^a & 0 & 0 & V_q^{ab} & 0 & V_q^{ac} \\ 0 & V_p^b & 0 & V_p^{ba} & V_p^{bc} & 0 & 0 & V_q^b & 0 & V_q^{ba} & V_q^{bc} & 0 \\ 0 & 0 & V_p^c & 0 & V_p^{cb} & V_p^{ca} & 0 & 0 & V_q^c & 0 & V_q^{cb} & V_q^{ca} \end{bmatrix} \quad (2.9)$$

$$\boldsymbol{\theta}_{sh} = [B_p^a \ B_p^b \ B_p^c \ B_p^{ab} \ B_p^{bc} \ B_p^{ca} \ B_q^a \ B_q^b \ B_q^c \ B_q^{ab} \ B_q^{bc} \ B_q^{ca}]^T \quad (2.10)$$

Similarly, matrices in the regression model corresponding to (2.7) are given by,

$$\mathbf{Z}_{se} = \begin{bmatrix} V_p^a - V_q^a \\ V_p^b - V_q^b \\ V_p^c - V_q^c \end{bmatrix} \quad (2.11)$$

$$\boldsymbol{\theta}_{se} = [Z_{pq}^a \ Z_{pq}^b \ Z_{pq}^c \ Z_{pq}^{ab} \ Z_{pq}^{bc} \ Z_{pq}^{ca}]^T \quad (2.12)$$

$$\mathbf{H}_{se} = \begin{bmatrix} h1 & 0 & 0 & h2 & 0 & h3 \\ 0 & h2 & 0 & h1 & h3 & 0 \\ 0 & 0 & h3 & 0 & h2 & h1 \end{bmatrix} \quad (2.13)$$

$$h_1 = I_{pq}^a - j[B_p^a + B_p^{ab} + B_p^{ac} \quad -B_p^{ab} \quad -B_p^{ac}] \begin{bmatrix} V_p^a \\ V_p^b \\ V_p^c \end{bmatrix} \quad (2.14)$$

$$h_2 = I_{pq}^b - j[-B_p^{ba} \quad B_p^b + B_p^{ba} + B_p^{bc} \quad -B_p^{bc}] \begin{bmatrix} V_p^a \\ V_p^b \\ V_p^c \end{bmatrix} \quad (2.15)$$

$$h_3 = I_{pq}^c - j[-B_p^{ca} \quad -B_p^{cb} \quad B_p^c + B_p^{ca} + B_p^{cb}] \begin{bmatrix} V_p^a \\ V_p^b \\ V_p^c \end{bmatrix} \quad (2.16)$$

2.2. Unsymmetrical Formulation

In the unsymmetrical formulation, the impedance and susceptance matrices are asymmetric. Therefore, the matrices in the regression model described by (2.6) are given by,

$$\mathbf{Z}_{sh} = \begin{bmatrix} I_{pq}^a + I_{qp}^a \\ I_{pq}^b + I_{qp}^b \\ I_{pq}^c + I_{qp}^c \end{bmatrix} \quad (2.17)$$

\mathbf{H}_{sh}

$$= \begin{bmatrix} V_p^a & 0 & 0 & V_p^{ab} & 0 & 0 & 0 & 0 & V_p^{ac} & V_q^a & 0 & 0 & V_q^{ab} & 0 & 0 & 0 & 0 & V_q^{ac} \\ 0 & V_p^b & 0 & 0 & V_p^{ba} & V_p^{bc} & 0 & 0 & 0 & 0 & V_q^b & 0 & 0 & V_q^{ba} & V_q^{bc} & 0 & 0 & 0 \\ 0 & 0 & V_p^c & 0 & 0 & 0 & V_p^{cb} & V_p^{ca} & 0 & 0 & 0 & V_q^c & 0 & 0 & 0 & V_q^{cb} & V_q^{ca} & 0 \end{bmatrix} \quad (2.18)$$

$\boldsymbol{\theta}_{sh}$

$$= [B_p^a \ B_p^b \ B_p^c \ B_p^{ab} \ B_p^{ba} \ B_p^{bc} \ B_p^{cb} \ B_p^{ca} \ B_p^{ac} \ B_q^a \ B_q^b \ B_q^c \ B_q^{ab} \ B_q^{ba} \ B_q^{bc} \ B_q^{cb} \ B_q^{ca} \ B_q^{ac}]^T \quad (2.19)$$

Similarly, matrices in the regression model corresponding to (2.7) are given by,

$$\mathbf{Z}_{se} = \begin{bmatrix} V_p^a - V_q^a \\ V_p^b - V_q^b \\ V_p^c - V_q^c \end{bmatrix} \quad (2.20)$$

$$\boldsymbol{\theta}_{se} = [Z_{pq}^a \quad Z_{pq}^b \quad Z_{pq}^c \quad Z_{pq}^{ab} \quad Z_{pq}^{ba} \quad Z_{pq}^{bc} \quad Z_{pq}^{cb} \quad Z_{pq}^{ca} \quad Z_{pq}^{ac}]^T \quad (2.21)$$

$$\mathbf{H}_{se} = \begin{bmatrix} h_1 & 0 & 0 & h_2 & 0 & 0 & 0 & 0 & h_3 \\ 0 & h_2 & 0 & 0 & h_1 & h_3 & 0 & 0 & 0 \\ 0 & 0 & h_3 & 0 & 0 & 0 & h_2 & h_1 & 0 \end{bmatrix} \quad (2.22)$$

$$h_1 = I_{pq}^a - j[B_p^a + B_p^{ab} + B_p^{ac} \quad -B_p^{ab} \quad -B_p^{ac}] \begin{bmatrix} V_p^a \\ V_p^b \\ V_p^c \end{bmatrix} \quad (2.23)$$

$$h_2 = I_{pq}^b - j[-B_p^{ba} \quad B_p^b + B_p^{ba} + B_p^{bc} \quad -B_p^{bc}] \begin{bmatrix} V_p^a \\ V_p^b \\ V_p^c \end{bmatrix} \quad (2.24)$$

$$h_3 = I_{pq}^c - j[-B_p^{ca} \quad -B_p^{cb} \quad B_p^c + B_p^{ca} + B_p^{cb}] \begin{bmatrix} V_p^a \\ V_p^b \\ V_p^c \end{bmatrix} \quad (2.25)$$

The matrices \mathbf{Z}_{sh} , \mathbf{H}_{sh} , \mathbf{Z}_{se} , \mathbf{H}_{se} are calculated using PMU measurements and therefore, have real and imaginary components. Hence, (2.6) and (2.7) can be expressed as follows

$$\overbrace{\begin{bmatrix} \text{real}(\mathbf{Z}_{sh}) \\ \text{imag}(\mathbf{Z}_{sh}) \end{bmatrix}}^{\mathbf{Z}_{sus}} = \overbrace{\begin{bmatrix} -\text{imag}(\mathbf{H}_{sh}) \\ \text{real}(\mathbf{H}_{sh}) \end{bmatrix}}^{\mathbf{H}_{sus}} \times \overbrace{\begin{bmatrix} \boldsymbol{\theta}_{sh} \end{bmatrix}}^{\boldsymbol{\theta}_{sus}} \quad (2.26)$$

$$\overbrace{\begin{bmatrix} \text{real}(\mathbf{Z}_{se}) \\ \text{imag}(\mathbf{Z}_{se}) \end{bmatrix}}^{\mathbf{Z}_{imp}} = \overbrace{\begin{bmatrix} \text{real}(\mathbf{H}_{se}) & -\text{imag}(\mathbf{H}_{se}) \\ \text{imag}(\mathbf{H}_{se}) & \text{real}(\mathbf{H}_{se}) \end{bmatrix}}^{\mathbf{H}_{imp}} \times \overbrace{\begin{bmatrix} \text{real}(\boldsymbol{\theta}_{se}) \\ \text{imag}(\boldsymbol{\theta}_{se}) \end{bmatrix}}^{\boldsymbol{\theta}_{imp}} \quad (2.27)$$

Initially, (2.26) is used for the calculation of the shunt susceptance matrix and the estimated susceptance parameters are used to solve (2.27) to calculate the series impedance parameters.

CHAPTER 3

ALGORITHMS

The transmission line parameters can be estimated by solving the linear equations (2.26) and (2.27), where the entries of the matrices are obtained from PMU measurements. Traditionally, linear regression models are solved by using the least squares method, where we minimize the squared error between the measurements \mathbf{Z} and the estimate $\mathbf{H}\hat{\boldsymbol{\theta}}$ [30] as shown in (3.1).

$$\mathbf{J} = \boldsymbol{\epsilon}^T \boldsymbol{\epsilon} = (\mathbf{Z} - \mathbf{H}\hat{\boldsymbol{\theta}})^T (\mathbf{Z} - \mathbf{H}\hat{\boldsymbol{\theta}}) \quad (3.1)$$

\mathbf{J} can be minimized by equating the partial derivative of \mathbf{J} with respect to $\boldsymbol{\theta}$ and by solving for $\boldsymbol{\theta}$. On doing the minimization, we get,

$$\hat{\boldsymbol{\theta}} = (\mathbf{H}^T \mathbf{H})^{-1} \mathbf{H}^T \mathbf{Z} \quad (3.2)$$

In the least squares method, it is assumed that the data matrix \mathbf{H} is free of errors. However, this assumption does not hold good when \mathbf{H} is composed of real PMU measurements obtained from the field. This is because field PMU may data contain sampling errors, human errors, modeling errors, and instrument transformer errors [31]-[33]. The errors in the data matrix can be modeled as,

$$\mathbf{Z} = (\mathbf{H} + \boldsymbol{\epsilon}_H) * \boldsymbol{\theta} + \boldsymbol{\epsilon}_Z \quad (3.3)$$

which cannot be solved by the traditional least squares approach.

Several alternate methods were proposed in the literature, which accounts for the errors in the \mathbf{Z} matrix as well as \mathbf{H} matrix. Two such popular algorithms, moving window total least squares (MWTLS) and recursive Kalman filter (RKF), are considered in this work.

3.1. Moving Window Total Least Squares Method

Total least squares method was developed in [34] to solve a system of linear equations with errors in the data matrix as well as measurement matrix. The TLS method is widely used in signal processing to estimate the line parameters. The algorithm tries to minimize the orthogonal distance between the estimate and the true value [35]-[37]

$$\min\|\begin{bmatrix} \mathbf{H} & \mathbf{Z} \end{bmatrix} - \begin{bmatrix} \hat{\mathbf{H}} & \hat{\mathbf{Z}} \end{bmatrix}\|_2 \quad (3.4)$$

In MWTLS, the matrices \mathbf{Z} and \mathbf{H} are calculated using an ‘n’ sample measurement window. As the new measurements arrive, the old measurements are replaced by the moving window. The procedure is repeated continuously until the measurements are exhausted. It is easy to observe that an increase in window size will lead to improvement in the accuracy of the results. To estimate the parameters, calculating the singular value decomposition of $\begin{bmatrix} \mathbf{H} & \mathbf{Z} \end{bmatrix}$ is the first step. The singular value decomposition is the factorization of a matrix into the form $\mathbf{U}\mathbf{\Sigma}\mathbf{V}^T$. Therefore,

$$\begin{bmatrix} \mathbf{H} & \mathbf{Z} \end{bmatrix} = \mathbf{U}\mathbf{\Sigma}\mathbf{V}^T \quad (3.5)$$

In (3.5), \mathbf{U} denotes the left singular vectors, $\mathbf{\Sigma}$ denotes the singular values, and \mathbf{V} denotes the right singular vectors. Let cH be the number of columns in \mathbf{H} . Then the parameters can be estimated using (3.6) [28].

$$\hat{\boldsymbol{\theta}} = -\frac{\mathbf{V}(1:cH, cH+1)}{\mathbf{V}(cH+1, cH+1)} \quad (3.6)$$

3.2. Recursive Kalman Filter Method

Kalman filter is extensively used in signal processing to estimate the parameters of unknown signals. For a linear discrete system, the Kalman filter formulation is given by (3.7)–(3.12),

$$\boldsymbol{\theta}_k^- = \mathbf{F}_{k-1} * \boldsymbol{\theta}_{k-1} + \mathbf{G}_{k-1} * \mathbf{u}_{k-1} \quad (3.7)$$

$$\mathbf{Z}_k = \mathbf{H}_k \boldsymbol{\theta}_k \quad (3.8)$$

$$\mathbf{P}_k^- = \mathbf{F}_{k-1} \mathbf{P}_{k-1} \mathbf{F}_{k-1}^T \quad (3.9)$$

$$\boldsymbol{\theta}_k = \boldsymbol{\theta}_k^- + \mathbf{K}_k * (\mathbf{Z}_k - \mathbf{H}_k \boldsymbol{\theta}_k^-) \quad (3.10)$$

$$\mathbf{K}_k = \mathbf{P}_k^- \mathbf{H}_k^T * [\mathbf{H}_k \mathbf{P}_k^- \mathbf{H}_k^T + \mathbf{R}]^{-1} \quad (3.11)$$

$$\mathbf{P}_k = [\mathbf{I} - \mathbf{K}_k \mathbf{H}_k] * \mathbf{P}_k^- \quad (3.12)$$

where, k denotes the sample number, $\boldsymbol{\theta}_k^-$ is the priori estimate, $\boldsymbol{\theta}_k$ is the posteriori state estimate, \mathbf{F}_{k-1} is the state transition matrix, \mathbf{G}_{k-1} is the input matrix, \mathbf{u}_{k-1} is the priori input, \mathbf{P}_k^- is the error covariance matrix of priori estimate, \mathbf{P}_k is the error covariance matrix of posteriori estimate, \mathbf{R} is the measurement covariance matrix.

For the transmission system with line parameters as states, the state transition matrix is identity, and there is no input matrix [29]. Therefore (3.7) and (3.9) can be reformulated as,

$$\boldsymbol{\theta}_k^- = \boldsymbol{\theta}_{k-1}, \mathbf{P}_k^- = \mathbf{P}_{k-1} \quad (3.13)$$

The operation of the RKF is shown in Figure 3.1 where \mathbf{K} represents the Kalman gain. A modified covariance matrix (\mathbf{R}) is employed [39] to account for errors in the regression matrix, \mathbf{H} as well as in data matrix, \mathbf{Z} . The modified covariance matrix is used to solve (2.26) and (2.27), to estimate the line parameters, $\boldsymbol{\theta}$. In [29], it was assumed that the impedance and susceptance matrices are symmetrical, which may not always be true. As a result, two mathematical formulations, namely, the symmetrical formulation and the unsymmetrical formulation are investigated in this work. The modified covariance matrices accounting for errors in data matrix (\mathbf{Z}) as well as regression matrix (\mathbf{H}) are presented in the Appendices A and B, respectively. For the detailed derivation of these formulae please see the Appendix C.

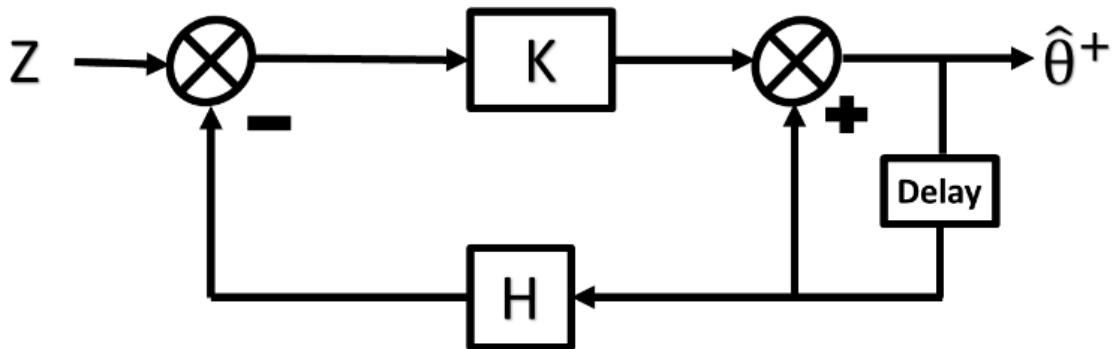


Figure 3.1. Recursive Kalman filter

CHAPTER 4

TRANSMISSION LINE PARAMETER ESTIMATION

4.1. Data Pre-Processing

The sequence of steps for pre-processing the PMU data before setting them as inputs to the parameter estimation algorithms are as follows.

File conversion

Data synchronization

Data cleaning

Estimation of complex voltages and currents

4.1.1. File Conversion

The synchrophasor data for this work are obtained from a local utility and are in a proprietary file format. The PMU data corresponding to the period of interest are converted to CSV files using a file exporter software provided by the utility. The CSV files thus obtained are used for the development and testing of parameter estimation algorithms in MATLAB [40].

4.1.2. Data Synchronization

PMU devices have an internal clock (usually a crystal oscillator) and are synchronized with the global positioning system (GPS) for high-precision time sampling [41]. The high-precision timestamps can be used to synchronize PMU measurements taken at different locations. Since measurements taken at the sending end as well as the receiving are being

used in the estimation process in the proposed algorithm, the measurements are synchronized based on the timestamps.

4.1.3. Data Cleaning

PMU measurements samples are synchronized with universal coordinated time (UTC) using the GPS signals. The PMU data may be affected by the data losses [41]-[42] due to loss of GPS synchronization or external factors. Therefore, the PMU data must be cleaned before starting the estimation process. Several methods have been proposed in the literature to deal with the PMU data losses [43]-[44]. However, for the initial estimation procedure, the measurements affected by the data losses are ignored. It was observed that at times of data losses, the voltage and current measurements are replaced by '0' in the data files. Since this is not possible in the traditional power system, the measurements with '0' magnitudes are omitted.

4.1.4. Estimation of Complex Voltages and Currents

The pre-processed data are used to calculate voltages and current in this step. The measured synchrophasor angle can increase or decrease based on the operating conditions and is usually wrapped between -180° and $+180^\circ$ [45]. Therefore, the phasor angles measured by the synchrophasor device are unwrapped using MATLAB's unwrap command. Thus, unwrapped phase angles and magnitudes for voltages and currents are used to calculate the phasor using (4.1),

$$M_{\text{complex}} = M_{\text{magnitude}} * e^{-i(M_{\text{phase angle}})} \quad (4.1)$$

where $M_{\text{magnitude}}$ is voltage or current magnitude, $M_{\text{phase angle}}$ is voltage or current unwrapped phase angle. Finally, the calculated voltage and current measurements are used for the parameter estimation process.

4.2. Test Procedure

A three-stage test procedure is adopted in this work as shown in Figure 4.1. The reason for doing so is that algorithms developed using purely synthetic data may not give the desired performance when implemented in the field. Conversely, algorithms cannot be directly tested using field data, because the true values of the line parameters are not known.

In the first stage, the algorithm is tested on a purely synthetic dataset. The dataset is generated using a known set of line parameters. A white Gaussian noise is added to the voltage and current measurements to replicate the measurement noise and the performance of the selected algorithms (MWTLs and RKF) is evaluated by measuring the accuracy of the estimated parameters.

In the second stage, the algorithm is tested on a pseudo-synthetic dataset generated using field data. Voltage measurements (PMU data) are taken from both ends of a transmission line and current measurements are generated with a known set of line parameters using (4.2) - (4.3).

$$\mathbf{I}_{pq}^{abc} = \mathbf{Y}_{pq}^{abc} * (\mathbf{V}_p^{abc} - \mathbf{V}_q^{abc}) + \mathbf{B}_p^{abc} \mathbf{V}_p^{abc} \quad (4.2)$$

$$\mathbf{I}_{qp}^{abc} = \mathbf{Y}_{pq}^{abc} * (\mathbf{V}_q^{abc} - \mathbf{V}_p^{abc}) + \mathbf{B}_q^{abc} \mathbf{V}_q^{abc} \quad (4.3)$$

White Gaussian noise is added to the data similar to what was done in the first stage and performance of the selected algorithms is assessed once more.

Finally, the algorithm is implemented on the real system, using both voltage and current measurements obtained from PMU data obtained from the field. The performance of the algorithm is evaluated by estimating the parameters over different time-periods.

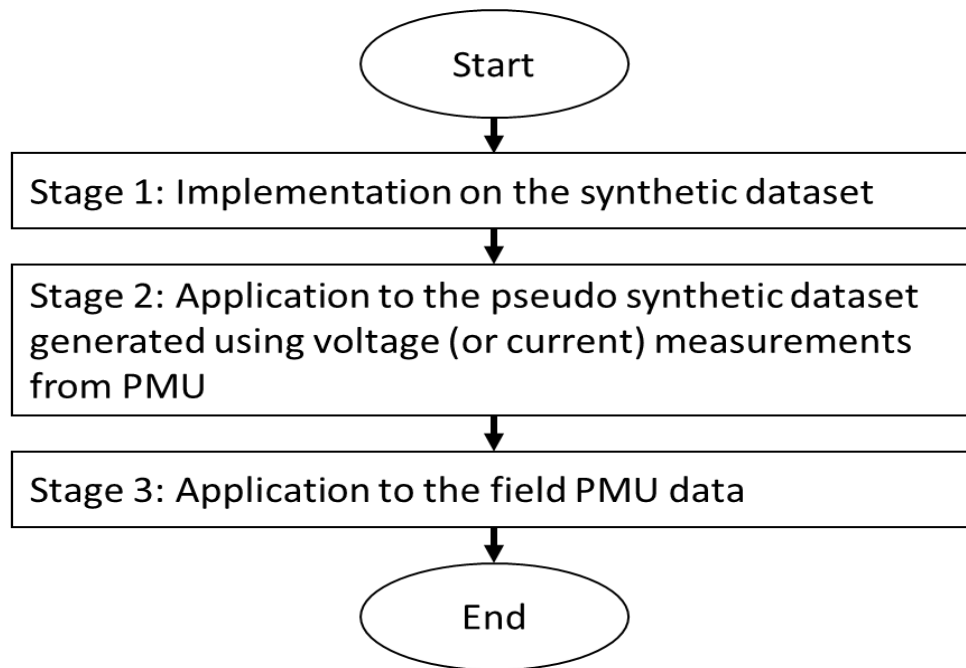


Figure 4.1. Three-stage test procedure for algorithm validation

4.3. Line Parameter Estimation Using Synthetic Data

In this stage, the algorithms were tested on a synthetic dataset. A training set consisting of 1,200 measurements was generated in MATLAB using the parameters of a 362 kV transmission line with horizontal configuration [46]. The length of the transmission line was chosen to be 50 miles with the parameters given by (4.4) - (4.5).

$$\mathbf{Z}_{pq}^{abc} = \begin{bmatrix} 15.1 + 52.1i & 8.98 + 22.5i & 8.77 + 18.4i \\ 8.9 + 22.5i & 12.26 + 51.6i & 8.98 + 22.5i \\ 8.7 + 18.4i & 8.98 + 22.5i & 15.18 + 52.1i \end{bmatrix} \Omega \quad (4.4)$$

$$\mathbf{B}_p^{abc} = \mathbf{B}_q^{abc} = j \begin{bmatrix} 0.329 & -0.057 & -0.017 \\ -0.057 & 0.341 & -0.057 \\ -0.017 & -0.057 & 0.329 \end{bmatrix} 10^{-3} \Omega^{-1} \quad (4.5)$$

To replicate the field conditions, measurement noises having characteristics $N(0, 0.001^2)$ and $N(0, 0.01^2)$ were added to the voltage and current measurements, respectively. A window size of 80 was chosen for the two methods (MWTLS and RKF). Initially, the algorithm was employed to estimate the susceptance parameters by solving (2.26) using the symmetrical formulation. The estimated susceptance parameters were then used to estimate impedance parameters using (2.27). Subsequently, the sequence impedance matrix (\mathbf{Z}_{pq}^{012}) was calculated using (4.6).

$$\mathbf{Z}_{pq}^{012} = \mathbf{S}^{-1} * \mathbf{Z}_{pq}^{abc} * \mathbf{S} \quad (4.6)$$

In (4.5), $\mathbf{Z}_{pq}^{012} = \begin{bmatrix} Z_{pq}^0 & Z_{pq}^{01} & Z_{pq}^{02} \\ Z_{pq}^{10} & Z_{pq}^1 & Z_{pq}^{12} \\ Z_{pq}^{20} & Z_{pq}^{21} & Z_{pq}^{22} \end{bmatrix}$, $\mathbf{S} = \begin{bmatrix} 1 & 1 & 1 \\ 1 & a^2 & a \\ 1 & a & a^2 \end{bmatrix}$, $a = 1 \angle 120^\circ$. The simulations

were repeated 100 times and the average results presented in Table 4.1. The simulation results show that both RKF and MWTLS were able to estimate the line parameters using synthetic data. It can also be inferred from Table 4.1 that RKF performs slightly better than MWTLS.

Table 4.1. Simulation results on synthetic data

Susceptance Parameter	Mean % error		Impedance Parameter	Mean % error	
	RKF	MWTLs		RKF	MWTLs
B_p^a	0.6380	5.0108	Z_{pq}^a	0.0171	0.0369
B_p^{ba}	1.3280	5.6225	Z_{pq}^{ba}	0.0176	0.0334
B_p^{ca}	4.1649	23.7815	Z_{pq}^{ca}	0.0147	0.0414
B_p^{ab}	1.2674	7.3276	Z_{pq}^{ab}	0.0151	0.0410
B_p^b	0.7116	4.3268	Z_{pq}^b	0.0143	0.0369
B_p^{cb}	1.4785	6.9901	Z_{pq}^{cb}	0.0161	0.0443
B_p^{ac}	4.6813	24.6559	Z_{pq}^{ca}	0.0188	0.0344
B_p^{bc}	1.2906	5.8178	Z_{pq}^{cb}	0.0154	0.0366
B_p^c	0.6411	4.8460	Z_{pq}^c	0.0171	0.0352
B_q^a	0.7449	5.0730			
B_q^{ba}	1.4241	6.2243			
B_q^{ca}	4.8987	23.9759			
B_q^{ab}	1.5420	7.0436			
B_q^b	0.6816	4.7564			
B_q^{cb}	1.4482	7.1809			
B_q^{ac}	4.5762	25.303			
B_q^{bc}	1.2380	6.2442			
B_q^c	0.6812	4.8879			

4.3.1. Sensitivity analysis

A sensitivity analysis is conducted to study the effect of noise present in voltage, and current measurements on the performance of the RKF algorithm using symmetrical formulation. Gaussian noise of varying standard deviations (0.0005-0.01 p.u.) are added to the voltage, and current measurements and the simulations are repeated. The results are shown in Figures 4.2-4.3. It can be observed that even though the standard deviations of the introduced noise increase, the percentage of error in the estimated parameters remain less than 2%. Therefore, it can be concluded that the RKF algorithm is robust and is capable of estimating parameters even in the presence of varying magnitude of measurement noise.

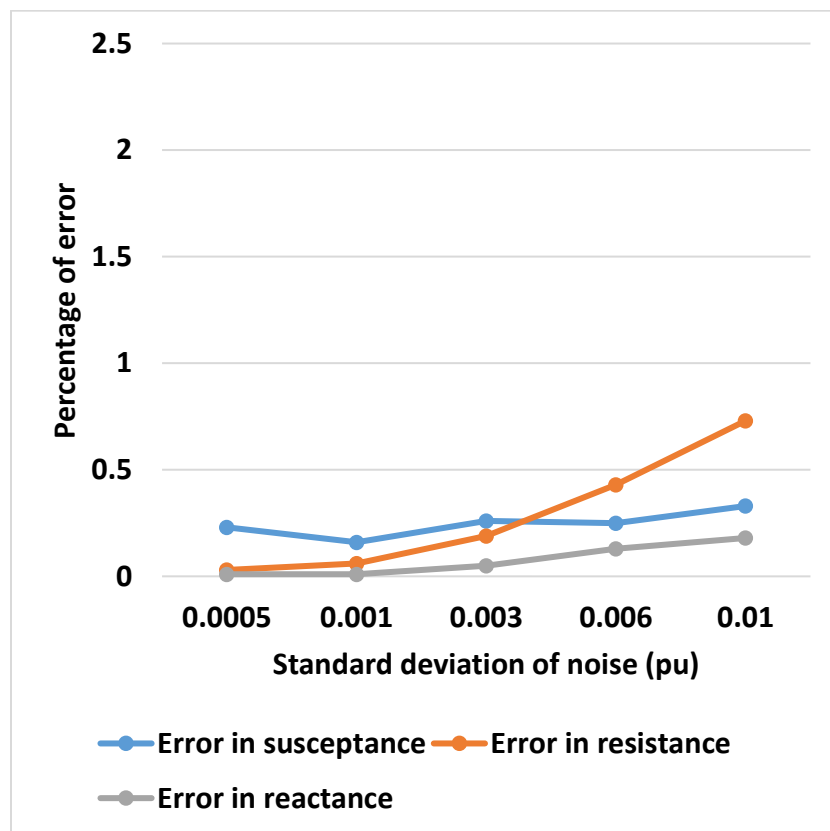


Figure 4.2. Noise in voltage vs percentage of error

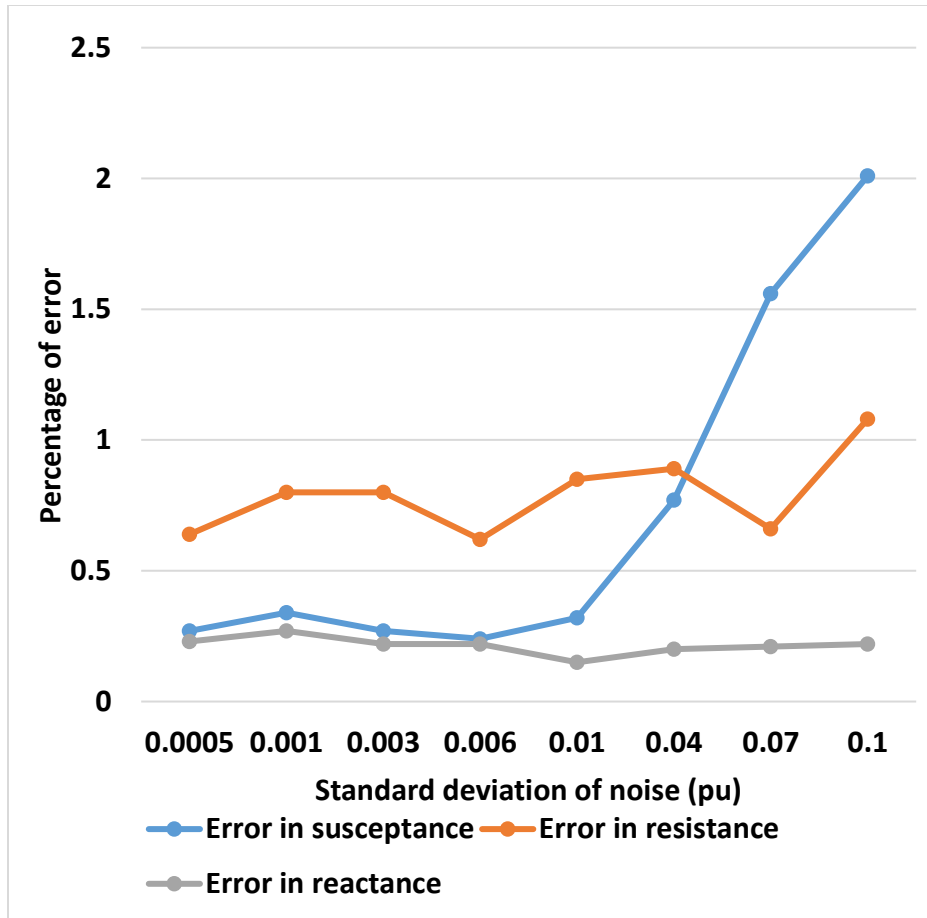


Figure 4.3. Noise in current vs percentage of error

4.4. Line Parameter Estimation Using Pseudo-Synthetic Data

In the next stage, pseudo-synthetic dataset was generated using voltage measurements taken from both ends of a 500 kV transmission line during 7 AM and 8 AM. A training set of 9,000 measurements were generated using PMU data and (4.2) - (4.3). To study the effect of errors on the performance of the algorithms, Gaussian noise of varying magnitude were added to the data and a sensitivity study was conducted. The results are summarized in Figures 4.4 and 4.5.

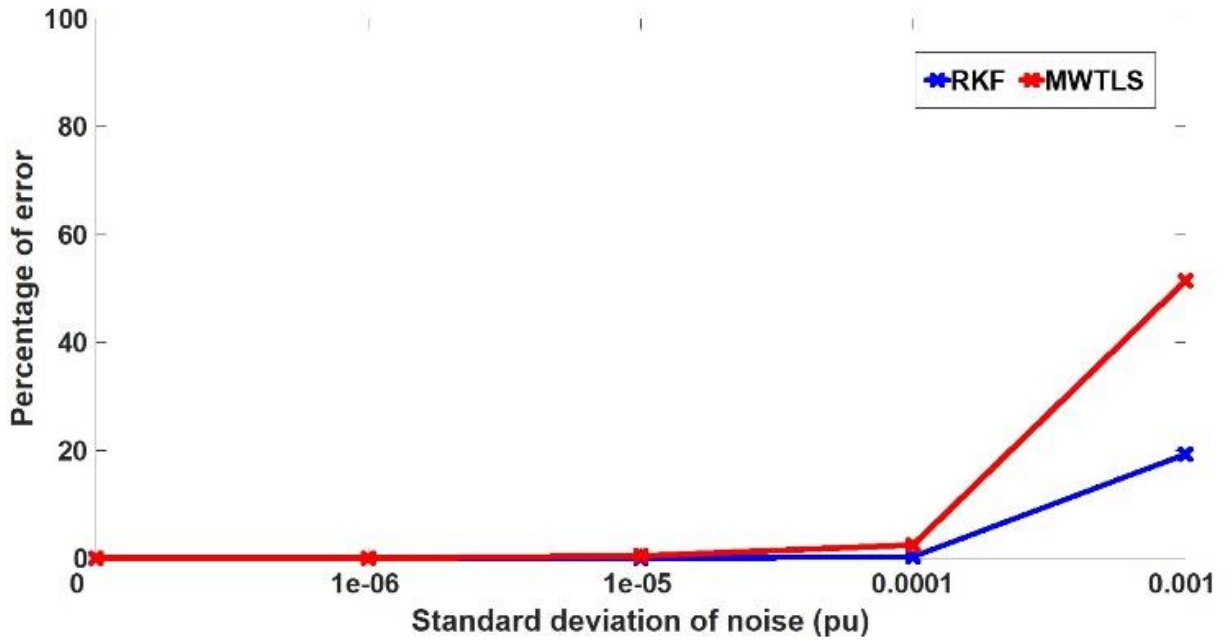


Figure 4.4. Noise in current vs percentage of error

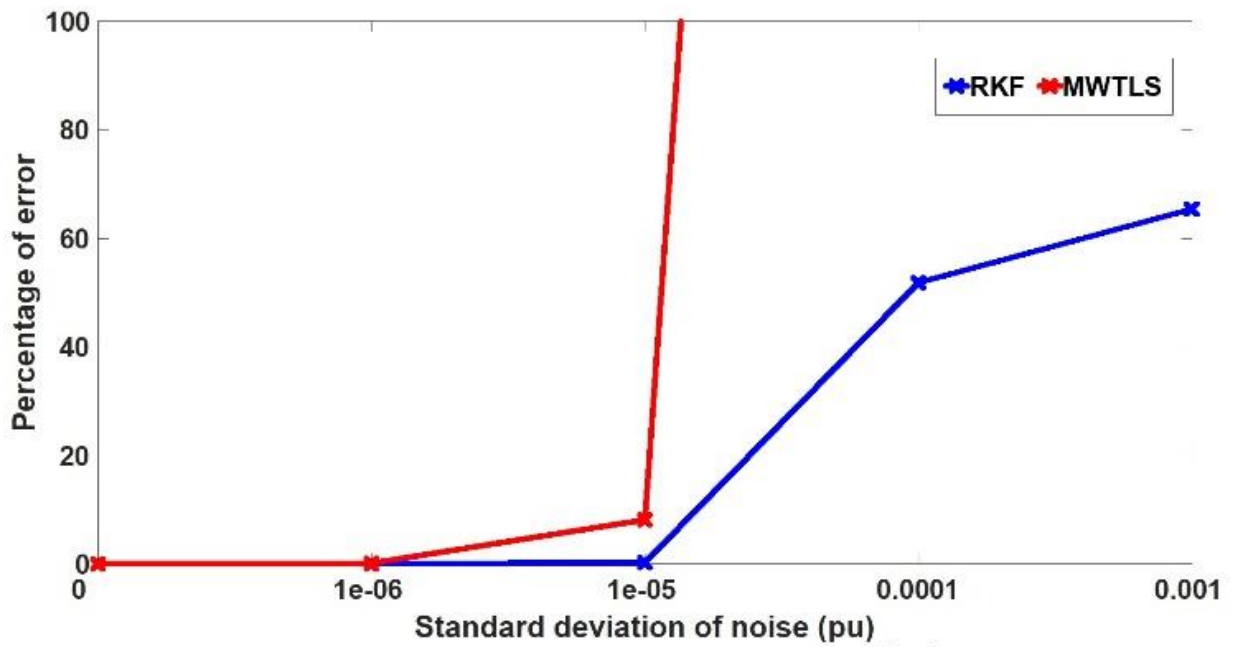


Figure 4.5. Noise in voltage vs percentage of error

Two inferences can be drawn from the results shown in Figures 4.4 and 4.5:

1) RKF algorithm yields better results compared to MWTLs. Consequently, RKF was chosen to estimate the parameters using real data.

2) The accuracy of the estimates falls drastically with increase in measurement noise.

After an in-depth analysis, it was concluded that the variation in voltage is small for the real system as shown in Figure 4.6. This is because utilities try to maintain the voltage constant, which eventually leads to the parameter estimation problem becoming ill-conditioned. Table 4.2 shows the condition number of the regression matrices, and it can be observed that the condition number of pseudo-synthetic data, in particular, H_{sh} (made of voltage measurements) is considerably high.

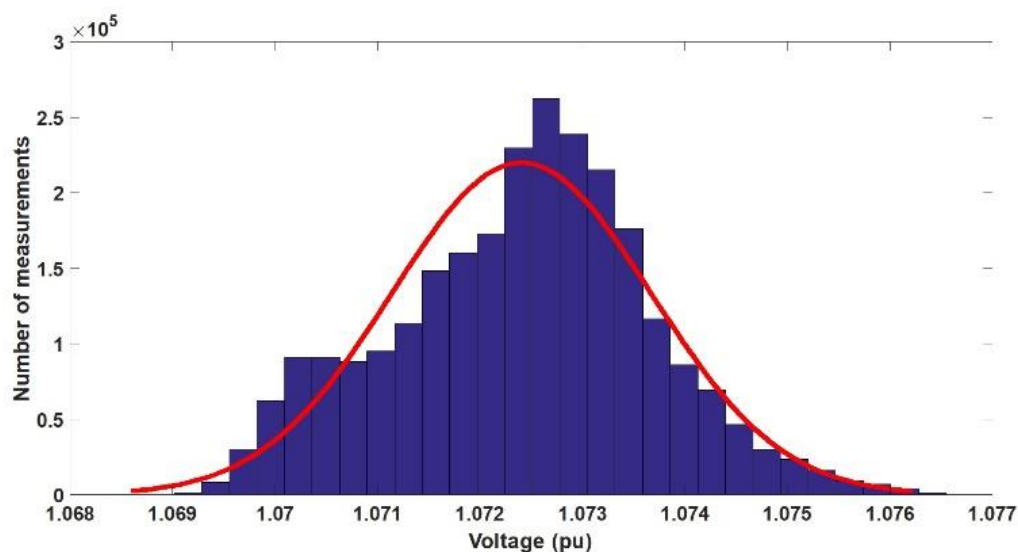


Figure 4.6. Variation of the voltage of 500 kV transmission line

During this analysis, it was realized that one way to further enhance the performance of RKF (even in presence of the ill-conditioning problem), could be by improving the quality

of the initial estimates. Traditionally, parameters are calculated using software such as ASPEN and stored in the SCADA database at the time of commissioning. Therefore, the hypothesis that needed to be tested was: *if ASPEN data could be utilized to calculate the initial estimates and thereby improve the performance of RKF.*

Table 4.2. Condition number of regression matrix

	Condition Number of H_{sh}	Condition Number of H_{se}
Synthetic data	54.74	3.81
Pseudo-synthetic data	1.14e05	3.8e03

The transmission line is initially assumed to be transposed and symmetrical, to calculate initial estimates using ASPEN data. Therefore, the impedance matrix is modified as shown below.

$$\mathbf{Z}_{pq}^{abc} = \begin{bmatrix} Z_{pq}^a & Z_{pq}^{ab} & Z_{pq}^{ac} \\ Z_{pq}^{ba} & Z_{pq}^b & Z_{pq}^{bc} \\ Z_{pq}^{ca} & Z_{pq}^{cb} & Z_{pq}^c \end{bmatrix} = \begin{bmatrix} Z_{pq}^s & Z_{pq}^m & Z_{pq}^m \\ Z_{pq}^m & Z_{pq}^s & Z_{pq}^m \\ Z_{pq}^m & Z_{pq}^m & Z_{pq}^s \end{bmatrix} \quad (4.7)$$

In (4.7), Z_{pq}^s denotes the self-impedance, Z_{pq}^m denotes the mutual impedance. From (4.6)-(4.7), the relation between Z_{pq}^s , Z_{pq}^m , Z_{pq}^0 , Z_{pq}^1 are derived as follows,

$$Z_{pq}^s + 2 * Z_{pq}^m = Z_{pq}^0 \quad (4.8)$$

$$Z_{pq}^s - Z_{pq}^m = Z_{pq}^1 \quad (4.9)$$

The calculated self and mutual impedance are used to populate the initial estimate of impedance matrix using (4.7). The resultant matrix is used to calculate the initial estimate of parameter vector θ_1^- . The block diagram of the modified RKF is shown in Figure 4.7.

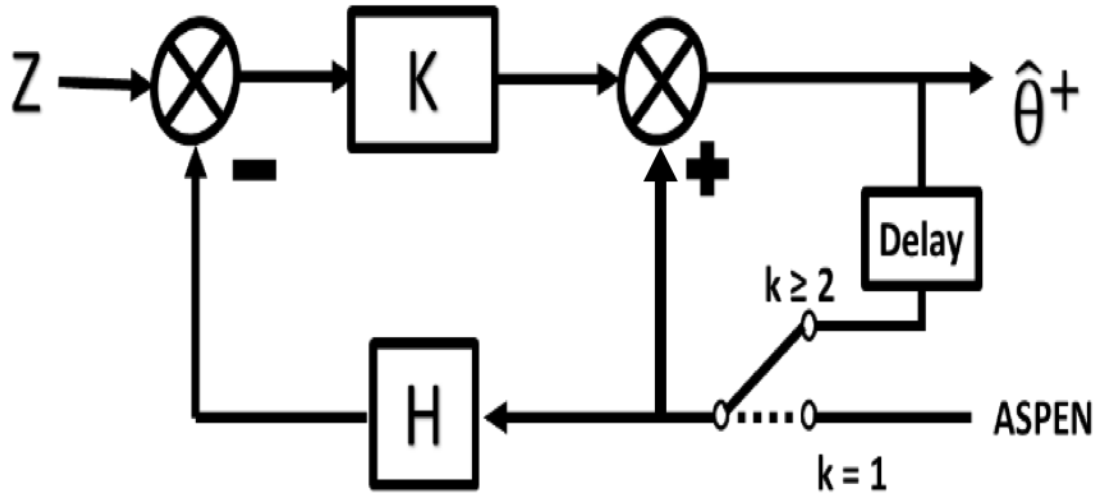


Figure 4.7. Recursive Kalman filter with initial estimates calculated from ASPEN

4.5. Implementation on the Real System

Finally, the RKF algorithm was implemented on the 500 kV transmission line with PMUs installed at both ends. PMU data are collected over 38 consecutive days for the time-period 7 AM to 8 AM. Since line parameters did not change significantly over this time-period, the consistency of the estimates was taken as a metric for validation. Each dataset consisted of a one-hour duration of PMU data measured at 30 samples per second. The initial estimates were calculated utilizing ASPEN data from utility database employing (4.8) - (4.9) and fed to RKF for final estimation. The parameters are estimated using symmetrical formulation as well as unsymmetrical formulation and the results are summarized in Figures 4.8-4.15. It can be observed that the estimated parameters lie in a narrow band. From the narrowness of

the band, it can be concluded that RKF algorithm in conjunction with ASPEN data was able to estimate the line parameters *consistently*.

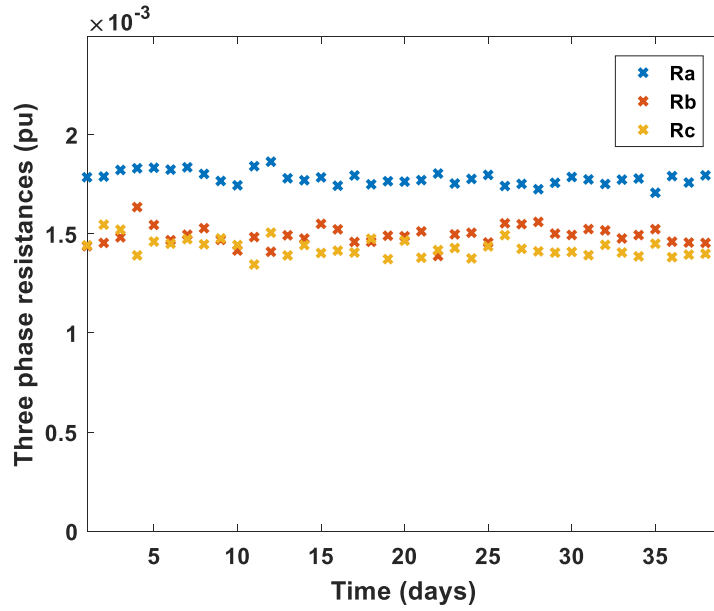


Figure 4.8. Estimated three-phase resistance using symmetrical formulation

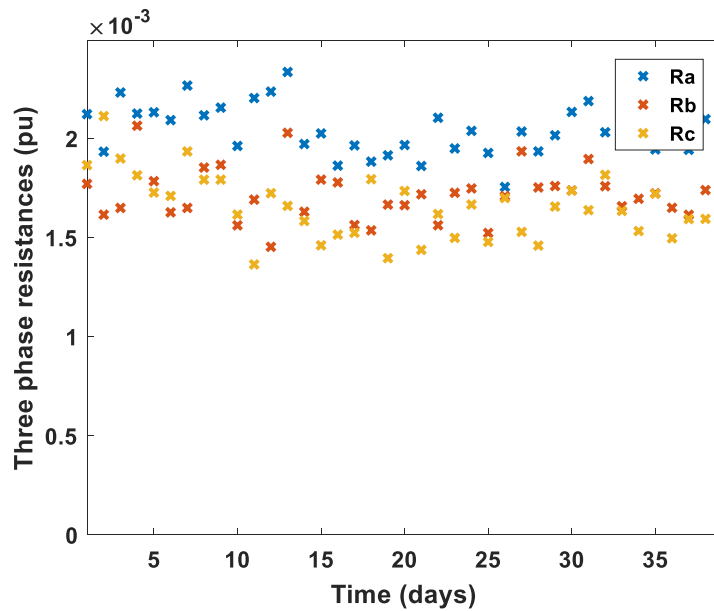


Figure 4.9. Estimated three-phase resistance using unsymmetrical formulation

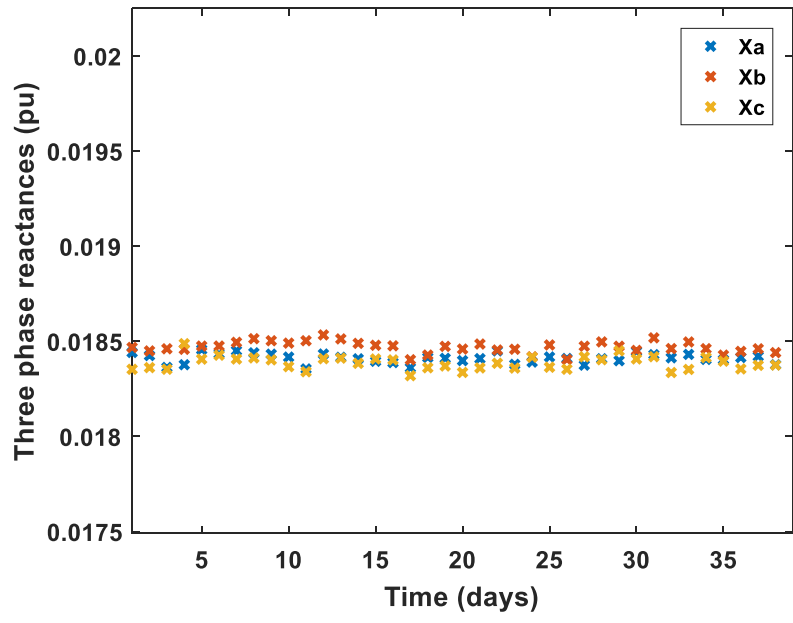


Figure 4.10. Estimated three-phase reactance using symmetrical formulation

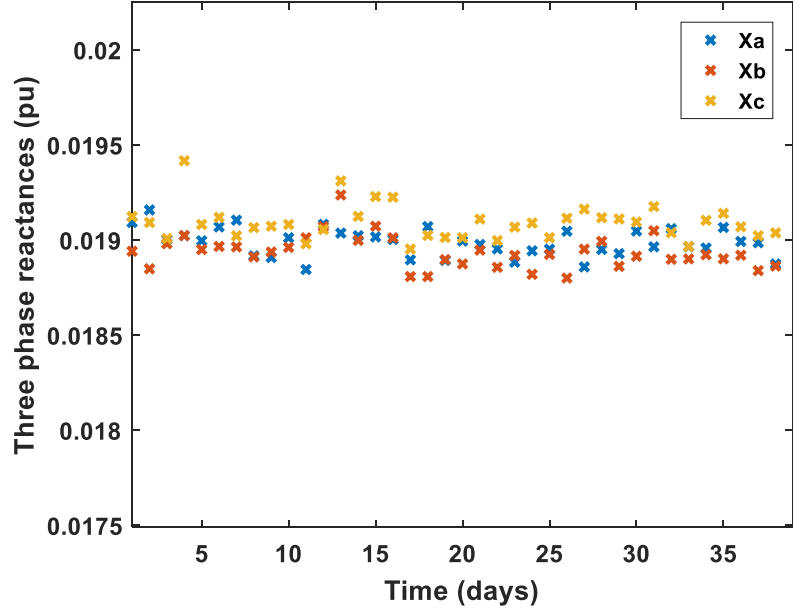


Figure 4.11. Estimated three-phase reactance using unsymmetrical formulation

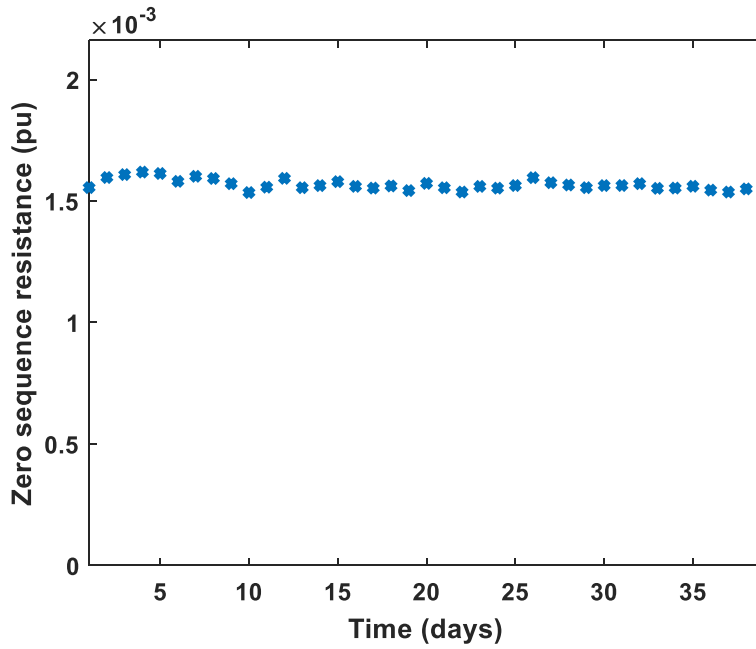


Figure 4.12. Estimated zero-sequence resistance using symmetrical formulation

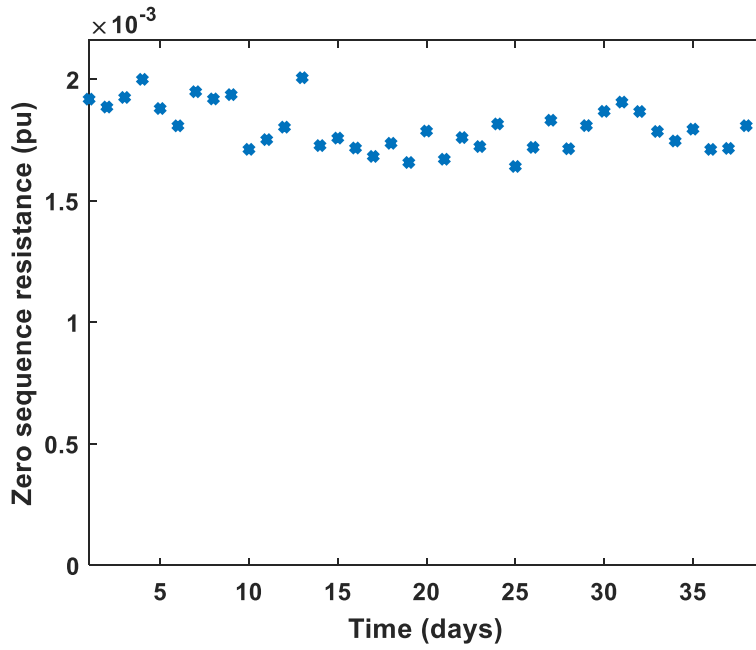


Figure 4.13. Estimated zero-sequence resistance using unsymmetrical formulation

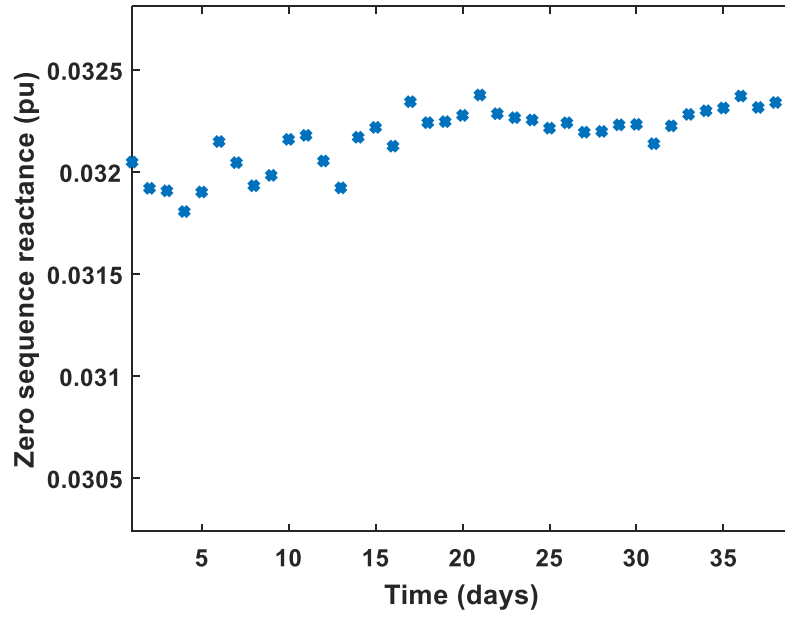


Figure 4.14. Estimated zero-sequence reactance using symmetrical formulation

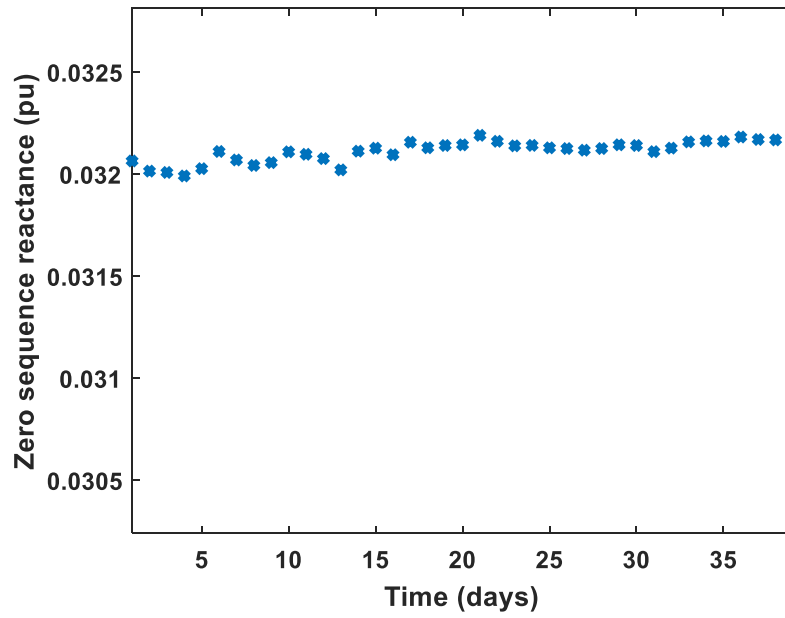


Figure 4.15. Estimated zero-sequence reactance using unsymmetrical formulation

4.5.1. Time Series Analysis of Sequence Impedances

Transmission line parameters are a function of operating conditions and tend to change as the day progresses. Therefore, to study the variation of line parameters, the estimation procedure using the RKF algorithm (symmetrical as well as unsymmetrical formulation) is repeated every hour and the results are presented in Figures 4.16-4.23. It can be observed that the algorithm was able to capture the variation in line parameters with time. Further, it can be inferred that the number of outliers in the unsymmetrical formulation is more as compared to the symmetrical formulation. The possible reason could be the increased number of unknowns in the unsymmetrical formulation. Since both the formulations utilized the same sized dataset, as the number of unknowns increased, the accuracy of the unsymmetrical formulation algorithm decreased. Also, it could be that the transmission line under examination was symmetrical and forcing it to not be so, was leading to higher errors.

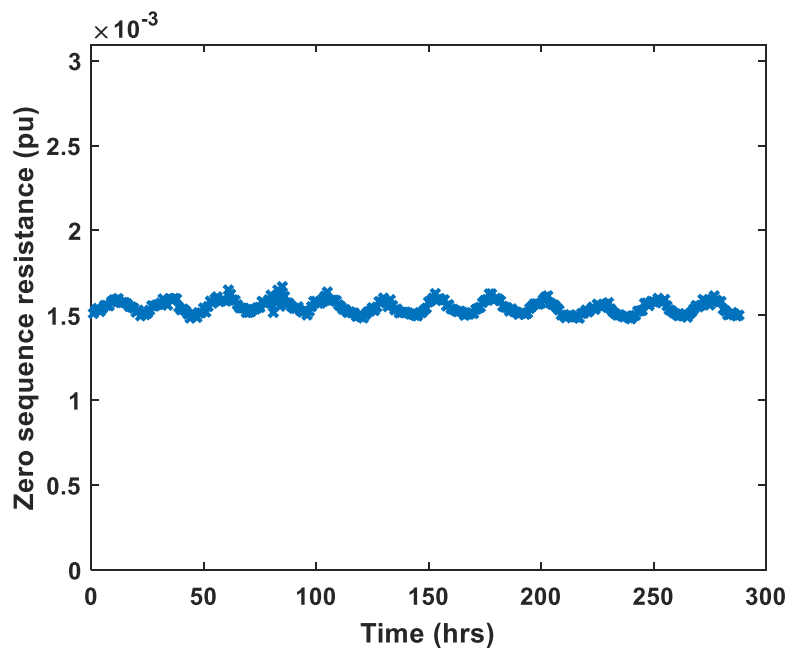


Figure 4.16. Estimated zero-sequence resistance using symmetrical formulation

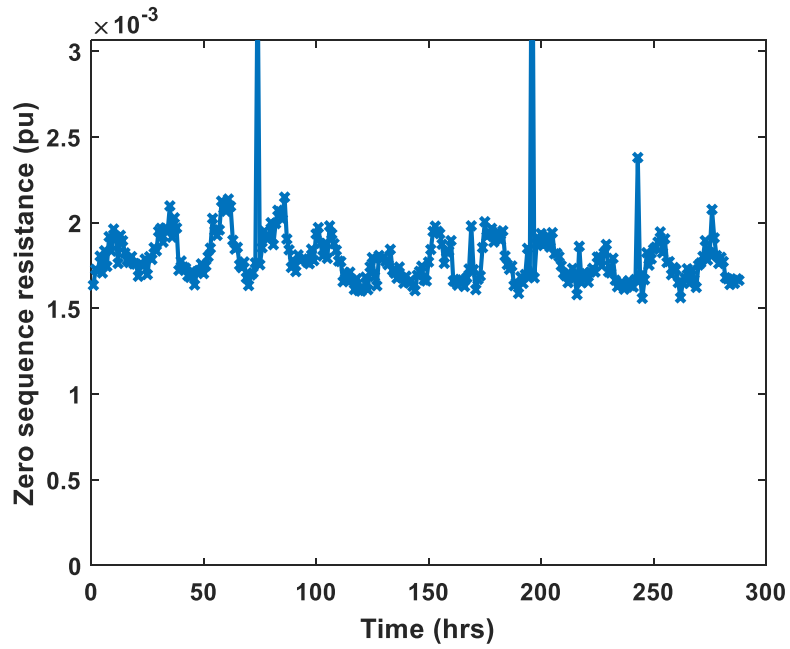


Figure 4.17. Estimated zero-sequence resistance using unsymmetrical formulation

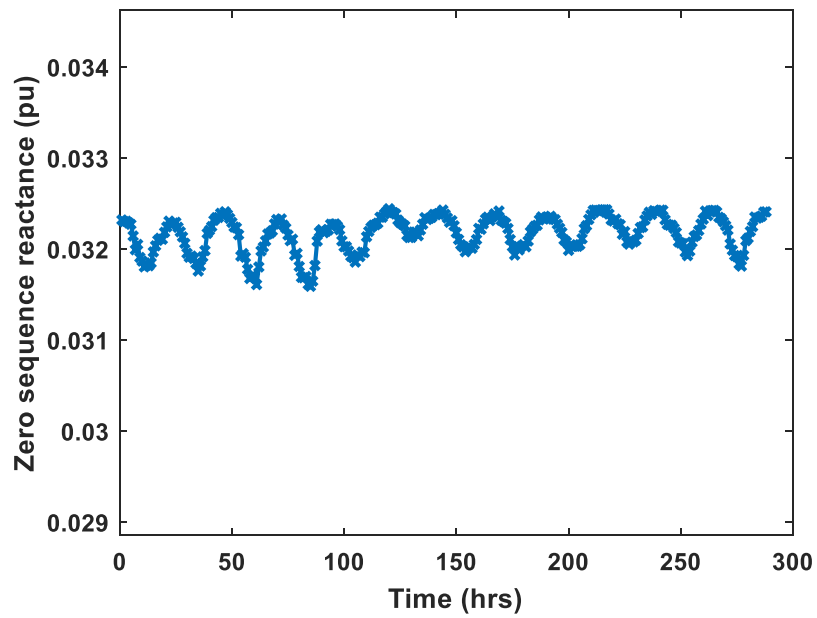


Figure 4.18. Estimated zero-sequence reactance using symmetrical formulation

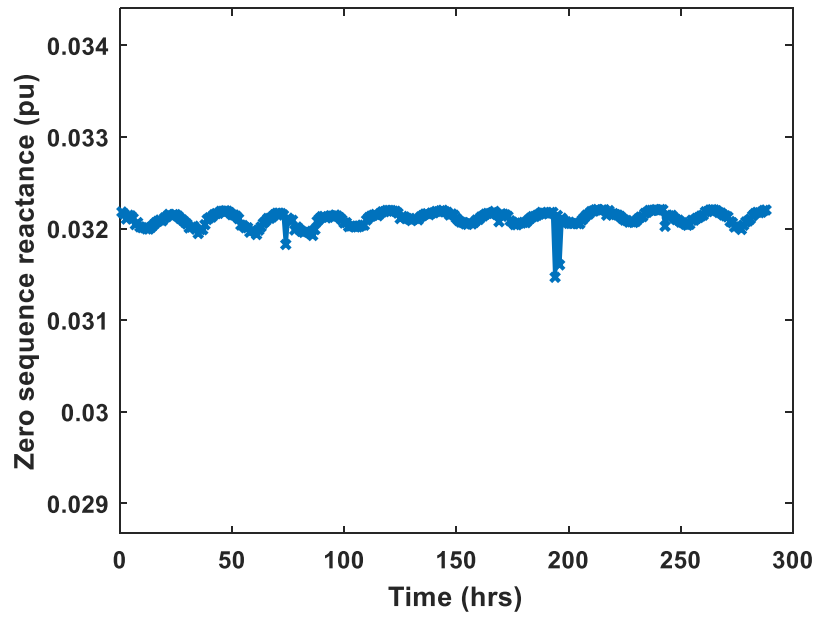


Figure 4.19. Estimated zero-sequence reactance using unsymmetrical formulation

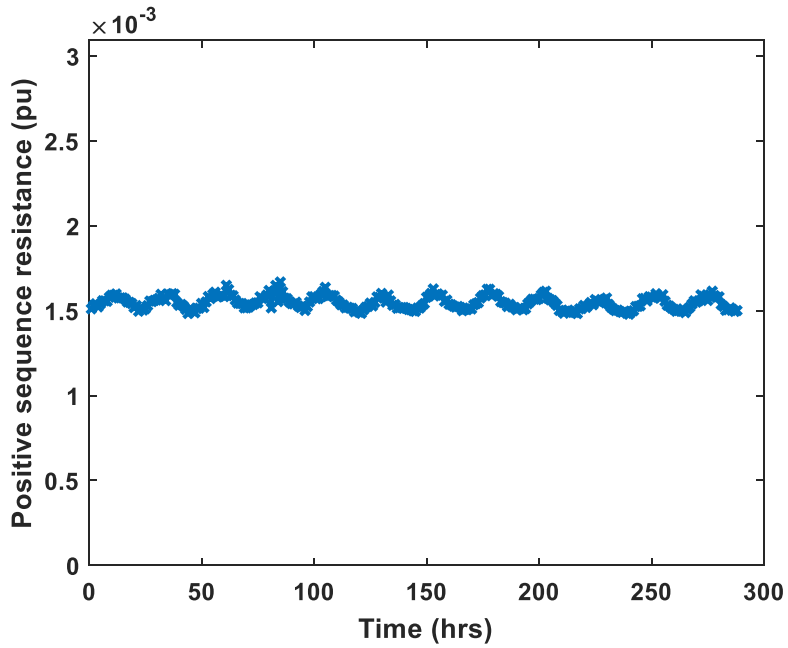


Figure 4.20. Estimated positive-sequence resistance using symmetrical formulation

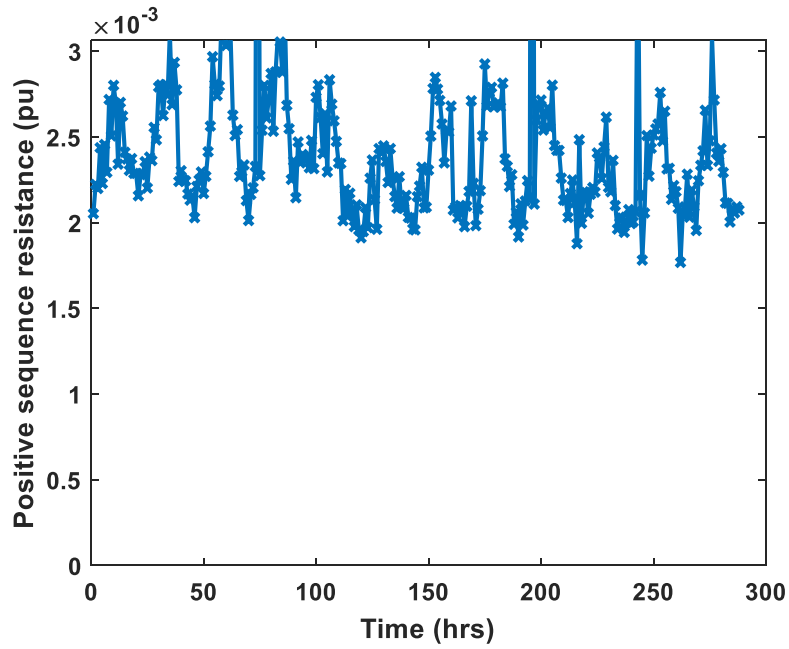


Figure 4.21. Estimated positive-sequence resistance using unsymmetrical formulation

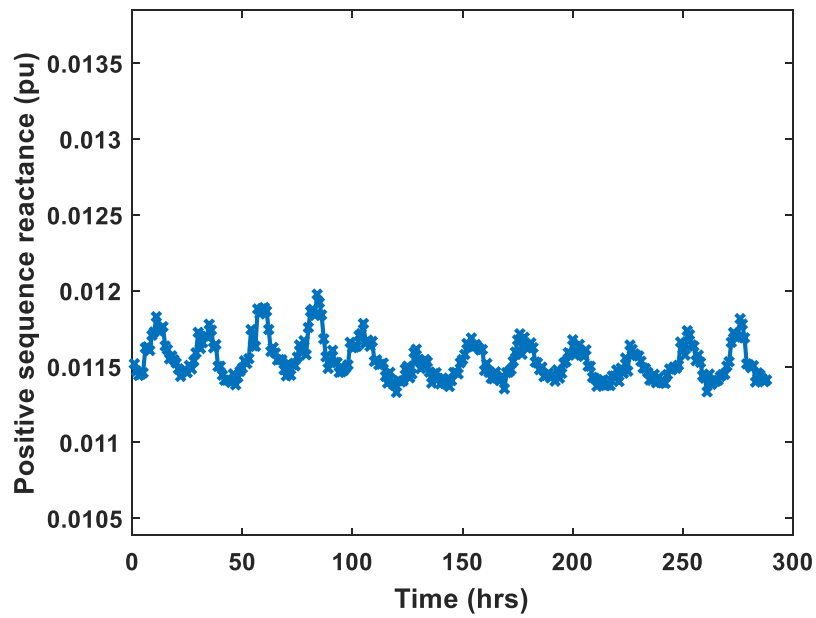


Figure 4.22. Estimated positive-sequence reactance using symmetrical formulation

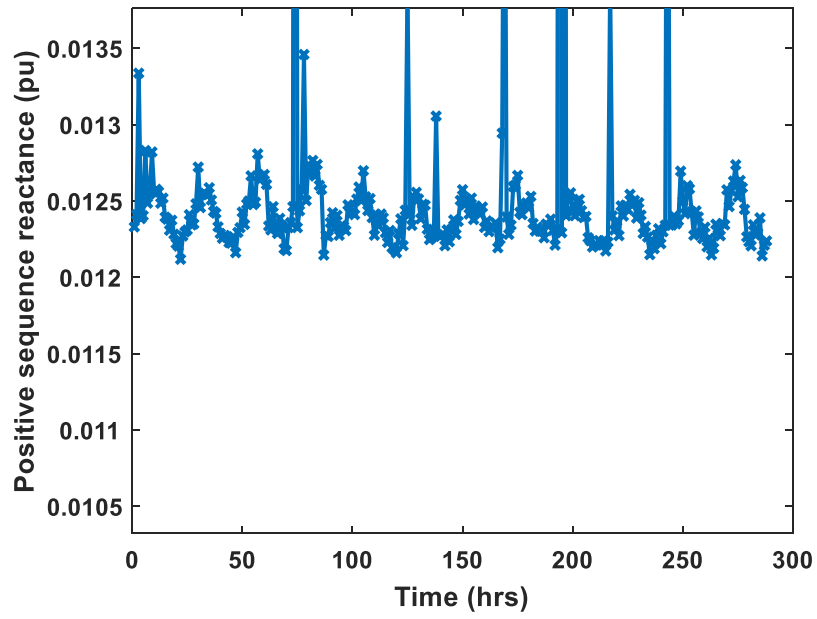


Figure 4.23. Estimated positive-sequence reactance using unsymmetrical formulation

CHAPTER 5

LINE PARAMETER ESTIMATION DURING DATA-DROPOUTS

Power system applications, such as state estimation and dynamic line rating (DLR), utilize line parameters in their analyses as discussed below:

- In state estimation, the network model, line parameters and SCADA (and/or PMU) measurements are used to estimate the complex bus voltages of the system. It is typical to assume line parameters as accurately known for the estimation procedure [47]-[48].
- Dynamic line rating (DLR) is an alternative to static line rating. Typically, static line rating is determined based upon the operating temperature, solar radiation, wind speed, ground clearance, all of which are assumed to be constant [49]. As these assumptions are usually conservative, real-time capacity can be higher than the static rating. As the transmission line parameters are a function of conditions such as temperature, sag (which varies with time) it is imperative that the line parameters, modeled as a function of these time-varying quantities, should be included in the DLR studies [50]-[51].

In Section 4.5.1, the variation of line parameters with time was presented. It can be clearly seen that there is a considerable change in parameters as time progresses. Therefore, it is crucial to include the dependency of line parameter variation with time in power system analysis. However, the applications are limited by the availability of estimated parameters, which in turn is affected by the quality of PMU data. PMUs are occasionally affected by

data losses as discussed in Section 4.1.3. The severity of data dropouts on a typical day for real PMU data can be observed in Figure 5.1. To overcome this problem, transmission line parameters need to be predicted at times of data dropouts using past estimates. Auto Regressive Integrated Moving Average (ARIMA) [52] model can be used for this purpose.

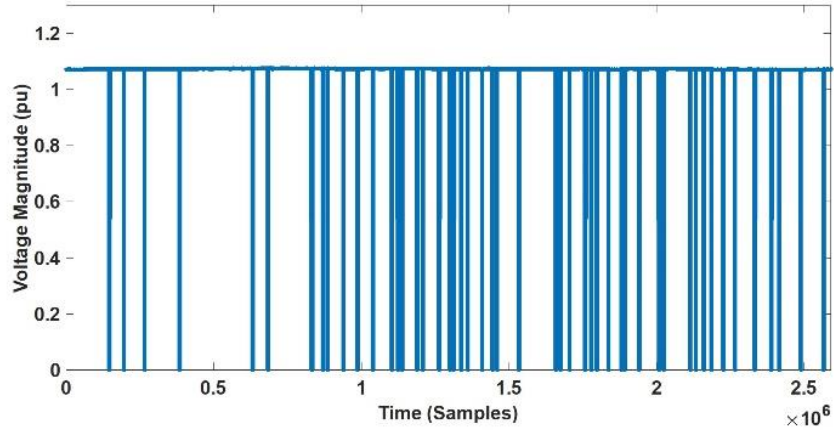


Figure 5.1. Voltage magnitude of a 500 kV transmission line for 24 hours

5.1. Overview of ARIMA

ARIMA models are widely used for time series analysis such as forecasting wind power [53] and electricity prices [54]. Autoregressive component of ARIMA model uses ‘p’ past values to estimate the current value of the time-series. Here, the current value is estimated as a linear combination of previous values [55]. The auto-regressive (AR) model is given by

$$f(B) = 1 - f_1 B^1 - f_2 B^2 - \dots - f_p B^p \quad (5.1)$$

In (5.1), B is the Backshift operator and a_t is the error at time t . On the other hand, moving average model uses a linear combination of white noise in the previous measurements to estimate the present value. The moving average (MA) model is given by

$$g(B) = 1 - g_1 B^1 - g_2 B^2 \dots - g_q B^q \quad (5.2)$$

It is assumed that the orders of AR and MA components are p and q , respectively. The integration component (w_t) of the ARIMA model is used to capture the non-stationary behavior of the parameters and is given by (5.3)-(5.4).

$$w_t = \nabla^d z_t \text{ or } z_t = S^d w_t \quad (5.3)$$

$$S w_t = \sum_{j=0}^{\infty} w_t + w_{t-1} + w_{t-2} + \dots \quad (5.4)$$

An ARIMA model [52] is a combination of auto-regressive, moving average, and integration models, and is given by,

$$f(B)w_t = g(B)a_t \quad (5.5)$$

To design an ARIMA model, the order of auto-regressive, moving average, and integration models must be determined. The order of integration component is the number of times of difference of z_t required to produce a stationary process. On the other hand, the orders of AR and MA components are determined iteratively until the requirements of the accuracy are met. The chosen model is trained using past estimates and percentage of error of predicted values are calculated. If the accuracy of the model is less than the desired value, the procedure is repeated by changing the order of the model.

An independent ARIMA model can be designed for each parameter of interest. Once a data dropout is detected, the model is trained using the estimates up to the time of dropout and is used for forecasting until good data become available.

5.2. Application of ARIMA Models

In this section, the use of ARIMA models to predict the parameter values using past estimates is investigated. The estimation results from the previous section are utilized for this work and a dataset of 372 estimates is created. The dataset is split into two subsets: a training set of 300 estimates, and a testing set comprising of 72 estimates. First, the proposed ARIMA model is used to forecast zero sequence resistance. An ARIMA model of order (80,1,1) is chosen for this analysis. The model is trained in MATLAB using the training dataset and the trained model is used to predict the subsequent 72 estimates (testing dataset). The procedure is repeated for zero-sequence reactance. The zero-sequence impedance was used for this purpose because the power utility was interested in tracking the values of their zero sequence impedances over time.

The forecasted values are compared with the test set and the results are summarized in Figures 5.2-5.3, and Table 5.1. It can be observed from the figures that the zero-sequence resistance varies between 0.9 and 1.2 p.u., while, the zero-sequence reactance varies between 0.995 and 1.005 p.u. As the forecasted error will be small if the parameter variation is low, the accuracy of the forecast of zero sequence resistance is comparatively less in comparison to the zero-sequence reactance. From Table 5.1, it is observed that the mean and median estimation errors are less than 4% and less than 0.2% for zero-sequence resistance and zero-sequence reactance, respectively. Therefore, it can be concluded that

ARIMA models can be successfully used to forecast line parameters from past estimates. An added advantage is that ARIMA model can also be used to detect an outlier in the actual estimation results (highlighted by red ovals in Figures 5.2 and 5.3).

Table 5.1. Results of ARIMA model

Parameter	Mean Error (%)	Median Error (%)
Zero-sequence resistance	3.8654	2.87
Zero-sequence reactance	0.1128	0.10

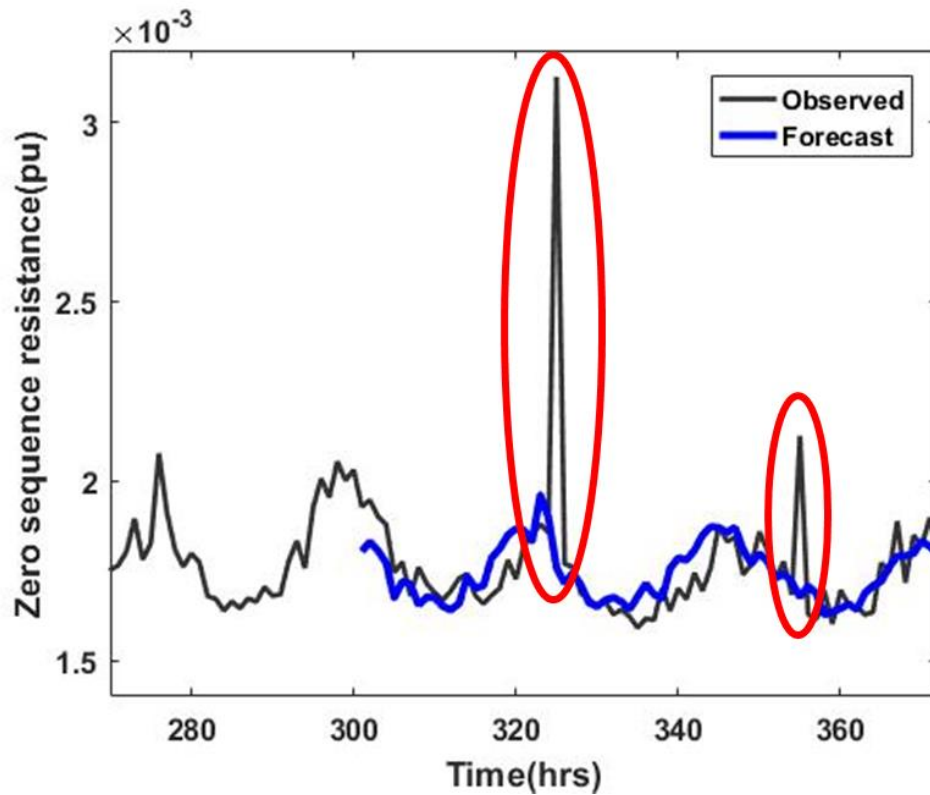


Figure 5.2. Observed and forecasted zero-sequence resistance using ARIMA model; outliers are highlighted by red ovals

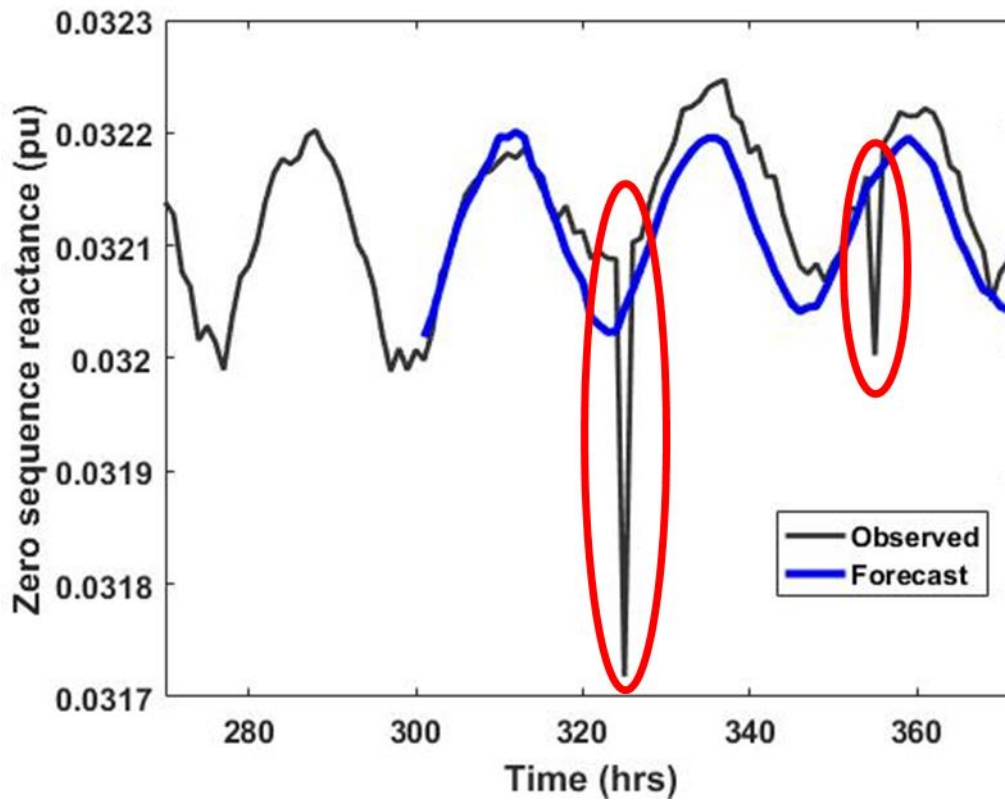


Figure 5.3. Observed and forecasted zero-sequence reactance using ARIMA model; outliers are highlighted by red ovals

CHAPTER 6

CONCLUSION & FUTURE SCOPE

6.1. Conclusion

Transmission line parameters, in general, and zero-sequence impedance, in particular, play an important role in power systems operations, control, and protection. Online methods for transmission line parameter estimation using synchrophasor data were investigated in this work. Two popular algorithms for parameter estimation problems, namely, MWTLS and RKF were selected. The algorithms were tested on a synthetic dataset generated in MATLAB and it was concluded that the algorithms can estimate the line parameters with less than 2% error.

In the next stage, a pseudo-synthetic dataset was generated using PMU data and the algorithms were re-applied. The results showed that the performance of RKF was better than MWTLS. In addition, it was observed that the accuracy of the estimates was sensitive to noise in the voltage measurements. After a thorough investigation, it was found that the variation of voltages with time was small because utilities maintained their voltages close to 1 p.u., which led to the problem becoming ill-conditioned. As a result, the effect of noise on the accuracy of the results was magnified.

One way to improve the accuracy of the estimates was by providing an improved initial estimate. Therefore, for the third stage, the RKF algorithm with initial estimates obtained from ASPEN data was implemented on a 500 kV transmission line operated by a local utility. The estimation procedure was repeated over a period of one month and the results

were documented. The estimation results proved that the algorithm was able to estimate the zero-sequence impedance consistently. Furthermore, it was able to follow the variation of line parameters over the course of a day.

Lastly, an auto regressive integrated moving average (ARIMA) model was implemented to predict the variations in sequence impedances during data dropouts. The simulation results indicated that the mean and median estimation errors were less than 4% and 0.2% for zero-sequence resistance and zero-sequence reactance, respectively. Additionally, ARIMA model was capable of detecting outliers in the estimates.

6.2. Future Scope

In this work, focus has only been on the noises added by the PMUs themselves, and not those that are added by the instrument transformers (ITs). The transformation ratios associated with each IT can change with time introducing additional errors into the measurements. Therefore, these additional errors must be accounted for, to increase the estimation accuracy.

Several methods were proposed in recent years to estimate the line parameters considering instrument transformer errors. In [56], the physical behavior of the conductor is used to determine the positive sequence parameters on laboratory datasets considering instrument transformer errors. In [44], an iterative algorithm is employed to estimate positive sequence parameters of a distribution network using MATLAB simulations. In [45], a robust estimator insensitive to bad data are used to estimate three-phase line parameters. However, it was tested on a fully transposed line and it required a minimum of 10% loading which

may not be possible in real-life. It can be observed that current work either focuses on positive sequence or is not sufficiently validated using field data. Therefore, the algorithms for three-phase line parameter estimation considering PMU errors as well as instrument transformer errors need further attention and extensive testing before they are applied in practice.

REFERENCES

- [1] J. A. P. Lopes, F. J. Soares and P. M. R. Almeida, "Integration of electric vehicles in the electric power system," in *Proc. IEEE*, vol. 99, no. 1, pp. 168-183, Jan. 2011.
- [2] P. Denholm, W. Short, "An evaluation of utility system impacts and benefits of optimally dispatched plug-in hybrid electric vehicles," Oct. 2006, [Online]. Available: <https://www.nrel.gov/docs/fy07osti/40293.pdf>.
- [3] G. G. Karady, K. E. Holbert, *Electrical Energy Conversion and Transport: An Interactive Computer-Based Approach*, 2nd ed., New York: John Wiley & Sons, 2005.
- [4] J. R. Carson, "Wave propagation in overhead wires with ground return," *Bell Syst. Tech. J.*, vol. 5, no. 4, pp. 539-554, Oct. 1926.
- [5] J. D. Glover, M. S. Sarma, T. J. Overbye, *Power System Analysis and Design*, 4th ed., Canada, ON, Toronto, Thomson, 2008.
- [6] A. G. Phadke, "Synchronized phasor measurements-a historical overview," in *Proc. IEEE/PES Transmission and Distribution Conf. and Exhibition*, Yokohama, Japan, vol.1, pp. 476-479, Oct. 2002.
- [7] K. D. Jones, A. Pal and J. S. Thorp, "Methodology for performing synchrophasor data conditioning and validation," *IEEE Trans. on Power Syst.*, vol. 30, no. 3, pp. 1121-1130, May 2015.
- [8] A. Pal, G. A. Sanchez-Ayala, V. A. Centeno and J. S. Thorp, "A PMU placement scheme ensuring real-time monitoring of critical buses of the network," in *IEEE Trans. on Power Del.*, vol. 29, no. 2, pp. 510-517, April 2014.
- [9] M. Li, A. Pal, A. G. Phadke, J. S. Thorp, "Transient stability prediction based on apparent impedance trajectory recorded by PMUs," *Int. J. Elect. Power Energy Syst.*, vol. 54, pp. 498-504, Jan. 2014.
- [10] C. Mishra, K. D. Jones, A. Pal and V. A. Centeno, "Binary particle swarm optimisation-based optimal substation coverage algorithm for phasor measurement unit installations in practical systems," *IET Generation, Transmission & Distribution*, vol. 10, no. 2, pp. 555-562, Feb. 2016.
- [11] A. Pal, A. K. S. Vullikanti and S. S. Ravi, "A PMU placement scheme considering realistic costs and modern trends in relaying," *IEEE Trans. on Power Syst.*, vol. 32, no. 1, pp. 552-561, Jan. 2017.

- [12] A. G. Phadke, J. S. Thorp, *Synchronized Phasor Measurements and Their Applications*, New York: Springer, 2008.
- [13] A. Pal, C. Mishra, A. K. S. Vullikanti and S. S. Ravi, "General optimal substation coverage algorithm for phasor measurement unit placement in practical systems," *IET Generation, Transmission & Distribution*, vol. 11, no. 2, pp. 347-353, Jan. 2017.
- [14] G. A. Sanchez, A. Pal, V. A. Centeno, W. C. Flores, "PMU placement for the Central American power network and its possible impacts," in *Proc. IEEE Power Eng. Soc. Conf. Innovative Smart Grid Technol.*, pp. 1-7, Oct. 2011.
- [15] A. Pal, G. A. Sanchez-Ayala, J. S. Thorp, V. A. Centeno, "A community-based partitioning approach for PMU placement in large systems," *Electr. Power Compon. Syst.* 44, no. 12, pp. 1317 -1329, Jul. 2016.
- [16] A. Pal, I. Singh and B. Bhargava, "Stress assessment in power systems and its visualization using synchrophasor based metrics," in *Proc. North American Power Symposium (NAPS)*, Pullman, WA, pp. 1-6, Sept. 2014.
- [17] Pal, Anamitra, "PMU-based applications for improved monitoring and protection of power systems," PhD dissertation, Dept. Elect. Eng., Virginia Tech, Blacksburg, VA, 2014.
- [18] V. Chakati, M. Pore, A. Pal, A. Banerjee and S. K. S. Gupta, "Challenges and trade-offs of a cloud hosted phasor measurement unit-based linear state estimator," in *Proc. IEEE Power & Eng. Soc. Innovative Smart Grid Technol. Conf. (ISGT)*, Washington, DC, pp. 1-5, Oct 2017.
- [19] NASPI, "Synchrophasor fact sheet", Oct. 2014 [Online] Available: https://www.naspi.org/sites/default/files/reference_documents/33.pdf?fileID=1326A.
- [20] C. S. Chen, C. W. Liu, and J. A. Jiang, "A new adaptive PMU based protection scheme for transposed/untransposed parallel transmission lines," *IEEE Trans. Power Del.*, vol. 17, no. 2, pp. 395-404, Apr. 2002.
- [21] J.A. Jiang, J.Z. Yang, Y.H. Lin, C.W. Liu, and J.C. Ma, "An adaptive PMU based fault detection/location technique for transmission lines. I. theory and algorithms," *IEEE Trans. Power Del.*, vol. 15, no. 2, pp. 486-493, Apr. 2000.
- [22] S. V. Unde and S. S. Dambhare, "Double circuit transmission line parameter estimation using PMU," in *Proc. IEEE 6th Int. Conf. Power Syst.*, New Delhi, India, pp. 1-4, Jan. 2016.

- [23] M. Kato, T. Hisakado, H. Takani, H. Umezaki, and K. Sekiguchi, "Live line measurement of untransposed three phase transmission line parameters for relay settings," in *Proc. IEEE Power Eng. Soc. Gen. Meeting*, Minneapolis, MN, pp. 1-8, Jul. 2010.
- [24] Y. Liao and M. Kezunovic, "Online optimal transmission line parameter estimation for relaying applications," *IEEE Trans. Power Del.*, vol. 24, no. 1, pp. 96-102, Jan. 2009.
- [25] H. K. Karegar and B. Alinejad, "On-line transmission line zero sequence impedance estimation using phasor measurement units," in *Proc. 22nd Australasian Universities Power Eng. Conf.*, Bali, pp. 1-5, Sep 2012.
- [26] Z. Wu, L. T. Zora, and A. G. Phadke, "Simultaneous transmission line parameter and PMU measurement calibration," in *Proc. IEEE Power Eng. Soc. Gen. Meeting*, Denver, CO, pp. 1-5, Jul. 2015.
- [27] D. Shi, D. J. Tylavsky, N. Logic, K. M. Koellner, and D. Wheeler, "Transmission line parameter identification using PMU measurements," *Eur. Trans. Electr. Power*, vol. 21, no. 4, pp. 1574-1588, May 2011.
- [28] L. Ding, T. Bi, and D. Zhang, "Transmission line parameters identification based on moving-window tls and pmu data," in *Proc. Int. Conf. Advanced Power Syst. Automation Protection*, Beijing, China, pp. 2187-2191, Oct. 2011.
- [29] C. Mishra, A. Pal, and V. A. Centeno, "Kalman-filter based recursive regression for three-phase line parameter estimation using phasor measurements," in *Proc. IEEE Power Eng. Soc. Gen. Meeting*, Denver, CO, pp. 1-5, Jul. 2015.
- [30] D. Simon, *Optimal State Estimation*, 1st ed., New York: John Wiley & Sons, 2006.
- [31] A. Pal, P. Chatterjee, J. S. Thorp and V. A. Centeno, "Online calibration of voltage transformers using synchrophasor measurements," in *IEEE Trans. Power Del.*, vol. 31, no. 1, pp. 370-380, Feb. 2016.
- [32] Z. Wu, K. Thomas, R. Sun, V. A. Centeno and A. G. Phadke, "Three-phase instrument transformer calibration with synchronized phasor measurements," in *Proc. IEEE PES Innovative Smart Grid Technologies (ISGT)*, Washington, DC, pp. 1-6, Jan. 2012.
- [33] P. Chatterjee, A. Pal, J. S. Thorp, J. De La Ree Lopez and V. A. Centeno, "Error reduction of phasor measurement unit data considering practical constraints," *IET Generation, Transmission & Distribution*, vol. 12, no. 10, pp. 2332-2339, May 2018.

- [34] G. H. Golub, "Some modified matrix eigenvalue problems," *SIAM Rev.*, vol. 15, pp. 318-334, 1973.
- [35] I. Markovsky, S. Van Huffel, "Overview of total least-squares methods," *Signal Process.*, vol. 87, no. 10, pp. 2283-2302, Oct. 2007.
- [36] G. Golub, P. Hansen, D. O'leary, "Tikhonov regularization and total least squares," *SIM J. Matrix Analysis Applications*, no. 1, pp. 185-194, Aug. 1999.
- [37] G. H. Golub, C. F. VanLoan, "An analysis of the total least squares problem," *SIAM J. Num. Anal.*, vol. 17, pp. 883-893, Dec. 1980.
- [38] D. Boley, E. Steinmetz, K. T. Sutherland, "Recursive total least squares: an alternative to using the discrete Kalman filter in robot navigation," *Lecture Notes Artificial Intelligence*, vol. 25, pp. 221-234, 1995.
- [39] C. Hajiyev, "Kalman filter for estimation of a linear regression model with account of the regression vector error and its application to calibration of measuring instruments," *Key Eng. Materials*, vol. 381-382, pp. 557-560, June 2008.
- [40] "MATLAB – MathWorks," *MathWorks - MATLAB & Simulink*, 2017, [online] Available: www.mathworks.com/products/matlab.html.
- [41] NASPI, "PMU data quality: a framework for the attributes of pmu data quality and quality impacts to synchrophasor applications," 2017, [online] Available: https://www.naspi.org/sites/default/files/reference_documents/PARTF_WhitePaper_2_0170314_Final_PNNL_26313.pdf.
- [42] Huang, Can, et al. "Data quality issues for synchrophasor applications part I: a review," *J. of Modern Power Syst. and Clean Energy*, vol. 4, no. 3, pp. 342-352, July 2016.
- [43] Huang, Can, et al. "Data quality issues for synchrophasor applications part II: problem formulation and potential solutions," *J. of Modern Power Syst. and Clean Energy*, vol. 4, no. 3, pp. 353-361, July 2016.
- [44] Yao, Wenxuan, et al. "GPS signal loss in the wide area monitoring system: prevalence, impact, and solution," *Elec. Power Syst. Res.*, vol. 147, pp. 254-262, 2017.
- [45] NASPI, "Phase angle calculations: considerations and use cases," 2016, [online] Available: https://www.naspi.org/sites/default/files/reference_documents/naspi_2016_tr_006_phase_angle_calculations_final.pdf.

- [46] G. Phadke and J. S. Thorp, *Computer Relaying for Power Systems*, 2nd ed., New York: John Wiley & Sons, 2009.
- [47] A. Abur, A. G. Exposito, *Power System State Estimation: Theory and Implementation*, USA, FL, Boca Raton: CRC, 2004.
- [48] A. Monticelli, "Electric power system state estimation," in *Proc. of the IEEE*, vol. 88, no. 2, pp. 262-282, Feb. 2000.
- [49] W. Wang, S. Pinter, "Dynamic line rating systems for transmission lines," Apr. 2014.
- [50] S. R. Jiliusson, "Using PMU measurements to assess dynamic line rating of transmission lines," M.Sc. thesis, Elect. Power Syst. and High Voltage Eng., Aalborg University, Aalborg, Denmark, 2013.
- [51] M. Weibel et al., "Overhead line temperature monitoring pilot project," *CIGRE General Session*, pp. B2-311, Aug. 2006.
- [52] G. E. P. Box, G. M. Jenkins, and G. C. Reinsel, *Time series analysis forecasting and control*, 3rd ed. Englewood Cliffs, NJ: PrenticeHall, 1994.
- [53] P. Chen, T. Pedersen, B. Bak-Jensen, and Z. Chen, "ARIMA-based time series model of stochastic wind power generation," *IEEE Trans. Power Syst.*, vol. 25, no. 2, pp. 667-676, May 2010.
- [54] J. Contreras, R. Espinola, F. J. Nogales, and A. J. Conejo, "ARIMA models to predict next-day electricity prices," *IEEE Trans. Power Syst.*, vol. 18, no. 3, pp. 1014-1020, Aug. 2003.
- [55] R. H. Shumway, D. S. Stoffer, *Time Series Analysis and Its Applications*, New York:Springer-Verlag, 2000.
- [56] D. Ritzmann, J. Rens, P. S. Wright, W. Holderbaum and B. Potter, "A novel approach to noninvasive measurement of overhead line impedance parameters," in *IEEE Trans. on Instrum. and Meas.*, vol. 66, no. 6, pp. 1155-1163, June 2017.
- [57] P. A. Pegoraro, K. Brady, P. Castello, C. Muscas and A. von Meier, "Line impedance estimation based on synchrophasor measurements for power distribution systems," *IEEE Trans. on Instrum. and Meas.*, to be published.
- [58] V. Milojević, S. Čalija, G. Rietveld, M. V. Ačanski and D. Colangelo, "Utilization of PMU measurements for three-phase line parameter estimation in power

systems,” *IEEE Trans. on Instrum. and Meas.*, vol. 67, no. 10, pp. 2453-2462, Oct. 2018.

APPENDIX A

MODIFIED MEASUREMENT COVARIANCE MATRIX FOR SYMMETRICAL FORMULATION

The modified measurement covariance matrix for the calculation of susceptance parameters using symmetrical formulation is presented in this section. If the susceptance parameter matrix to be estimated is denoted by \mathbf{t} , from (2.10), \mathbf{t} is found to be,

$$\mathbf{t} = \boldsymbol{\theta}_{sh} \quad (\text{A. 1})$$

For a Gaussian noise of $N(0, \text{sigv}^2)$, $N(0, \text{sigc}^2)$ in the voltage and current measurements, respectively, the covariance matrix is shown below.

$$\begin{aligned} \mathbf{Rnew}(1,1) = & \text{sigv}^2 [(\mathbf{t}(1) + \mathbf{t}(4) + \mathbf{t}(6))^2 + (\mathbf{t}(7) + \mathbf{t}(10) + \mathbf{t}(12))^2] + \mathbf{t}(4)^2 \\ & + \mathbf{t}(6)^2 + \mathbf{t}(10)^2 + \mathbf{t}(12)^2] + 2 \\ & * \text{sigc}^2 \end{aligned} \quad (\text{A. 2})$$

$$\begin{aligned} \mathbf{Rnew}(2,2) = & \text{sigv}^2 [(\mathbf{t}(2) + \mathbf{t}(4) + \mathbf{t}(5))^2 + (\mathbf{t}(8) + \mathbf{t}(10) + \mathbf{t}(11))^2] \\ & + \mathbf{t}(4)^2 + \mathbf{t}(5)^2 + \mathbf{t}(10)^2 + \mathbf{t}(11)^2] + 2 \\ & * \text{sigc}^2 \end{aligned} \quad (\text{A. 3})$$

$$\begin{aligned} \mathbf{Rnew}(3,3) = & \text{sigv}^2 [(\mathbf{t}(3) + \mathbf{t}(5) + \mathbf{t}(6))^2 + (\mathbf{t}(9) + \mathbf{t}(11) + \mathbf{t}(12))^2] \\ & + \mathbf{t}(5)^2 + \mathbf{t}(6)^2 + \mathbf{t}(11)^2 + \mathbf{t}(12)^2] + 2 \\ & * \text{sigc}^2 \end{aligned} \quad (\text{A. 4})$$

$$\begin{aligned} \mathbf{Rnew}(1,2) = & \text{sigv}^2 [-(\mathbf{t}(1) + \mathbf{t}(4) + \mathbf{t}(6)) * \mathbf{t}(4) - (\mathbf{t}(2) + \mathbf{t}(4) + \mathbf{t}(5)) * \mathbf{t}(4) \\ & + \mathbf{t}(5) * \mathbf{t}(6) - (\mathbf{t}(7) + \mathbf{t}(10) + \mathbf{t}(12)) * \mathbf{t}(10) \\ & - (\mathbf{t}(8) + \mathbf{t}(10) + \mathbf{t}(11)) * \mathbf{t}(10) + \mathbf{t}(11) * \mathbf{t}(12)] \end{aligned} \quad (\text{A. 5})$$

$$\begin{aligned}
\mathbf{Rnew}(1,3) = & \left[-(\mathbf{t}(1) + \mathbf{t}(4) + \mathbf{t}(6)) * \mathbf{t}(6) - (\mathbf{t}(5) + \mathbf{t}(3) + \mathbf{t}(6))(6) + \mathbf{t}(4) \right. \\
& * \mathbf{t}(5) - (\mathbf{t}(7) + \mathbf{t}(10) + \mathbf{t}(12)) * \mathbf{t}(12) - (\mathbf{t}(11) + \mathbf{t}(9) + \mathbf{t}(12)) \\
& \left. * \mathbf{t}(12) + \mathbf{t}(10) * \mathbf{t}(11) \right] * \text{sigv}^2 \tag{A.6}
\end{aligned}$$

$$\begin{aligned}
\mathbf{Rnew}(2,3) = & \left[-(\mathbf{t}(2) + \mathbf{t}(4) + \mathbf{t}(5)) * \mathbf{t}(5) - (\mathbf{t}(3) + \mathbf{t}(5) + \mathbf{t}(6)) * \mathbf{t}(5) + \mathbf{t}(4) \right. \\
& * \mathbf{t}(6) - (\mathbf{t}(8) + \mathbf{t}(10) + \mathbf{t}(11)) * \mathbf{t}(11) - (\mathbf{t}(9) + \mathbf{t}(11) + \mathbf{t}(12)) \\
& \left. * \mathbf{t}(11) + \mathbf{t}(10) * \mathbf{t}(12) \right] * \text{sigv}^2 \tag{A.7}
\end{aligned}$$

$$\mathbf{Rnew}(2,1) = \mathbf{Rnew}(1,2) \tag{A.8}$$

$$\mathbf{Rnew}(3,1) = \mathbf{Rnew}(1,3) \tag{A.9}$$

$$\mathbf{Rnew}(3,2) = \mathbf{Rnew}(2,3) \tag{A.10}$$

Let the impedance parameter matrix to be estimated be denoted by \mathbf{t} . Then, from (2.12), \mathbf{t} is found to be,

$$\mathbf{t} = \begin{bmatrix} \text{real}(\boldsymbol{\theta}_{se}) \\ \text{imag}(\boldsymbol{\theta}_{se}) \end{bmatrix} \tag{A.11}$$

The modified measurement covariance matrix for the calculation of impedance parameters using symmetrical formulation is presented below.

$$\begin{aligned}
\mathbf{Rnewimp}(1,1) & = \text{sigc}^2 * (\mathbf{t}(1)^2 + \mathbf{t}(4)^2 + \mathbf{t}(6)^2 + \mathbf{t}(7)^2 + \mathbf{t}(10)^2 + \mathbf{t}(12)^2) - \text{sigv}^2 \\
& * ([\mathbf{t}(1) \ \mathbf{t}(4) \ \mathbf{t}(6)] * \mathbf{Bp} * (\mathbf{Bp})^T * ([\mathbf{t}(1) \ \mathbf{t}(4) \ \mathbf{t}(6)])^T) - \text{sigv}^2 \\
& * ([\mathbf{t}(7) \ \mathbf{t}(10) \ \mathbf{t}(12)] * \mathbf{Bp} * (\mathbf{Bp})^T * ([\mathbf{t}(7) \ \mathbf{t}(10) \ \mathbf{t}(12)])^T) \\
& + \text{sigv}^2 \tag{A.12}
\end{aligned}$$

Rnewimp(1,2)

$$\begin{aligned}
&= \text{sigc}^2 ([\mathbf{t}(1) \ \mathbf{t}(4) \ \mathbf{t}(6) \ \mathbf{t}(7) \ \mathbf{t}(10) \ \mathbf{t}(12)]) \\
&\quad * ([\mathbf{t}(4) \ \mathbf{t}(2) \ \mathbf{t}(5) \ \mathbf{t}(10) \ \mathbf{t}(8) \ \mathbf{t}(11)])^T) - \text{sigv}^2 ([\mathbf{t}(1) \ \mathbf{t}(4) \ \mathbf{t}(6)] \\
&\quad * \mathbf{Bp} * (\mathbf{Bp})^T * ([\mathbf{t}(4) \ \mathbf{t}(2) \ \mathbf{t}(5)])^T) - \text{sigv}^2 ([\mathbf{t}(7) \ \mathbf{t}(10) \ \mathbf{t}(12)] * \mathbf{Bp} \\
&\quad * (\mathbf{Bp})^T * ([\mathbf{t}(10) \ \mathbf{t}(8) \ \mathbf{t}(11)])^T) \tag{A.13}
\end{aligned}$$

Rnewimp(1,3)

$$\begin{aligned}
&= ([\mathbf{t}(1) \ \mathbf{t}(4) \ \mathbf{t}(6) \ \mathbf{t}(7) \ \mathbf{t}(10) \ \mathbf{t}(12)] \\
&\quad * ([\mathbf{t}(6) \ \mathbf{t}(5) \ \mathbf{t}(3) \ \mathbf{t}(12) \ \mathbf{t}(11) \ \mathbf{t}(9)])^T) \text{sigc}^2 - \text{sigv}^2 \\
&\quad * ([\mathbf{t}(1) \ \mathbf{t}(4) \ \mathbf{t}(6)] * \mathbf{Bp} * (\mathbf{Bp})^T * ([\mathbf{t}(6) \ \mathbf{t}(5) \ \mathbf{t}(3)])^T) - \text{sigv}^2 \\
&\quad * ([\mathbf{t}(7) \ \mathbf{t}(10) \ \mathbf{t}(12)] * \mathbf{Bp} * (\mathbf{Bp})^T \\
&\quad * ([\mathbf{t}(12) \ \mathbf{t}(11) \ \mathbf{t}(9)])^T) \tag{A.14}
\end{aligned}$$

Rnewimp(1,4)

$$\begin{aligned}
&= ([\mathbf{t}(1) \ \mathbf{t}(4) \ \mathbf{t}(6) \ -\mathbf{t}(7) \ -\mathbf{t}(10) \ -\mathbf{t}(12)] \\
&\quad * ([\mathbf{t}(7) \ \mathbf{t}(10) \ \mathbf{t}(12) \ \mathbf{t}(1) \ \mathbf{t}(4) \ \mathbf{t}(6)])^T) \text{sigc}^2 - \text{sigv}^2 \\
&\quad * ([\mathbf{t}(1) \ \mathbf{t}(4) \ \mathbf{t}(6)] * \mathbf{Bp} * (\mathbf{Bp})^T * ([\mathbf{t}(7) \ \mathbf{t}(10) \ \mathbf{t}(12)])^T) + \text{sigv}^2 \\
&\quad * ([\mathbf{t}(7) \ \mathbf{t}(10) \ \mathbf{t}(12)] * \mathbf{Bp} * (\mathbf{Bp})^T * ([\mathbf{t}(1) \ \mathbf{t}(4) \ \mathbf{t}(6)])^T) \tag{A.15}
\end{aligned}$$

Rnewimp(1,5)

$$\begin{aligned}
&= ([\mathbf{t}(1) \ \mathbf{t}(4) \ \mathbf{t}(6) \ -\mathbf{t}(7) \ -\mathbf{t}(10) \ -\mathbf{t}(12)] \\
&\quad * ([\mathbf{t}(10) \ \mathbf{t}(8) \ \mathbf{t}(11) \ \mathbf{t}(4) \ \mathbf{t}(2) \ \mathbf{t}(5)])^T) \text{sigc}^2 - \text{sigv}^2 \\
&\quad * ([\mathbf{t}(1) \ \mathbf{t}(4) \ \mathbf{t}(6)] * \mathbf{Bp} * (\mathbf{Bp})^T * ([\mathbf{t}(10) \ \mathbf{t}(8) \ \mathbf{t}(11)])^T) + \text{sigv}^2 \\
&\quad * ([\mathbf{t}(7) \ \mathbf{t}(10) \ \mathbf{t}(12)] * \mathbf{Bp} * (\mathbf{Bp})^T * ([\mathbf{t}(4) \ \mathbf{t}(2) \ \mathbf{t}(5)])^T) \tag{A.16}
\end{aligned}$$

Rnewimp(1,6)

$$\begin{aligned}
&= ([\mathbf{t}(1) \ \mathbf{t}(4) \ \mathbf{t}(6) \ -\mathbf{t}(7) \ -\mathbf{t}(10) \ -\mathbf{t}(12)] \\
&\quad * ([\mathbf{t}(12) \ \mathbf{t}(11) \ \mathbf{t}(9) \ \mathbf{t}(6) \ \mathbf{t}(5) \ \mathbf{t}(3)])^T) \text{sigc}^2 - \text{sigv}^2 \\
&\quad * ([\mathbf{t}(1) \ \mathbf{t}(4) \ \mathbf{t}(6)] * \mathbf{Bp} * (\mathbf{Bp})^T * ([\mathbf{t}(12) \ \mathbf{t}(11) \ \mathbf{t}(9)])^T) + \text{sigv}^2 \\
&\quad * ([\mathbf{t}(7) \ \mathbf{t}(10) \ \mathbf{t}(12)] * \mathbf{Bp} * (\mathbf{Bp})^T \\
&\quad * ([\mathbf{t}(6) \ \mathbf{t}(5) \ \mathbf{t}(3)])^T)
\end{aligned} \tag{A.17}$$

$$\mathbf{Rnewimp}(2,1) = \mathbf{Rnewimp}(1,2) \tag{A.18}$$

Rnewimp(2,2)

$$\begin{aligned}
&= \text{sigc}^2 * (\mathbf{t}(4)^2 + \mathbf{t}(2)^2 + \mathbf{t}(5)^2 + \mathbf{t}(10)^2 + \mathbf{t}(8)^2 + \mathbf{t}(11)^2) - \text{sigv}^2 \\
&\quad * ([\mathbf{t}(4) \ \mathbf{t}(2) \ \mathbf{t}(5)] * \mathbf{Bp} * (\mathbf{Bp})^T * ([\mathbf{t}(4) \ \mathbf{t}(2) \ \mathbf{t}(5)])^T) - \text{sigv}^2 \\
&\quad * ([\mathbf{t}(10) \ \mathbf{t}(8) \ \mathbf{t}(11)] * \mathbf{Bp} * (\mathbf{Bp})^T * ([\mathbf{t}(10) \ \mathbf{t}(8) \ \mathbf{t}(11)])^T) \\
&\quad + \text{sigv}^2
\end{aligned} \tag{A.19}$$

Rnewimp(2,3)

$$\begin{aligned}
&= ([\mathbf{t}(4) \ \mathbf{t}(2) \ \mathbf{t}(5) \ \mathbf{t}(10) \ \mathbf{t}(8) \ \mathbf{t}(11)] \\
&\quad * ([\mathbf{t}(6) \ \mathbf{t}(5) \ \mathbf{t}(3) \ \mathbf{t}(12) \ \mathbf{t}(11) \ \mathbf{t}(9)])^T) \text{sigc}^2 - \text{sigv}^2 \\
&\quad * ([\mathbf{t}(4) \ \mathbf{t}(2) \ \mathbf{t}(5)] * \mathbf{Bp} * (\mathbf{Bp})^T * ([\mathbf{t}(6) \ \mathbf{t}(5) \ \mathbf{t}(3)])^T) - \text{sigv}^2 \\
&\quad * ([\mathbf{t}(10) \ \mathbf{t}(8) \ \mathbf{t}(11)] * \mathbf{Bp} * (\mathbf{Bp})^T \\
&\quad * ([\mathbf{t}(12) \ \mathbf{t}(11) \ \mathbf{t}(9)])^T)
\end{aligned} \tag{A.20}$$

Rnewimp(2,4)

$$\begin{aligned}
&= \text{sigc}^2 * ([\mathbf{t}(4) \ \mathbf{t}(2) \ \mathbf{t}(5) \ -\mathbf{t}(10) \ -\mathbf{t}(8) \ -\mathbf{t}(11)] \\
&* ([\mathbf{t}(7) \ \mathbf{t}(10) \ \mathbf{t}(12) \ \mathbf{t}(1) \ \mathbf{t}(4) \ \mathbf{t}(6)])^T) - \text{sigv}^2 * ([\mathbf{t}(4) \ \mathbf{t}(2) \ \mathbf{t}(5)] \\
&* \mathbf{B}_p * (\mathbf{B}_p)^T * ([\mathbf{t}(7) \ \mathbf{t}(10) \ \mathbf{t}(12)])^T) \\
&+ \text{sigv}^2([\mathbf{t}(10) \ \mathbf{t}(8) \ \mathbf{t}(11)] * \mathbf{B}_p * (\mathbf{B}_p)^T \\
&* ([\mathbf{t}(1) \ \mathbf{t}(4) \ \mathbf{t}(6)])^T)
\end{aligned} \tag{A.21}$$

Rnewimp(2,5)

$$\begin{aligned}
&= ([\mathbf{t}(4) \ \mathbf{t}(2) \ \mathbf{t}(5) \ -\mathbf{t}(10) \ -\mathbf{t}(8) \ -\mathbf{t}(11)] \\
&* ([\mathbf{t}(10) \ \mathbf{t}(8) \ \mathbf{t}(11) \ \mathbf{t}(4) \ \mathbf{t}(2) \ \mathbf{t}(5)])^T) \text{sigc}^2 - \text{sigv}^2 \\
&* ([\mathbf{t}(4) \ \mathbf{t}(2) \ \mathbf{t}(5)] * \mathbf{B}_p * (\mathbf{B}_p)^T * ([\mathbf{t}(10) \ \mathbf{t}(8) \ \mathbf{t}(11)])^T) + \text{sigv}^2 \\
&* ([\mathbf{t}(10) \ \mathbf{t}(8) \ \mathbf{t}(11)] * \mathbf{B}_p * (\mathbf{B}_p)^T \\
&* ([\mathbf{t}(4) \ \mathbf{t}(2) \ \mathbf{t}(5)])^T)
\end{aligned} \tag{A.22}$$

Rnewimp(2,6)

$$\begin{aligned}
&= ([\mathbf{t}(4) \ \mathbf{t}(2) \ \mathbf{t}(5) \ -\mathbf{t}(10) \ -\mathbf{t}(8) \ -\mathbf{t}(11)] \\
&* ([\mathbf{t}(12) \ \mathbf{t}(11) \ \mathbf{t}(9) \ \mathbf{t}(6) \ \mathbf{t}(5) \ \mathbf{t}(3)])^T) \text{sigc}^2 - \text{sigv}^2 \\
&* ([\mathbf{t}(4) \ \mathbf{t}(2) \ \mathbf{t}(5)] * \mathbf{B}_p * (\mathbf{B}_p)^T * ([\mathbf{t}(12) \ \mathbf{t}(11) \ \mathbf{t}(9)])^T) + \text{sigv}^2 \\
&* ([\mathbf{t}(10) \ \mathbf{t}(8) \ \mathbf{t}(11)] * \mathbf{B}_p * (\mathbf{B}_p)^T \\
&* ([\mathbf{t}(6) \ \mathbf{t}(5) \ \mathbf{t}(3)])^T)
\end{aligned} \tag{A.23}$$

$$\mathbf{Rnewimp}(3,1) = \mathbf{Rnewimp}(1,3) \tag{A.24}$$

$$\mathbf{Rnewimp}(3,2) = \mathbf{Rnewimp}(2,3) \tag{A.25}$$

Rnewimp(3,3)

$$\begin{aligned}
&= \text{sigc}^2 * (\mathbf{t}(6)^2 + \mathbf{t}(5)^2 + \mathbf{t}(3)^2 + \mathbf{t}(12)^2 + \mathbf{t}(11)^2 + \mathbf{t}(9)^2) - \text{sigv}^2 \\
&* ([\mathbf{t}(6) \ \mathbf{t}(5) \ \mathbf{t}(3)] * \mathbf{Bp} * (\mathbf{Bp})^T * ([\mathbf{t}(6) \ \mathbf{t}(5) \ \mathbf{t}(3)])^T) - \text{sigv}^2 \\
&* ([\mathbf{t}(12) \ \mathbf{t}(11) \ \mathbf{t}(9)] * \mathbf{Bp} * (\mathbf{Bp})^T * ([\mathbf{t}(12) \ \mathbf{t}(11) \ \mathbf{t}(9)])^T) \\
&+ \text{sigv}^2 \tag{A. 26}
\end{aligned}$$

Rnewimp(3,4)

$$\begin{aligned}
&= ([\mathbf{t}(6) \ \mathbf{t}(5) \ \mathbf{t}(3) \ - \ \mathbf{t}(12) \ - \ \mathbf{t}(11) \ - \ \mathbf{t}(9)] \\
&* ([\mathbf{t}(7) \ \mathbf{t}(10) \ \mathbf{t}(12) \ \mathbf{t}(1) \ \mathbf{t}(4) \ \mathbf{t}(6)])^T) \text{sigc}^2 - \text{sigv}^2 \\
&* ([\mathbf{t}(6) \ \mathbf{t}(5) \ \mathbf{t}(3)] * \mathbf{Bp} * (\mathbf{Bp})^T * ([\mathbf{t}(7) \ \mathbf{t}(10) \ \mathbf{t}(12)])^T) + \text{sigv}^2 \\
&* ([\mathbf{t}(12) \ \mathbf{t}(11) \ \mathbf{t}(9)] * \mathbf{Bp} * ([\mathbf{t}(1) \ \mathbf{t}(4) \ \mathbf{t}(6)])^T) \tag{A. 27}
\end{aligned}$$

Rnewimp(3,5)

$$\begin{aligned}
&= ([\mathbf{t}(6) \ \mathbf{t}(5) \ \mathbf{t}(3) \ - \ \mathbf{t}(12) \ - \ \mathbf{t}(11) \ - \ \mathbf{t}(9)] \\
&* ([\mathbf{t}(10) \ \mathbf{t}(8) \ \mathbf{t}(11) \ \mathbf{t}(4) \ \mathbf{t}(2) \ \mathbf{t}(5)])^T) \text{sigc}^2 - \text{sigv}^2 \\
&* ([\mathbf{t}(6) \ \mathbf{t}(5) \ \mathbf{t}(3)] * \mathbf{Bp} * (\mathbf{Bp})^T * ([\mathbf{t}(10) \ \mathbf{t}(8) \ \mathbf{t}(11)])^T) + \text{sigv}^2 \\
&* ([\mathbf{t}(12) \ \mathbf{t}(11) \ \mathbf{t}(9)] * \mathbf{Bp} * (\mathbf{Bp})^T * ([\mathbf{t}(4) \ \mathbf{t}(2) \ \mathbf{t}(5)])^T) \tag{A. 28}
\end{aligned}$$

Rnewimp(3,6)

$$\begin{aligned}
&= ([\mathbf{t}(6) \ \mathbf{t}(5) \ \mathbf{t}(3) \ - \ \mathbf{t}(12) \ - \ \mathbf{t}(11) \ - \ \mathbf{t}(9)] \\
&* ([\mathbf{t}(12) \ \mathbf{t}(11) \ \mathbf{t}(9) \ \mathbf{t}(6) \ \mathbf{t}(5) \ \mathbf{t}(3)])^T) \text{sigc}^2 - \text{sigv}^2 \\
&* ([\mathbf{t}(6) \ \mathbf{t}(5) \ \mathbf{t}(3)] * \mathbf{Bp} * (\mathbf{Bp})^T * ([\mathbf{t}(12) \ \mathbf{t}(11) \ \mathbf{t}(9)])^T) + \text{sigv}^2 \\
&* ([\mathbf{t}(12) \ \mathbf{t}(11) \ \mathbf{t}(9)] * \mathbf{Bp} * (\mathbf{Bp})^T * ([\mathbf{t}(6) \ \mathbf{t}(5) \ \mathbf{t}(3)])^T) \tag{A. 29}
\end{aligned}$$

$$\mathbf{Rnewimp}(4,1) = \mathbf{Rnewimp}(1,4) \tag{A. 30}$$

$$\mathbf{Rnewimp}(4,2) = \mathbf{Rnewimp}(2,4) \quad (\text{A. 31})$$

$$\mathbf{Rnewimp}(4,3) = \mathbf{Rnewimp}(3,4) \quad (\text{A. 32})$$

$$\mathbf{Rnewimp}(4,4) = \mathbf{Rnewimp}(1,1) \quad (\text{A. 33})$$

$$\mathbf{Rnewimp}(4,5)$$

$$\begin{aligned} &= ([\mathbf{t}(7) \ \mathbf{t}(10) \ \mathbf{t}(12) \ \mathbf{t}(1) \ \mathbf{t}(4) \ \mathbf{t}(6)] \\ &\quad * ([\mathbf{t}(10) \ \mathbf{t}(8) \ \mathbf{t}(11) \ \mathbf{t}(4) \ \mathbf{t}(2) \ \mathbf{t}(5)])^T) \text{sigc}^2 - \text{sigv}^2 \\ &\quad * ([\mathbf{t}(7) \ \mathbf{t}(10) \ \mathbf{t}(12)] * \mathbf{Bp} * (\mathbf{Bp})^T * ([\mathbf{t}(10) \ \mathbf{t}(8) \ \mathbf{t}(11)])^T) - \text{sigv}^2 \\ &\quad * ([\mathbf{t}(1) \ \mathbf{t}(4) \ \mathbf{t}(6)] * \mathbf{Bp} * (\mathbf{Bp})^T * ([\mathbf{t}(4) \ \mathbf{t}(2) \ \mathbf{t}(5)])^T) \end{aligned} \quad (\text{A. 34})$$

$$\mathbf{Rnewimp}(4,6)$$

$$\begin{aligned} &= ([\mathbf{t}(7) \ \mathbf{t}(10) \ \mathbf{t}(12) \ \mathbf{t}(1) \ \mathbf{t}(4) \ \mathbf{t}(6)] \\ &\quad * ([\mathbf{t}(12) \ \mathbf{t}(11) \ \mathbf{t}(9) \ \mathbf{t}(6) \ \mathbf{t}(5) \ \mathbf{t}(3)])^T) \text{sigc}^2 - \text{sigv}^2 \\ &\quad * ([\mathbf{t}(7) \ \mathbf{t}(10) \ \mathbf{t}(12)] * \mathbf{Bp} * (\mathbf{Bp})^T * ([\mathbf{t}(12) \ \mathbf{t}(11) \ \mathbf{t}(9)])^T) - \text{sigv}^2 \\ &\quad * ([\mathbf{t}(1) \ \mathbf{t}(4) \ \mathbf{t}(6)] * \mathbf{Bp} * (\mathbf{Bp})^T * ([\mathbf{t}(6) \ \mathbf{t}(5) \ \mathbf{t}(3)])^T) \end{aligned} \quad (\text{A. 35})$$

$$\mathbf{Rnewimp}(5,1) = \mathbf{Rnewimp}(1,5) \quad (\text{A. 36})$$

$$\mathbf{Rnewimp}(5,2) = \mathbf{Rnewimp}(2,5) \quad (\text{A. 37})$$

$$\mathbf{Rnewimp}(5,3) = \mathbf{Rnewimp}(3,5) \quad (\text{A. 38})$$

$$\mathbf{Rnewimp}(5,4) = \mathbf{Rnewimp}(4,5) \quad (\text{A. 39})$$

$$\mathbf{Rnewimp}(5,5) = \mathbf{Rnewimp}(2,2) \quad (\text{A. 40})$$

Rnewimp(5,6)

$$\begin{aligned} &= ([\mathbf{t}(10) \ \mathbf{t}(8) \ \mathbf{t}(11) \ \mathbf{t}(4) \ \mathbf{t}(2) \ \mathbf{t}(5)] \\ &\quad * ([\mathbf{t}(12) \ \mathbf{t}(11) \ \mathbf{t}(9) \ \mathbf{t}(6) \ \mathbf{t}(5) \ \mathbf{t}(3)])^T) \text{sigc}^2 - \text{sigv}^2 \\ &\quad * ([\mathbf{t}(10) \ \mathbf{t}(8) \ \mathbf{t}(11)] * \mathbf{Bp} * (\mathbf{Bp})^T * ([\mathbf{t}(12) \ \mathbf{t}(11) \ \mathbf{t}(9)])^T) - \text{sigv}^2 \\ &\quad * ([\mathbf{t}(4) \ \mathbf{t}(2) \ \mathbf{t}(5)] * \mathbf{Bp} * (\mathbf{Bp})^T * ([\mathbf{t}(6) \ \mathbf{t}(5) \ \mathbf{t}(3)])^T) \end{aligned} \quad (\text{A. 41})$$

$$\mathbf{Rnewimp}(6,1) = \mathbf{Rnewimp}(1,6) \quad (\text{A. 42})$$

$$\mathbf{Rnewimp}(6,2) = \mathbf{Rnewimp}(2,6) \quad (\text{A. 43})$$

$$\mathbf{Rnewimp}(6,3) = \mathbf{Rnewimp}(3,6) \quad (\text{A. 44})$$

$$\mathbf{Rnewimp}(6,4) = \mathbf{Rnewimp}(4,6) \quad (\text{A. 45})$$

$$\mathbf{Rnewimp}(6,5) = \mathbf{Rnewimp}(5,6) \quad (\text{A. 46})$$

$$\mathbf{Rnewimp}(6,6) = \mathbf{Rnewimp}(3,3) \quad (\text{A. 47})$$

APPENDIX B

MODIFIED MEASUREMENT COVARIANCE MATRIX FOR UNSYMMETRICAL FORMULATION

Let the susceptance parameter matrix to be estimated be denoted by \mathbf{t} . Then, from (2.19), \mathbf{t} is given by,

$$\mathbf{t} = \boldsymbol{\theta}_{sh} \quad (\text{B. 1})$$

The modified measurement covariance matrix for the calculation of susceptance parameters using unsymmetrical formulation is presented below.

$$\begin{aligned} \mathbf{Rnew}(1,1) = & 2 * \text{sigc}^2 + \text{sigv}^2 * [(\mathbf{t}(1) + \mathbf{t}(4) + \mathbf{t}(9))^2 + \mathbf{t}(4)^2 + \mathbf{t}(9)^2 \\ & + (\mathbf{t}(10) + \mathbf{t}(13) + \mathbf{t}(18))^2 + \mathbf{t}(13)^2 + \mathbf{t}(18)^2] \end{aligned} \quad (\text{B. 2})$$

$$\begin{aligned} \mathbf{Rnew}(2,2) = & 2 * \text{sigc}^2 + \text{sigv}^2 * [(\mathbf{t}(2) + \mathbf{t}(5) + \mathbf{t}(7))^2 + \mathbf{t}(5)^2 + \mathbf{t}(7)^2 \\ & + (\mathbf{t}(11) + \mathbf{t}(14) + \mathbf{t}(16))^2 + \mathbf{t}(14)^2 + \mathbf{t}(16)^2] \end{aligned} \quad (\text{B. 3})$$

$$\begin{aligned} \mathbf{Rnew}(3,3) = & \text{sigv}^2 * [(\mathbf{t}(3) + \mathbf{t}(6) + \mathbf{t}(8))^2 + \mathbf{t}(6)^2 + \mathbf{t}(8)^2 \\ & + (\mathbf{t}(12) + \mathbf{t}(15) + \mathbf{t}(17))^2 + \mathbf{t}(15)^2 + \mathbf{t}(17)^2] + 2 \\ & * \text{sigc}^2 \end{aligned} \quad (\text{B. 4})$$

$$\begin{aligned} \mathbf{Rnew}(1,2) = & \text{sigv}^2 [-(\mathbf{t}(1) + \mathbf{t}(4) + \mathbf{t}(9)) * \mathbf{t}(7) - (\mathbf{t}(2) + \mathbf{t}(8) + \mathbf{t}(7)) * \mathbf{t}(4) \\ & + \mathbf{t}(9) * \mathbf{t}(5) - (\mathbf{t}(10) + \mathbf{t}(13) + \mathbf{t}(18)) * \mathbf{t}(16) \\ & - (\mathbf{t}(11) + \mathbf{t}(14) + \mathbf{t}(16)) * \mathbf{t}(13) + \mathbf{t}(18) * \mathbf{t}(11)] \end{aligned} \quad (\text{B. 5})$$

$$\begin{aligned} \mathbf{Rnew}(1,3) = & \text{sigv}^2 [-(\mathbf{t}(1) + \mathbf{t}(4) + \mathbf{t}(9)) * \mathbf{t}(6) - (\mathbf{t}(3) + \mathbf{t}(6) + \mathbf{t}(8)) * \mathbf{t}(9) \\ & + \mathbf{t}(4) * \mathbf{t}(8) - (\mathbf{t}(10) + \mathbf{t}(13) + \mathbf{t}(18)) * \mathbf{t}(15) \\ & - (\mathbf{t}(12) + \mathbf{t}(15) + \mathbf{t}(17)) * \mathbf{t}(18) + \mathbf{t}(13) * \mathbf{t}(17)] \end{aligned} \quad (\text{B. 6})$$

$$\begin{aligned}
\mathbf{Rnew}(2,3) = & \text{sigv}^2 [-(\mathbf{t}(2) + \mathbf{t}(5) + \mathbf{t}(7)) * \mathbf{t}(8) - (\mathbf{t}(3) + \mathbf{t}(6) + \mathbf{t}(8)) * \mathbf{t}(5) \\
& + \mathbf{t}(7) * \mathbf{t}(6) - (\mathbf{t}(12) + \mathbf{t}(15) + \mathbf{t}(17)) * \mathbf{t}(14) \\
& - (\mathbf{t}(11) + \mathbf{t}(14) + \mathbf{t}(16)) * \mathbf{t}(17) + \mathbf{t}(16) * \mathbf{t}(15)] \quad (\text{B. 7})
\end{aligned}$$

$$\mathbf{Rnew}(2,1) = \mathbf{Rnew}(1,2) \quad (\text{B. 8})$$

$$\mathbf{Rnew}(3,1) = \mathbf{Rnew}(1,3) \quad (\text{B. 9})$$

$$\mathbf{Rnew}(3,2) = \mathbf{Rnew}(2,3) \quad (\text{B. 10})$$

Let the impedance parameter matrix to be estimated be denoted by \mathbf{t} . Then, from (2.21), \mathbf{t} is given by,

$$\mathbf{t} = \begin{bmatrix} \text{real}(\boldsymbol{\theta}_{se}) \\ \text{imag}(\boldsymbol{\theta}_{se}) \end{bmatrix} \quad (\text{B. 11})$$

The modified measurement covariance matrix for the calculation of impedance parameters using unsymmetrical formulation is presented below.

$$\mathbf{Rnewimp}(1,1)$$

$$\begin{aligned}
= & \text{sigc}^2 (\mathbf{t}(1)^2 + \mathbf{t}(4)^2 + \mathbf{t}(9)^2 + \mathbf{t}(10)^2 + \mathbf{t}(13)^2 + \mathbf{t}(18)^2) \\
& - \text{sigv}^2 ([\mathbf{t}(1) \ \mathbf{t}(4) \ \mathbf{t}(9)] * \mathbf{Bp} * (\mathbf{Bp})^T * ([\mathbf{t}(1) \ \mathbf{t}(4) \ \mathbf{t}(9)])^T) - \text{sigv}^2 \\
& * ([\mathbf{t}(10) \ \mathbf{t}(13) \ \mathbf{t}(18)] * \mathbf{Bp} * (\mathbf{Bp})^T * ([\mathbf{t}(10) \ \mathbf{t}(13) \ \mathbf{t}(18)])^T) + 2 \\
& * \text{sigv}^2 \quad (\text{B. 12})
\end{aligned}$$

Rnewimp(1,2)

$$\begin{aligned}
&= ([\mathbf{t}(1) \ \mathbf{t}(4) \ \mathbf{t}(9) \ \mathbf{t}(10) \ \mathbf{t}(13) \ \mathbf{t}(18)] ([\mathbf{t}(7) \ \mathbf{t}(2) \ \mathbf{t}(5) \ \mathbf{t}(16) \ \mathbf{t}(11) \ \mathbf{t}(14)])^T) \\
&- \text{sigv}^2 * ([\mathbf{t}(1) \ \mathbf{t}(4) \ \mathbf{t}(9)] * \mathbf{Bp} * (\mathbf{Bp})^T * ([\mathbf{t}(7) \ \mathbf{t}(2) \ \mathbf{t}(5)])^T) - \text{sigv}^2 \\
&* ([\mathbf{t}(10) \ \mathbf{t}(13) \ \mathbf{t}(18)] * \mathbf{Bp} * (\mathbf{Bp})^T * ([\mathbf{t}(16) \ \mathbf{t}(11) \ \mathbf{t}(14)])^T) \quad (\text{B.13})
\end{aligned}$$

Rnewimp(1,3)

$$\begin{aligned}
&= \text{sigc}^2([\mathbf{t}(1) \ \mathbf{t}(4) \ \mathbf{t}(9) \ \mathbf{t}(10) \ \mathbf{t}(13) \ \mathbf{t}(18)] \\
&* ([\mathbf{t}(6) \ \mathbf{t}(8) \ \mathbf{t}(3) \ \mathbf{t}(15) \ \mathbf{t}(17) \ \mathbf{t}(12)])^T) - \text{sigv}^2 \\
&* ([\mathbf{t}(1) \ \mathbf{t}(4) \ \mathbf{t}(9)] * \mathbf{Bp} * (\mathbf{Bp})^T * ([\mathbf{t}(6) \ \mathbf{t}(8) \ \mathbf{t}(3)])^T) - \text{sigv}^2 \\
&* ([\mathbf{t}(10) \ \mathbf{t}(13) \ \mathbf{t}(18)] * \mathbf{Bp} * (\mathbf{Bp})^T * ([\mathbf{t}(15) \ \mathbf{t}(17) \ \mathbf{t}(12)])^T) \quad (\text{B.14})
\end{aligned}$$

Rnewimp(1,4)

$$\begin{aligned}
&= \text{sigc}^2([\mathbf{t}(1) \ \mathbf{t}(4) \ \mathbf{t}(9) \ -\mathbf{t}(10) \ -\mathbf{t}(13) \ -\mathbf{t}(18)] \\
&* ([\mathbf{t}(10) \ \mathbf{t}(13) \ \mathbf{t}(18) \ \mathbf{t}(1) \ \mathbf{t}(4) \ \mathbf{t}(9)])^T) - \text{sigv}^2 \\
&* ([\mathbf{t}(1) \ \mathbf{t}(4) \ \mathbf{t}(9)] * \mathbf{Bp} * (\mathbf{Bp})^T * ([\mathbf{t}(10) \ \mathbf{t}(13) \ \mathbf{t}(18)])^T) + \text{sigv}^2 \\
&* ([\mathbf{t}(10) \ \mathbf{t}(13) \ \mathbf{t}(18)] * \mathbf{Bp} * (\mathbf{Bp})^T * ([\mathbf{t}(1) \ \mathbf{t}(4) \ \mathbf{t}(9)])^T) \quad (\text{B.15})
\end{aligned}$$

Rnewimp(1,5)

$$\begin{aligned}
&= \text{sigc}^2([\mathbf{t}(1) \ \mathbf{t}(4) \ \mathbf{t}(9) \ -\mathbf{t}(10) \ -\mathbf{t}(13) \ -\mathbf{t}(18)] \\
&* ([\mathbf{t}(16) \ \mathbf{t}(11) \ \mathbf{t}(14) \ \mathbf{t}(7) \ \mathbf{t}(2) \ \mathbf{t}(5)])^T) - \text{sigv}^2 \\
&* ([\mathbf{t}(1) \ \mathbf{t}(4) \ \mathbf{t}(9)] * \mathbf{Bp} * (\mathbf{Bp})^T * ([\mathbf{t}(16) \ \mathbf{t}(11) \ \mathbf{t}(14)])^T) + \text{sigv}^2 \\
&* ([\mathbf{t}(10) \ \mathbf{t}(13) \ \mathbf{t}(18)] * \mathbf{Bp} * (\mathbf{Bp})^T * ([\mathbf{t}(7) \ \mathbf{t}(2) \ \mathbf{t}(5)])^T) \quad (\text{B.16})
\end{aligned}$$

Rnewimp(1,6)

$$\begin{aligned}
&= \text{sigc}^2([\mathbf{t}(1) \ \mathbf{t}(4) \ \mathbf{t}(9) \ -\mathbf{t}(10) \ -\mathbf{t}(13) \ -\mathbf{t}(18)] \\
&\quad * ([\mathbf{t}(15) \ \mathbf{t}(17) \ \mathbf{t}(12) \ \mathbf{t}(6) \ \mathbf{t}(8) \ \mathbf{t}(3)])^T) - \text{sigv}^2 \\
&\quad * ([\mathbf{t}(1) \ \mathbf{t}(4) \ \mathbf{t}(9)] * \mathbf{Bp} * (\mathbf{Bp})^T * ([\mathbf{t}(15) \ \mathbf{t}(17) \ \mathbf{t}(12)])^T) + \text{sigv}^2 \\
&\quad * ([\mathbf{t}(10) \ \mathbf{t}(13) \ \mathbf{t}(18)] * \mathbf{Bp} * (\mathbf{Bp})^T * ([\mathbf{t}(6) \ \mathbf{t}(8) \ \mathbf{t}(3)])^T) \quad (\text{B.17})
\end{aligned}$$

$$\mathbf{Rnewimp}(2,1) = \mathbf{Rnewimp}(1,2) \quad (\text{B.18})$$

Rnewimp(2,2)

$$\begin{aligned}
&= (\mathbf{t}(7)^2 + \mathbf{t}(2)^2 + \mathbf{t}(5)^2 + \mathbf{t}(16)^2 + \mathbf{t}(11)^2 + \mathbf{t}(14)^2)\text{sigc}^2 - \text{sigv}^2 \\
&\quad * ([\mathbf{t}(7) \ \mathbf{t}(2) \ \mathbf{t}(5)] * \mathbf{Bp} * (\mathbf{Bp})^T * ([\mathbf{t}(7) \ \mathbf{t}(2) \ \mathbf{t}(5)])^T) - \text{sigv}^2 \\
&\quad * ([\mathbf{t}(16) \ \mathbf{t}(11) \ \mathbf{t}(14)] * \mathbf{Bp} * (\mathbf{Bp})^T * ([\mathbf{t}(16) \ \mathbf{t}(11) \ \mathbf{t}(14)])^T) + 2 \\
&\quad * \text{sigv}^2 \quad (\text{B.19})
\end{aligned}$$

Rnewimp(2,3)

$$\begin{aligned}
&= \text{sigc}^2([\mathbf{t}(7) \ \mathbf{t}(2) \ \mathbf{t}(5) \ \mathbf{t}(16) \ \mathbf{t}(11) \ \mathbf{t}(14)] \\
&\quad * ([\mathbf{t}(6) \ \mathbf{t}(8) \ \mathbf{t}(3) \ \mathbf{t}(15) \ \mathbf{t}(17) \ \mathbf{t}(12)])^T) - \text{sigv}^2 \\
&\quad * ([\mathbf{t}(7) \ \mathbf{t}(2) \ \mathbf{t}(5)] * \mathbf{Bp} * (\mathbf{Bp})^T * ([\mathbf{t}(6) \ \mathbf{t}(8) \ \mathbf{t}(3)])^T) - \text{sigv}^2 \\
&\quad * ([\mathbf{t}(16) \ \mathbf{t}(11) \ \mathbf{t}(14)] * \mathbf{Bp} * (\mathbf{Bp})^T * ([\mathbf{t}(15) \ \mathbf{t}(17) \ \mathbf{t}(12)])^T) \quad (\text{B.20})
\end{aligned}$$

Rnewimp(2,4)

$$\begin{aligned}
&= \text{sigc}^2([\mathbf{t}(7) \ \mathbf{t}(2) \ \mathbf{t}(5) \ -\mathbf{t}(16) \ -\mathbf{t}(11) \ -\mathbf{t}(14)] \\
&\quad * ([\mathbf{t}(10) \ \mathbf{t}(13) \ \mathbf{t}(18) \ \mathbf{t}(1) \ \mathbf{t}(4) \ \mathbf{t}(9)])^T) - \text{sigv}^2 \\
&\quad * ([\mathbf{t}(7) \ \mathbf{t}(2) \ \mathbf{t}(5)] * \mathbf{Bp} * (\mathbf{Bp})^T * ([\mathbf{t}(10) \ \mathbf{t}(13) \ \mathbf{t}(18)])^T) + \text{sigv}^2 \\
&\quad * ([\mathbf{t}(16) \ \mathbf{t}(11) \ \mathbf{t}(14)] * \mathbf{Bp} * (\mathbf{Bp})^T * ([\mathbf{t}(1) \ \mathbf{t}(4) \ \mathbf{t}(9)])^T) \quad (\text{B.21})
\end{aligned}$$

Rnewimp(2,5)

$$\begin{aligned}
&= \text{sigc}^2([\mathbf{t}(7) \ \mathbf{t}(2) \ \mathbf{t}(5) \ -\mathbf{t}(16) \ -\mathbf{t}(11) \ -\mathbf{t}(14)] \\
&\quad * ([\mathbf{t}(16) \ \mathbf{t}(11) \ \mathbf{t}(14) \ \mathbf{t}(7) \ \mathbf{t}(2) \ \mathbf{t}(5)])^T) - \text{sigv}^2 \\
&\quad * ([\mathbf{t}(7) \ \mathbf{t}(2) \ \mathbf{t}(5)] * \mathbf{Bp} * (\mathbf{Bp})^T * ([\mathbf{t}(16) \ \mathbf{t}(11) \ \mathbf{t}(14)])^T) + \text{sigv}^2 \\
&\quad * ([\mathbf{t}(16) \ \mathbf{t}(11) \ \mathbf{t}(14)] * \mathbf{Bp} * (\mathbf{Bp})^T * ([\mathbf{t}(7) \ \mathbf{t}(2) \ \mathbf{t}(5)])^T) \quad (\text{B. 22})
\end{aligned}$$

Rnewimp(2,6)

$$\begin{aligned}
&= \text{sigc}^2([\mathbf{t}(7) \ \mathbf{t}(2) \ \mathbf{t}(5) \ -\mathbf{t}(16) \ -\mathbf{t}(11) \ -\mathbf{t}(14)] \\
&\quad * ([\mathbf{t}(15) \ \mathbf{t}(17) \ \mathbf{t}(12) \ \mathbf{t}(6) \ \mathbf{t}(8) \ \mathbf{t}(3)])^T) - \text{sigv}^2 \\
&\quad * ([\mathbf{t}(7) \ \mathbf{t}(2) \ \mathbf{t}(5)] * \mathbf{Bp} * (\mathbf{Bp})^T * ([\mathbf{t}(15) \ \mathbf{t}(17) \ \mathbf{t}(12)])^T) + \text{sigv}^2 \\
&\quad * ([\mathbf{t}(16) \ \mathbf{t}(11) \ \mathbf{t}(14)] * \mathbf{Bp} * (\mathbf{Bp})^T * ([\mathbf{t}(6) \ \mathbf{t}(8) \ \mathbf{t}(3)])^T) \quad (\text{B. 23})
\end{aligned}$$

$$\mathbf{Rnewimp}(3,1) = \mathbf{Rnewimp}(1,3) \quad (\text{B. 24})$$

$$\mathbf{Rnewimp}(3,2) = \mathbf{Rnewimp}(2,3) \quad (\text{B. 25})$$

Rnewimp(3,3)

$$\begin{aligned}
&= \text{sigc}^2 * (\mathbf{t}(6)^2 + \mathbf{t}(8)^2 + \mathbf{t}(3)^2 + \mathbf{t}(15)^2 + \mathbf{t}(17)^2 + \mathbf{t}(12)^2) \\
&\quad - \text{sigv}^2 * ([\mathbf{t}(6) \ \mathbf{t}(8) \ \mathbf{t}(3)] * \mathbf{Bp} * (\mathbf{Bp})^T * ([\mathbf{t}(6) \ \mathbf{t}(8) \ \mathbf{t}(3)])^T) \\
&\quad - ([\mathbf{t}(15) \ \mathbf{t}(17) \ \mathbf{t}(12)] * \mathbf{Bp} * (\mathbf{Bp})^T \\
&\quad * ([\mathbf{t}(15) \ \mathbf{t}(17) \ \mathbf{t}(12)])^T) * \text{sigv}^2 + 2 * \text{sigv}^2 \quad (\text{B. 26})
\end{aligned}$$

Rnewimp(3,4)

$$\begin{aligned} &= ([\mathbf{t}(6) \ \mathbf{t}(8) \ \mathbf{t}(3) \ -\mathbf{t}(15) \ -\mathbf{t}(17) \ -\mathbf{t}(12)] \\ &* ([\mathbf{t}(10) \ \mathbf{t}(13) \ \mathbf{t}(18) \ \mathbf{t}(1) \ \mathbf{t}(4) \ \mathbf{t}(9)])^T) \text{sigc}^2 - \text{sigv}^2 \\ &* ([\mathbf{t}(6) \ \mathbf{t}(8) \ \mathbf{t}(3)] * \mathbf{Bp} * (\mathbf{Bp})^T * ([\mathbf{t}(10) \ \mathbf{t}(13) \ \mathbf{t}(18)])^T) + \text{sigv}^2 \\ &* ([\mathbf{t}(15) \ \mathbf{t}(17) \ \mathbf{t}(12)] * \mathbf{Bp} * (\mathbf{Bp})^T * ([\mathbf{t}(1) \ \mathbf{t}(4) \ \mathbf{t}(9)])^T) \quad (\text{B.27}) \end{aligned}$$

Rnewimp(3,5)

$$\begin{aligned} &= \text{sigc}^2([\mathbf{t}(6) \ \mathbf{t}(8) \ \mathbf{t}(3) \ -\mathbf{t}(15) \ -\mathbf{t}(17) \ -\mathbf{t}(12)] \\ &* ([\mathbf{t}(16) \ \mathbf{t}(11) \ \mathbf{t}(14) \ \mathbf{t}(7) \ \mathbf{t}(2) \ \mathbf{t}(5)])^T) - \text{sigv}^2 \\ &* ([\mathbf{t}(6) \ \mathbf{t}(8) \ \mathbf{t}(3)] * \mathbf{Bp} * (\mathbf{Bp})^T * ([\mathbf{t}(16) \ \mathbf{t}(11) \ \mathbf{t}(14)])^T) + \text{sigv}^2 \\ &* ([\mathbf{t}(15) \ \mathbf{t}(17) \ \mathbf{t}(12)] * \mathbf{Bp} * (\mathbf{Bp})^T * ([\mathbf{t}(7) \ \mathbf{t}(2) \ \mathbf{t}(5)])^T) \quad (\text{B.28}) \end{aligned}$$

Rnewimp(3,6)

$$\begin{aligned} &= \text{sigc}^2([\mathbf{t}(6) \ \mathbf{t}(5) \ \mathbf{t}(3) \ -\mathbf{t}(15) \ -\mathbf{t}(17) \ -\mathbf{t}(12)] \\ &* ([\mathbf{t}(15) \ \mathbf{t}(17) \ \mathbf{t}(12) \ \mathbf{t}(6) \ \mathbf{t}(8) \ \mathbf{t}(3)])^T) - \text{sigv}^2 \\ &* ([\mathbf{t}(6) \ \mathbf{t}(8) \ \mathbf{t}(3)] * \mathbf{Bp} * (\mathbf{Bp})^T * ([\mathbf{t}(15) \ \mathbf{t}(17) \ \mathbf{t}(12)])^T) + \text{sigv}^2 \\ &* ([\mathbf{t}(15) \ \mathbf{t}(17) \ \mathbf{t}(12)] * \mathbf{Bp} * (\mathbf{Bp})^T * ([\mathbf{t}(6) \ \mathbf{t}(8) \ \mathbf{t}(3)])^T) \quad (\text{B.29}) \end{aligned}$$

$$\mathbf{Rnewimp}(4,1) = \mathbf{Rnewimp}(1,4) \quad (\text{B.30})$$

$$\mathbf{Rnewimp}(4,2) = \mathbf{Rnewimp}(2,4) \quad (\text{B.31})$$

$$\mathbf{Rnewimp}(4,3) = \mathbf{Rnewimp}(3,4) \quad (\text{B.32})$$

$$\mathbf{Rnewimp}(4,4) = \mathbf{Rnewimp}(1,1) \quad (\text{B.33})$$

Rnewimp(4,5)

$$\begin{aligned} &= \text{sigc}^2([\mathbf{t}(10) \ \mathbf{t}(13) \ \mathbf{t}(18) \ -\mathbf{t}(1) \ -\mathbf{t}(4) \ -\mathbf{t}(9)] \\ &* ([\mathbf{t}(16) \ \mathbf{t}(11) \ \mathbf{t}(14) \ \mathbf{t}(7) \ \mathbf{t}(2) \ \mathbf{t}(5)])^T) - \text{sigv}^2 \\ &* ([\mathbf{t}(10) \ \mathbf{t}(13) \ \mathbf{t}(18)] * \mathbf{Bp} * (\mathbf{Bp})^T * ([\mathbf{t}(16) \ \mathbf{t}(11) \ \mathbf{t}(14)])^T) - \text{sigv}^2 \\ &* ([\mathbf{t}(1) \ \mathbf{t}(4) \ \mathbf{t}(9)] * \mathbf{Bp} * (\mathbf{Bp})^T * ([\mathbf{t}(7) \ \mathbf{t}(2) \ \mathbf{t}(5)])^T) \quad (\text{B.34}) \end{aligned}$$

Rnewimp(4,6)

$$\begin{aligned} &= \text{sigc}^2([\mathbf{t}(10) \ \mathbf{t}(13) \ \mathbf{t}(18) \ -\mathbf{t}(1) \ -\mathbf{t}(4) \ -\mathbf{t}(9)] \\ &* ([\mathbf{t}(15) \ \mathbf{t}(17) \ \mathbf{t}(12) \ \mathbf{t}(6) \ \mathbf{t}(8) \ \mathbf{t}(3)])^T) - \text{sigv}^2 \\ &* ([\mathbf{t}(10) \ \mathbf{t}(13) \ \mathbf{t}(18)] * \mathbf{Bp} * (\mathbf{Bp})^T * ([\mathbf{t}(15) \ \mathbf{t}(17) \ \mathbf{t}(12)])^T) - \text{sigv}^2 \\ &* ([\mathbf{t}(1) \ \mathbf{t}(4) \ \mathbf{t}(9)] * \mathbf{Bp} * (\mathbf{Bp})^T * ([\mathbf{t}(6) \ \mathbf{t}(8) \ \mathbf{t}(3)])^T) \quad (\text{B.35}) \end{aligned}$$

$$\mathbf{Rnewimp}(5,1) = \mathbf{Rnewimp}(1,5) \quad (\text{B.36})$$

$$\mathbf{Rnewimp}(5,2) = \mathbf{Rnewimp}(2,5) \quad (\text{B.37})$$

$$\mathbf{Rnewimp}(5,3) = \mathbf{Rnewimp}(3,5) \quad (\text{B.38})$$

$$\mathbf{Rnewimp}(5,4) = \mathbf{Rnewimp}(4,5) \quad (\text{B.39})$$

$$\mathbf{Rnewimp}(5,5) = \mathbf{Rnewimp}(2,2) \quad (\text{B.40})$$

Rnewimp(5,6)

$$\begin{aligned} &= \text{sigc}^2([\mathbf{t}(16) \ \mathbf{t}(11) \ \mathbf{t}(14) \ -\mathbf{t}(7) \ -\mathbf{t}(2) \ -\mathbf{t}(5)] \\ &* ([\mathbf{t}(15) \ \mathbf{t}(17) \ \mathbf{t}(12) \ \mathbf{t}(6) \ \mathbf{t}(8) \ \mathbf{t}(3)])^T) - \text{sigv}^2 \\ &* ([\mathbf{t}(16) \ \mathbf{t}(11) \ \mathbf{t}(14)] * \mathbf{Bp} * (\mathbf{Bp})^T * ([\mathbf{t}(15) \ \mathbf{t}(17) \ \mathbf{t}(12)])^T) - \text{sigv}^2 \\ &* ([\mathbf{t}(7) \ \mathbf{t}(2) \ \mathbf{t}(5)] * \mathbf{Bp} * (\mathbf{Bp})^T * ([\mathbf{t}(6) \ \mathbf{t}(8) \ \mathbf{t}(3)])^T) \quad (\text{B.41}) \end{aligned}$$

$$\mathbf{Rnewimp}(6,1) = \mathbf{Rnewimp}(1,6) \quad (\text{B. 42})$$

$$\mathbf{Rnewimp}(6,2) = \mathbf{Rnewimp}(2,6) \quad (\text{B. 43})$$

$$\mathbf{Rnewimp}(6,3) = \mathbf{Rnewimp}(3,6) \quad (\text{B. 44})$$

$$\mathbf{Rnewimp}(6,4) = \mathbf{Rnewimp}(4,6) \quad (\text{B. 45})$$

$$\mathbf{Rnewimp}(6,5) = \mathbf{Rnewimp}(5,6) \quad (\text{B. 46})$$

$$\mathbf{Rnewimp}(6,6) = \mathbf{Rnewimp}(3,3) \quad (\text{B. 47})$$

APPENDIX C

CALCULATION OF IMPEDANCE COVARIANCE MATRIX: SYMMETRICAL

FORMULATION

Let the impedance parameter matrix to be estimated is given by $\boldsymbol{\theta}$, from (2.12)

$$\boldsymbol{\theta} = [\text{real}\{\boldsymbol{\theta}_{se}\} \quad \text{imag}\{\boldsymbol{\theta}_{se}\}] = [\theta_1 \ \theta_2 \ \theta_3 \ \theta_4 \ \theta_5 \ \theta_6 \ \theta_7 \ \theta_8 \ \theta_9 \ \theta_{10} \ \theta_{11} \ \theta_{12}] \quad (\text{C.1})$$

From (2.11) – (2.16), the derivation of the covariance matrix is presented below.

Calculation of diagonal element:

$$\begin{aligned} R(1,1) &= 2(\sigma_v)^2 \\ &+ \text{Var}\{\text{real}(h_1\theta_1 + h_2\theta_4 + h_3\theta_6) \\ &- \text{imag}(h_1\theta_7 + h_2\theta_{10} + h_3\theta_{12})\} \end{aligned} \quad (\text{C.2})$$

Using property, $\text{Var}(a\mathbf{X} - b\mathbf{Y}) = a^2\text{Var}(\mathbf{X}) + b^2\text{Var}(\mathbf{Y}) - 2ab\text{COV}(\mathbf{X}, \mathbf{Y})$, we get

$$\begin{aligned} R(1,1) &= 2(\sigma_v)^2 + \text{Var}\{\text{real}(h_1\theta_1 + h_2\theta_4 + h_3\theta_6)\} \\ &+ \text{Var}\{\text{imag}(h_1\theta_7 + h_2\theta_{10} + h_3\theta_{12})\} \\ &- 2\text{COV}\{\text{real}(h_1\theta_1 + h_2\theta_4 + h_3\theta_6), \text{imag}(h_1\theta_7 + h_2\theta_{10} + h_3\theta_{12})\} \end{aligned} \quad (\text{C.3})$$

$$\begin{aligned} \Rightarrow R(1,1) &= 2(\sigma_v)^2 + \text{Var}\left\{\text{real}\left([\theta_1 \ \theta_4 \ \theta_6] \begin{bmatrix} h_1 \\ h_2 \\ h_3 \end{bmatrix}\right)\right\} \\ &+ \text{Var}\left\{\text{imag}\left([\theta_7 \ \theta_{10} \ \theta_{12}] \begin{bmatrix} h_1 \\ h_2 \\ h_3 \end{bmatrix}\right)\right\} \\ &- 2\text{COV}\left\{\text{real}\left([\theta_1 \ \theta_4 \ \theta_6] \begin{bmatrix} h_1 \\ h_2 \\ h_3 \end{bmatrix}\right), \text{imag}\left([\theta_7 \ \theta_{10} \ \theta_{12}] \begin{bmatrix} h_1 \\ h_2 \\ h_3 \end{bmatrix}\right)\right\} \end{aligned} \quad (\text{C.4})$$

Using property, $\text{COV}(\mathbf{AX} + a, \mathbf{B}^T\mathbf{Y} + b) = \mathbf{ACOV}(\mathbf{X}, \mathbf{Y})\mathbf{B}$, we get

$$\begin{aligned}
& 2\text{COV}\left\{\text{real}\left([\theta_1 \ \theta_4 \ \theta_6] \begin{bmatrix} h_1 \\ h_2 \\ h_3 \end{bmatrix}\right), \text{imag}\left([\theta_7 \ \theta_{10} \ \theta_{12}] \begin{bmatrix} h_1 \\ h_2 \\ h_3 \end{bmatrix}\right)\right\} \\
& = 2[\theta_1 \ \theta_4 \ \theta_6]\text{COV}\left\{\text{real}\left(\begin{bmatrix} h_1 \\ h_2 \\ h_3 \end{bmatrix}\right), \text{imag}\left(\begin{bmatrix} h_1 \\ h_2 \\ h_3 \end{bmatrix}\right)\right\} \begin{bmatrix} \theta_7 \\ \theta_{10} \\ \theta_{12} \end{bmatrix}
\end{aligned} \tag{C.5}$$

Using property that real and imaginary components of a complex number are uncorrelated (same as orthogonal in geometric terms), we get

$$\text{COV}\left\{\text{real}\left(\begin{bmatrix} h_1 \\ h_2 \\ h_3 \end{bmatrix}\right), \text{imag}\left(\begin{bmatrix} h_1 \\ h_2 \\ h_3 \end{bmatrix}\right)\right\} = 0 \tag{C.6}$$

Therefore,

$$\begin{aligned}
R(1,1) &= 2(\sigma_V)^2 + \text{Var}\left\{\text{real}\left([\theta_1 \ \theta_4 \ \theta_6] \begin{bmatrix} h_1 \\ h_2 \\ h_3 \end{bmatrix}\right)\right\} \\
&+ \text{Var}\left\{\text{imag}\left([\theta_7 \ \theta_{10} \ \theta_{12}] \begin{bmatrix} h_1 \\ h_2 \\ h_3 \end{bmatrix}\right)\right\}
\end{aligned} \tag{C.7}$$

$$\begin{aligned}
\Rightarrow R(1,1) &= 2(\sigma_V)^2 + \text{Var}\left\{\text{real}\left([\theta_1 \ \theta_4 \ \theta_6] \left(\begin{bmatrix} I_{pq}^a \\ I_{pq}^b \\ I_{pq}^c \end{bmatrix} - \mathbf{B}_p^{abc} \begin{bmatrix} V_p^a \\ V_p^b \\ V_p^c \end{bmatrix}\right)\right)\right\} \\
&+ \text{Var}\left\{\text{imag}\left([\theta_7 \ \theta_{10} \ \theta_{12}] \left(\begin{bmatrix} I_{pq}^a \\ I_{pq}^b \\ I_{pq}^c \end{bmatrix} - \mathbf{B}_p^{abc} \begin{bmatrix} V_p^a \\ V_p^b \\ V_p^c \end{bmatrix}\right)\right)\right\}
\end{aligned} \tag{C.8}$$

$$\begin{aligned}
\Rightarrow R(1,1) = 2(\sigma_V)^2 + \text{Var} \left\{ \text{real} \left([\theta_1 \quad \theta_4 \quad \theta_6] \begin{bmatrix} I_{pq}^a \\ I_{pq}^b \\ I_{pq}^c \end{bmatrix} - [\theta_1 \quad \theta_4 \quad \theta_6] \mathbf{B}_p^{abc} \begin{bmatrix} V_p^a \\ V_p^b \\ V_p^c \end{bmatrix} \right) \right\} \\
+ \text{Var} \left\{ \text{imag} \left([\theta_7 \quad \theta_{10} \quad \theta_{12}] \begin{bmatrix} I_{pq}^a \\ I_{pq}^b \\ I_{pq}^c \end{bmatrix} \right. \right. \\
\left. \left. - [\theta_7 \quad \theta_{10} \quad \theta_{12}] \mathbf{B}_p^{abc} \begin{bmatrix} V_p^a \\ V_p^b \\ V_p^c \end{bmatrix} \right) \right\} \tag{C.9}
\end{aligned}$$

Combining properties, $\text{Var}(\mathbf{aX} - \mathbf{bY}) = \mathbf{a}^2\text{Var}(\mathbf{X}) + \mathbf{b}^2\text{Var}(\mathbf{Y}) - 2\mathbf{abCOV}(\mathbf{X}, \mathbf{Y})$ and $\text{Var}(\mathbf{AX} + \mathbf{b}) = \mathbf{A}\text{Var}(\mathbf{X})\mathbf{A}^T$, and knowing that voltages and currents are uncorrelated, we get

$$\begin{aligned}
R(1,1) = 2(\sigma_V)^2 + [\theta_1 \quad \theta_4 \quad \theta_6] \text{Var} \left\{ \text{real} \left(\begin{bmatrix} I_{pq}^a \\ I_{pq}^b \\ I_{pq}^c \end{bmatrix} \right) \right\} \begin{bmatrix} \theta_1 \\ \theta_4 \\ \theta_6 \end{bmatrix} \\
+ [\theta_1 \quad \theta_4 \quad \theta_6] \text{Var} \left\{ \text{real} \left(\mathbf{B}_p^{abc} \begin{bmatrix} V_p^a \\ V_p^b \\ V_p^c \end{bmatrix} \right) \right\} \begin{bmatrix} \theta_1 \\ \theta_4 \\ \theta_6 \end{bmatrix} \\
+ [\theta_7 \quad \theta_{10} \quad \theta_{12}] \text{Var} \left\{ \text{imag} \left(\begin{bmatrix} I_{pq}^a \\ I_{pq}^b \\ I_{pq}^c \end{bmatrix} \right) \right\} \begin{bmatrix} \theta_7 \\ \theta_{10} \\ \theta_{12} \end{bmatrix} \\
+ [\theta_7 \quad \theta_{10} \quad \theta_{12}] \text{Var} \left\{ \text{imag} \left(\mathbf{B}_p^{abc} \begin{bmatrix} V_p^a \\ V_p^b \\ V_p^c \end{bmatrix} \right) \right\} \begin{bmatrix} \theta_7 \\ \theta_{10} \\ \theta_{12} \end{bmatrix} \tag{C.10}
\end{aligned}$$

$$\begin{aligned}
\Rightarrow R(1,1) &= 2(\sigma_V)^2 + [\theta_1 \quad \theta_4 \quad \theta_6] \begin{bmatrix} (\sigma_C)^2 & 0 & 0 \\ 0 & (\sigma_C)^2 & 0 \\ 0 & 0 & (\sigma_C)^2 \end{bmatrix} \begin{bmatrix} \theta_1 \\ \theta_4 \\ \theta_6 \end{bmatrix} \\
&+ [\theta_1 \quad \theta_4 \quad \theta_6] \text{Var} \left\{ \text{real} \left(\mathbf{B}_p^{\text{abc}} \begin{bmatrix} V_p^a \\ V_p^b \\ V_p^c \end{bmatrix} \right) \right\} \begin{bmatrix} \theta_1 \\ \theta_4 \\ \theta_6 \end{bmatrix} \\
&+ [\theta_7 \quad \theta_{10} \quad \theta_{12}] \begin{bmatrix} (\sigma_C)^2 & 0 & 0 \\ 0 & (\sigma_C)^2 & 0 \\ 0 & 0 & (\sigma_C)^2 \end{bmatrix} \begin{bmatrix} \theta_7 \\ \theta_{10} \\ \theta_{12} \end{bmatrix} \\
&+ [\theta_7 \quad \theta_{10} \quad \theta_{12}] \text{Var} \left\{ \text{imag} \left(\mathbf{B}_p^{\text{abc}} \begin{bmatrix} V_p^a \\ V_p^b \\ V_p^c \end{bmatrix} \right) \right\} \begin{bmatrix} \theta_7 \\ \theta_{10} \\ \theta_{12} \end{bmatrix} \tag{C.11}
\end{aligned}$$

Now, since $\mathbf{B}_p^{\text{abc}}$ is purely imaginary, $\mathbf{B}_p^{\text{abc}} = j\mathbf{B}$, and therefore,

$$\text{Var} \left\{ \text{real} \left(\mathbf{B}_p^{\text{abc}} \begin{bmatrix} V_p^a \\ V_p^b \\ V_p^c \end{bmatrix} \right) \right\} = \text{Var} \left\{ \text{real} \left(j\mathbf{B} \begin{bmatrix} \text{real}(V_p^a) + j\text{imag}(V_p^a) \\ \text{real}(V_p^b) + j\text{imag}(V_p^b) \\ \text{real}(V_p^c) + j\text{imag}(V_p^c) \end{bmatrix} \right) \right\} \tag{C.12}$$

$$\Rightarrow \text{Var} \left\{ \text{real} \left(\mathbf{B}_p^{\text{abc}} \begin{bmatrix} V_p^a \\ V_p^b \\ V_p^c \end{bmatrix} \right) \right\} = \text{Var} \left\{ - \left(\mathbf{B} \begin{bmatrix} \text{imag}(V_p^a) \\ \text{imag}(V_p^b) \\ \text{imag}(V_p^c) \end{bmatrix} \right) \right\} \tag{C.13}$$

Defining, $\mathbf{C} = -\mathbf{B}$, and using property $\text{Var}(\mathbf{A}\mathbf{X} + \mathbf{b}) = \mathbf{A}\text{Var}(\mathbf{X})\mathbf{A}^T$, we get

$$\text{Var} \left\{ \text{real} \left(\mathbf{B}_p^{\text{abc}} \begin{bmatrix} V_p^a \\ V_p^b \\ V_p^c \end{bmatrix} \right) \right\} = \mathbf{C} \text{Var} \left\{ \begin{bmatrix} \text{imag}(V_p^a) \\ \text{imag}(V_p^b) \\ \text{imag}(V_p^c) \end{bmatrix} \right\} \mathbf{C}^T \tag{C.14}$$

$$\Rightarrow \text{Var} \left\{ \text{real} \left(\mathbf{B}_p^{\text{abc}} \begin{bmatrix} V_p^a \\ V_p^b \\ V_p^c \end{bmatrix} \right) \right\} = \mathbf{C} \begin{bmatrix} (\sigma_V)^2 & 0 & 0 \\ 0 & (\sigma_V)^2 & 0 \\ 0 & 0 & (\sigma_V)^2 \end{bmatrix} \mathbf{C}^T \tag{C.15}$$

$$\Rightarrow \text{Var} \left\{ \text{real} \left(\mathbf{B}_p^{\text{abc}} \begin{bmatrix} V_p^a \\ V_p^b \\ V_p^c \end{bmatrix} \right) \right\} = (\sigma_V)^2 \mathbf{C}\mathbf{C}^T = (\sigma_V)^2 \mathbf{B}\mathbf{B}^T \quad (\text{C.16})$$

Similarly,

$$\text{Var} \left\{ \text{imag} \left(\mathbf{B}_p^{\text{abc}} \begin{bmatrix} V_p^a \\ V_p^b \\ V_p^c \end{bmatrix} \right) \right\} = \mathbf{B} \text{Var} \left\{ \begin{bmatrix} \text{real}(V_p^a) \\ \text{real}(V_p^b) \\ \text{real}(V_p^c) \end{bmatrix} \right\} \mathbf{B}^T = (\sigma_V)^2 \mathbf{B}\mathbf{B}^T \quad (\text{C.17})$$

Substituting these values in the expression of R(1,1), and solving, we get

$$\begin{aligned} R(1,1) &= 2(\sigma_V)^2 + (\sigma_C)^2 \{(\theta_1)^2 + (\theta_4)^2 + (\theta_6)^2\} + (\sigma_V)^2 \left\{ [\theta_1 \quad \theta_4 \quad \theta_6] \mathbf{B}\mathbf{B}^T \begin{bmatrix} \theta_1 \\ \theta_4 \\ \theta_6 \end{bmatrix} \right\} \\ &\quad + (\sigma_C)^2 \{(\theta_7)^2 + (\theta_{10})^2 + (\theta_{12})^2\} \\ &\quad + (\sigma_V)^2 \left\{ [\theta_7 \quad \theta_{10} \quad \theta_{12}] \mathbf{B}\mathbf{B}^T \begin{bmatrix} \theta_7 \\ \theta_{10} \\ \theta_{12} \end{bmatrix} \right\} \end{aligned} \quad (\text{C.18})$$

Now as $\mathbf{B}\mathbf{B}^T = -\mathbf{B}_p^{\text{abc}}(\mathbf{B}_p^{\text{abc}})^T$, we get

$$\begin{aligned} R(1,1) &= 2(\sigma_V)^2 + (\sigma_C)^2 \{(\theta_1)^2 + (\theta_4)^2 + (\theta_6)^2 + (\theta_7)^2 + (\theta_{10})^2 + (\theta_{12})^2\} \\ &\quad - (\sigma_V)^2 \left\{ [\theta_1 \quad \theta_4 \quad \theta_6] \mathbf{B}_p^{\text{abc}} (\mathbf{B}_p^{\text{abc}})^T \begin{bmatrix} \theta_1 \\ \theta_4 \\ \theta_6 \end{bmatrix} \right\} \\ &\quad + [\theta_7 \quad \theta_{10} \quad \theta_{12}] \mathbf{B}_p^{\text{abc}} (\mathbf{B}_p^{\text{abc}})^T \begin{bmatrix} \theta_7 \\ \theta_{10} \\ \theta_{12} \end{bmatrix} \end{aligned} \quad (\text{C.19})$$

Calculation of non-diagonal element:

$$\begin{aligned}
R(1,2) = & \text{COV}\{\text{real}(h_1\theta_1 + h_2\theta_4 + h_3\theta_6) \\
& - \text{imag}(h_1\theta_7 + h_2\theta_{10} + h_3\theta_{12}), \text{real}(h_1\theta_4 + h_2\theta_2 + h_3\theta_5) \\
& - \text{imag}(h_1\theta_{10} + h_2\theta_8 + h_3\theta_{11})\} \tag{C.20}
\end{aligned}$$

$$\begin{aligned}
\Rightarrow R(1,2) = & \text{COV}\left\{\text{real}\left(\begin{bmatrix} \theta_1 & \theta_4 & \theta_6 \\ \theta_7 & \theta_{10} & \theta_{12} \end{bmatrix} \begin{bmatrix} h_1 \\ h_2 \\ h_3 \end{bmatrix}\right) \right. \\
& - \text{imag}\left(\begin{bmatrix} \theta_7 & \theta_{10} & \theta_{12} \\ \theta_{10} & \theta_8 & \theta_{11} \end{bmatrix} \begin{bmatrix} h_1 \\ h_2 \\ h_3 \end{bmatrix}\right), \text{real}\left(\begin{bmatrix} \theta_4 & \theta_2 & \theta_5 \\ \theta_4 & \theta_2 & \theta_5 \end{bmatrix} \begin{bmatrix} h_1 \\ h_2 \\ h_3 \end{bmatrix}\right) \\
& \left. - \text{imag}\left(\begin{bmatrix} \theta_4 & \theta_2 & \theta_5 \\ \theta_{10} & \theta_8 & \theta_{11} \end{bmatrix} \begin{bmatrix} h_1 \\ h_2 \\ h_3 \end{bmatrix}\right)\right\} \tag{C.21}
\end{aligned}$$

Combining properties, $\text{COV}(\mathbf{X}_1 + \mathbf{X}_2, \mathbf{Y}) = \text{COV}(\mathbf{X}_1, \mathbf{Y}) + \text{COV}(\mathbf{X}_2, \mathbf{Y})$ and $\text{COV}(a\mathbf{X}, b\mathbf{Y}) = ab\text{COV}(\mathbf{X}, \mathbf{Y})$, we get

$$\text{COV}(\mathbf{X}_1 - \mathbf{X}_2, \mathbf{X}_3 - \mathbf{X}_4) = \text{COV}(\mathbf{X}_1, \mathbf{X}_3) - \text{COV}(\mathbf{X}_1, \mathbf{X}_4) - \text{COV}(\mathbf{X}_2, \mathbf{X}_3) + \text{COV}(\mathbf{X}_2, \mathbf{X}_4)$$

Substituting this relation in the expression of $R(1,2)$, we get

$$\begin{aligned}
R(1,2) = & \text{COV}\left\{\text{real}\left(\begin{bmatrix} \theta_1 & \theta_4 & \theta_6 \\ \theta_7 & \theta_{10} & \theta_{12} \end{bmatrix} \begin{bmatrix} h_1 \\ h_2 \\ h_3 \end{bmatrix}\right), \text{real}\left(\begin{bmatrix} \theta_4 & \theta_2 & \theta_5 \\ \theta_4 & \theta_2 & \theta_5 \end{bmatrix} \begin{bmatrix} h_1 \\ h_2 \\ h_3 \end{bmatrix}\right)\right\} \\
& - \text{COV}\left\{\text{real}\left(\begin{bmatrix} \theta_1 & \theta_4 & \theta_6 \\ \theta_7 & \theta_{10} & \theta_{12} \end{bmatrix} \begin{bmatrix} h_1 \\ h_2 \\ h_3 \end{bmatrix}\right), \text{imag}\left(\begin{bmatrix} \theta_{10} & \theta_8 & \theta_{11} \\ \theta_{10} & \theta_8 & \theta_{11} \end{bmatrix} \begin{bmatrix} h_1 \\ h_2 \\ h_3 \end{bmatrix}\right)\right\} \\
& - \text{COV}\left\{\text{imag}\left(\begin{bmatrix} \theta_7 & \theta_{10} & \theta_{12} \\ \theta_7 & \theta_{10} & \theta_{12} \end{bmatrix} \begin{bmatrix} h_1 \\ h_2 \\ h_3 \end{bmatrix}\right), \text{real}\left(\begin{bmatrix} \theta_4 & \theta_2 & \theta_5 \\ \theta_4 & \theta_2 & \theta_5 \end{bmatrix} \begin{bmatrix} h_1 \\ h_2 \\ h_3 \end{bmatrix}\right)\right\} \\
& + \text{COV}\left\{\text{imag}\left(\begin{bmatrix} \theta_7 & \theta_{10} & \theta_{12} \\ \theta_7 & \theta_{10} & \theta_{12} \end{bmatrix} \begin{bmatrix} h_1 \\ h_2 \\ h_3 \end{bmatrix}\right), \text{imag}\left(\begin{bmatrix} \theta_{10} & \theta_8 & \theta_{11} \\ \theta_{10} & \theta_8 & \theta_{11} \end{bmatrix} \begin{bmatrix} h_1 \\ h_2 \\ h_3 \end{bmatrix}\right)\right\} \tag{C.22}
\end{aligned}$$

Using property, $\text{COV}(\mathbf{AX} + \mathbf{a}, \mathbf{B}^T\mathbf{Y} + \mathbf{b}) = \mathbf{A}\text{COV}(\mathbf{X}, \mathbf{Y})\mathbf{B}$, we get

$$\begin{aligned} & \text{COV}\left\{\text{real}\left([\theta_1 \ \theta_4 \ \theta_6] \begin{bmatrix} h_1 \\ h_2 \\ h_3 \end{bmatrix}\right), \text{imag}\left([\theta_{10} \ \theta_8 \ \theta_{11}] \begin{bmatrix} h_1 \\ h_2 \\ h_3 \end{bmatrix}\right)\right\} \\ &= [\theta_1 \ \theta_4 \ \theta_6] \text{COV}\left\{\text{real}\left(\begin{bmatrix} h_1 \\ h_2 \\ h_3 \end{bmatrix}\right), \text{imag}\left(\begin{bmatrix} h_1 \\ h_2 \\ h_3 \end{bmatrix}\right)\right\} \begin{bmatrix} \theta_{10} \\ \theta_8 \\ \theta_{11} \end{bmatrix} \end{aligned} \quad (\text{C.23})$$

$$\begin{aligned} & \text{COV}\left\{\text{imag}\left([\theta_7 \ \theta_{10} \ \theta_{12}] \begin{bmatrix} h_1 \\ h_2 \\ h_3 \end{bmatrix}\right), \text{real}\left([\theta_4 \ \theta_2 \ \theta_5] \begin{bmatrix} h_1 \\ h_2 \\ h_3 \end{bmatrix}\right)\right\} \\ &= [\theta_7 \ \theta_{10} \ \theta_{12}] \text{COV}\left\{\text{real}\left(\begin{bmatrix} h_1 \\ h_2 \\ h_3 \end{bmatrix}\right), \text{imag}\left(\begin{bmatrix} h_1 \\ h_2 \\ h_3 \end{bmatrix}\right)\right\} \begin{bmatrix} \theta_4 \\ \theta_2 \\ \theta_5 \end{bmatrix} \end{aligned} \quad (\text{C.24})$$

Using property that real and imaginary components of a complex number are uncorrelated (same as orthogonal in geometric terms), we get

$$\text{COV}\left\{\text{real}\left(\begin{bmatrix} h_1 \\ h_2 \\ h_3 \end{bmatrix}\right), \text{imag}\left(\begin{bmatrix} h_1 \\ h_2 \\ h_3 \end{bmatrix}\right)\right\} = 0$$

Therefore,

$$\begin{aligned} & \text{R(1,2)} \\ &= \text{COV}\left\{\text{real}\left([\theta_1 \ \theta_4 \ \theta_6] \begin{bmatrix} h_1 \\ h_2 \\ h_3 \end{bmatrix}\right), \text{real}\left([\theta_4 \ \theta_2 \ \theta_5] \begin{bmatrix} h_1 \\ h_2 \\ h_3 \end{bmatrix}\right)\right\} \\ &+ \text{COV}\left\{\text{imag}\left([\theta_7 \ \theta_{10} \ \theta_{12}] \begin{bmatrix} h_1 \\ h_2 \\ h_3 \end{bmatrix}\right), \text{imag}\left([\theta_{10} \ \theta_8 \ \theta_{11}] \begin{bmatrix} h_1 \\ h_2 \\ h_3 \end{bmatrix}\right)\right\} \end{aligned} \quad (\text{C.25})$$

$$\begin{aligned}
\Rightarrow R(1,2) = \text{COV} & \left\{ \text{real} \left([\theta_1 \quad \theta_4 \quad \theta_6] \begin{pmatrix} [I_{pq}^a] \\ [I_{pq}^b] \\ [I_{pq}^c] \end{pmatrix} \right. \right. \\
& \left. \left. - \mathbf{B}_p^{\text{abc}} \begin{pmatrix} [V_p^a] \\ [V_p^b] \\ [V_p^c] \end{pmatrix} \right) \right), \text{real} \left([\theta_4 \quad \theta_2 \quad \theta_5] \begin{pmatrix} [I_{pq}^a] \\ [I_{pq}^b] \\ [I_{pq}^c] \end{pmatrix} - \mathbf{B}_p^{\text{abc}} \begin{pmatrix} [V_p^a] \\ [V_p^b] \\ [V_p^c] \end{pmatrix} \right) \right\} \\
& + \text{COV} \left\{ \text{imag} \left([\theta_7 \quad \theta_{10} \quad \theta_{12}] \begin{pmatrix} [I_{pq}^a] \\ [I_{pq}^b] \\ [I_{pq}^c] \end{pmatrix} \right. \right. \\
& \left. \left. - \mathbf{B}_p^{\text{abc}} \begin{pmatrix} [V_p^a] \\ [V_p^b] \\ [V_p^c] \end{pmatrix} \right) \right), \text{imag} \left([\theta_{10} \quad \theta_8 \quad \theta_{11}] \begin{pmatrix} [I_{pq}^a] \\ [I_{pq}^b] \\ [I_{pq}^c] \end{pmatrix} - \mathbf{B}_p^{\text{abc}} \begin{pmatrix} [V_p^a] \\ [V_p^b] \\ [V_p^c] \end{pmatrix} \right) \right\} \quad (\text{C. 26})
\end{aligned}$$

$$\begin{aligned}
R(1,2) = \text{COV} & \left\{ \text{real} \left([\theta_1 \quad \theta_4 \quad \theta_6] \begin{pmatrix} [I_{pq}^a] \\ [I_{pq}^b] \\ [I_{pq}^c] \end{pmatrix} - [\theta_1 \quad \theta_4 \quad \theta_6] \mathbf{B}_p^{\text{abc}} \begin{pmatrix} [V_p^a] \\ [V_p^b] \\ [V_p^c] \end{pmatrix} \right), \text{real} \left([\theta_4 \quad \theta_2 \quad \theta_5] \begin{pmatrix} [I_{pq}^a] \\ [I_{pq}^b] \\ [I_{pq}^c] \end{pmatrix} \right. \right. \\
& \left. \left. - [\theta_4 \quad \theta_2 \quad \theta_5] \mathbf{B}_p^{\text{abc}} \begin{pmatrix} [V_p^a] \\ [V_p^b] \\ [V_p^c] \end{pmatrix} \right) \right\} \\
& + \text{COV} \left\{ \text{imag} \left([\theta_7 \quad \theta_{10} \quad \theta_{12}] \begin{pmatrix} [I_{pq}^a] \\ [I_{pq}^b] \\ [I_{pq}^c] \end{pmatrix} \right. \right. \\
& \left. \left. - [\theta_7 \quad \theta_{10} \quad \theta_{12}] \mathbf{B}_p^{\text{abc}} \begin{pmatrix} [V_p^a] \\ [V_p^b] \\ [V_p^c] \end{pmatrix} \right), \text{imag} \left([\theta_{10} \quad \theta_8 \quad \theta_{11}] \begin{pmatrix} [I_{pq}^a] \\ [I_{pq}^b] \\ [I_{pq}^c] \end{pmatrix} \right. \right. \\
& \left. \left. - [\theta_{10} \quad \theta_8 \quad \theta_{11}] \mathbf{B}_p^{\text{abc}} \begin{pmatrix} [V_p^a] \\ [V_p^b] \\ [V_p^c] \end{pmatrix} \right) \right\} \quad (\text{C. 27})
\end{aligned}$$

$$\begin{aligned}
\Rightarrow R(1,2) = & \text{COV} \left\{ [\theta_1 \quad \theta_4 \quad \theta_6] \text{real} \left(\begin{bmatrix} I_{pq}^a \\ I_{pq}^b \\ I_{pq}^c \end{bmatrix} \right) \right. \\
& - [\theta_1 \quad \theta_4 \quad \theta_6] \text{real} \left(\mathbf{B}_p^{abc} \begin{bmatrix} V_p^a \\ V_p^b \\ V_p^c \end{bmatrix} \right), [\theta_4 \quad \theta_2 \quad \theta_5] \text{real} \left(\begin{bmatrix} I_{pq}^a \\ I_{pq}^b \\ I_{pq}^c \end{bmatrix} \right) \\
& \left. - [\theta_4 \quad \theta_2 \quad \theta_5] \text{real} \left(\mathbf{B}_p^{abc} \begin{bmatrix} V_p^a \\ V_p^b \\ V_p^c \end{bmatrix} \right) \right\} \\
& + \text{COV} \left\{ [\theta_7 \quad \theta_{10} \quad \theta_{12}] \text{imag} \left(\begin{bmatrix} I_{pq}^a \\ I_{pq}^b \\ I_{pq}^c \end{bmatrix} \right) \right. \\
& - [\theta_7 \quad \theta_{10} \quad \theta_{12}] \text{imag} \left(\mathbf{B}_p^{abc} \begin{bmatrix} V_p^a \\ V_p^b \\ V_p^c \end{bmatrix} \right), [\theta_{10} \quad \theta_8 \quad \theta_{11}] \text{imag} \left(\begin{bmatrix} I_{pq}^a \\ I_{pq}^b \\ I_{pq}^c \end{bmatrix} \right) \\
& \left. - [\theta_{10} \quad \theta_8 \quad \theta_{11}] \text{imag} \left(\mathbf{B}_p^{abc} \begin{bmatrix} V_p^a \\ V_p^b \\ V_p^c \end{bmatrix} \right) \right\} \tag{C.28}
\end{aligned}$$

Combining properties, $\text{COV}(\mathbf{X}_1 + \mathbf{X}_2, \mathbf{Y}) = \text{COV}(\mathbf{X}_1, \mathbf{Y}) + \text{COV}(\mathbf{X}_2, \mathbf{Y})$ and $\text{COV}(a\mathbf{X}, b\mathbf{Y}) = ab\text{COV}(\mathbf{X}, \mathbf{Y})$, we get

$$\text{COV}(\mathbf{X}_1 - \mathbf{X}_2, \mathbf{X}_3 - \mathbf{X}_4) = \text{COV}(\mathbf{X}_1, \mathbf{X}_3) - \text{COV}(\mathbf{X}_1, \mathbf{X}_4) - \text{COV}(\mathbf{X}_2, \mathbf{X}_3) + \text{COV}(\mathbf{X}_2, \mathbf{X}_4)$$

Substituting this relation in the expression of R(1,2), and knowing that voltages and currents are uncorrelated, we get

R(1,2)

$$\begin{aligned}
&= \text{COV} \left\{ [\theta_1 \quad \theta_4 \quad \theta_6] \text{real} \left(\begin{bmatrix} I_{pq}^a \\ I_{pq}^b \\ I_{pq}^c \end{bmatrix} \right), [\theta_4 \quad \theta_2 \quad \theta_5] \text{real} \left(\begin{bmatrix} I_{pq}^a \\ I_{pq}^b \\ I_{pq}^c \end{bmatrix} \right) \right\} \\
&+ \text{COV} \left\{ [\theta_1 \quad \theta_4 \quad \theta_6] \text{real} \left(\mathbf{B}_p^{\text{abc}} \begin{bmatrix} V_p^a \\ V_p^b \\ V_p^c \end{bmatrix} \right), [\theta_4 \quad \theta_2 \quad \theta_5] \text{real} \left(\mathbf{B}_p^{\text{abc}} \begin{bmatrix} V_p^a \\ V_p^b \\ V_p^c \end{bmatrix} \right) \right\} \\
&+ \text{COV} \left\{ [\theta_7 \quad \theta_{10} \quad \theta_{12}] \text{imag} \left(\begin{bmatrix} I_{pq}^a \\ I_{pq}^b \\ I_{pq}^c \end{bmatrix} \right), [\theta_{10} \quad \theta_8 \quad \theta_{11}] \text{imag} \left(\begin{bmatrix} I_{pq}^a \\ I_{pq}^b \\ I_{pq}^c \end{bmatrix} \right) \right\} \\
&+ \text{COV} \left\{ [\theta_7 \quad \theta_{10} \quad \theta_{12}] \text{imag} \left(\mathbf{B}_p^{\text{abc}} \begin{bmatrix} V_p^a \\ V_p^b \\ V_p^c \end{bmatrix} \right), [\theta_{10} \quad \theta_8 \quad \theta_{11}] \text{imag} \left(\mathbf{B}_p^{\text{abc}} \begin{bmatrix} V_p^a \\ V_p^b \\ V_p^c \end{bmatrix} \right) \right\} \quad (\text{C. 29})
\end{aligned}$$

Using property, $\text{COV}(\mathbf{AX} + \mathbf{a}, \mathbf{B}^T \mathbf{Y} + \mathbf{b}) = \mathbf{A} \text{COV}(\mathbf{X}, \mathbf{Y}) \mathbf{B}$, we get

$$\begin{aligned}
\text{R(1,2)} &= [\theta_1 \quad \theta_4 \quad \theta_6] \text{COV} \left\{ \text{real} \left(\begin{bmatrix} I_{pq}^a \\ I_{pq}^b \\ I_{pq}^c \end{bmatrix} \right), \text{real} \left(\begin{bmatrix} I_{pq}^a \\ I_{pq}^b \\ I_{pq}^c \end{bmatrix} \right) \right\} \begin{bmatrix} \theta_4 \\ \theta_2 \\ \theta_5 \end{bmatrix} \\
&+ [\theta_1 \quad \theta_4 \quad \theta_6] \text{COV} \left\{ \text{real} \left(\mathbf{B}_p^{\text{abc}} \begin{bmatrix} V_p^a \\ V_p^b \\ V_p^c \end{bmatrix} \right), \text{real} \left(\mathbf{B}_p^{\text{abc}} \begin{bmatrix} V_p^a \\ V_p^b \\ V_p^c \end{bmatrix} \right) \right\} \begin{bmatrix} \theta_4 \\ \theta_2 \\ \theta_5 \end{bmatrix} \\
&+ [\theta_7 \quad \theta_{10} \quad \theta_{12}] \text{COV} \left\{ \text{imag} \left(\begin{bmatrix} I_{pq}^a \\ I_{pq}^b \\ I_{pq}^c \end{bmatrix} \right), \text{imag} \left(\begin{bmatrix} I_{pq}^a \\ I_{pq}^b \\ I_{pq}^c \end{bmatrix} \right) \right\} \begin{bmatrix} \theta_{10} \\ \theta_8 \\ \theta_{11} \end{bmatrix} \\
&+ [\theta_7 \quad \theta_{10} \quad \theta_{12}] \text{COV} \left\{ \text{imag} \left(\mathbf{B}_p^{\text{abc}} \begin{bmatrix} V_p^a \\ V_p^b \\ V_p^c \end{bmatrix} \right), \text{imag} \left(\mathbf{B}_p^{\text{abc}} \begin{bmatrix} V_p^a \\ V_p^b \\ V_p^c \end{bmatrix} \right) \right\} \begin{bmatrix} \theta_{10} \\ \theta_8 \\ \theta_{11} \end{bmatrix} \quad (\text{C. 30})
\end{aligned}$$

Using property $\text{COV}(\mathbf{X}, \mathbf{X}) = \text{Var}(\mathbf{X})$, we get

$$\begin{aligned}
R(1,2) &= [\theta_1 \quad \theta_4 \quad \theta_6] \text{Var} \left\{ \text{real} \left(\begin{bmatrix} I_{pq}^a \\ I_{pq}^b \\ I_{pq}^c \end{bmatrix} \right) \right\} \begin{bmatrix} \theta_4 \\ \theta_2 \\ \theta_5 \end{bmatrix} \\
&+ [\theta_1 \quad \theta_4 \quad \theta_6] \text{Var} \left\{ \text{real} \left(\mathbf{B}_p^{\text{abc}} \begin{bmatrix} V_p^a \\ V_p^b \\ V_p^c \end{bmatrix} \right) \right\} \begin{bmatrix} \theta_4 \\ \theta_2 \\ \theta_5 \end{bmatrix} \\
&+ [\theta_7 \quad \theta_{10} \quad \theta_{12}] \text{Var} \left\{ \text{imag} \left(\begin{bmatrix} I_{pq}^a \\ I_{pq}^b \\ I_{pq}^c \end{bmatrix} \right) \right\} \begin{bmatrix} \theta_{10} \\ \theta_8 \\ \theta_{11} \end{bmatrix} \\
&+ [\theta_7 \quad \theta_{10} \quad \theta_{12}] \text{Var} \left\{ \text{imag} \left(\mathbf{B}_p^{\text{abc}} \begin{bmatrix} V_p^a \\ V_p^b \\ V_p^c \end{bmatrix} \right) \right\} \begin{bmatrix} \theta_{10} \\ \theta_8 \\ \theta_{11} \end{bmatrix} \tag{C.31}
\end{aligned}$$

$$\text{As } \text{Var} \left\{ \text{real} \left(\begin{bmatrix} I_{pq}^a \\ I_{pq}^b \\ I_{pq}^c \end{bmatrix} \right) \right\} = \begin{bmatrix} (\sigma_C)^2 & 0 & 0 \\ 0 & (\sigma_C)^2 & 0 \\ 0 & 0 & (\sigma_C)^2 \end{bmatrix}, \quad \text{Var} \left\{ \text{real} \left(\mathbf{B}_p^{\text{abc}} \begin{bmatrix} V_p^a \\ V_p^b \\ V_p^c \end{bmatrix} \right) \right\} =$$

$$-(\sigma_V)^2 \mathbf{B}_p^{\text{abc}} (\mathbf{B}_p^{\text{abc}})^T, \quad \text{Var} \left\{ \text{imag} \left(\begin{bmatrix} I_{pq}^a \\ I_{pq}^b \\ I_{pq}^c \end{bmatrix} \right) \right\} = \begin{bmatrix} (\sigma_C)^2 & 0 & 0 \\ 0 & (\sigma_C)^2 & 0 \\ 0 & 0 & (\sigma_C)^2 \end{bmatrix} \quad \text{and}$$

$$\text{Var} \left\{ \text{imag} \left(\mathbf{B}_p^{\text{abc}} \begin{bmatrix} V_p^a \\ V_p^b \\ V_p^c \end{bmatrix} \right) \right\} = -(\sigma_V)^2 \mathbf{B}_p^{\text{abc}} (\mathbf{B}_p^{\text{abc}})^T, \text{ we get}$$

$$\begin{aligned}
R(1,2) = & [\theta_1 \quad \theta_4 \quad \theta_6] \begin{bmatrix} (\sigma_C)^2 & 0 & 0 \\ 0 & (\sigma_C)^2 & 0 \\ 0 & 0 & (\sigma_C)^2 \end{bmatrix} \begin{bmatrix} \theta_4 \\ \theta_2 \\ \theta_5 \end{bmatrix} \\
& - [\theta_1 \quad \theta_4 \quad \theta_6] (\sigma_V)^2 \mathbf{B}_p^{\text{abc}} (\mathbf{B}_p^{\text{abc}})^T \begin{bmatrix} \theta_4 \\ \theta_2 \\ \theta_5 \end{bmatrix} \\
& + [\theta_7 \quad \theta_{10} \quad \theta_{12}] \begin{bmatrix} (\sigma_C)^2 & 0 & 0 \\ 0 & (\sigma_C)^2 & 0 \\ 0 & 0 & (\sigma_C)^2 \end{bmatrix} \begin{bmatrix} \theta_{10} \\ \theta_8 \\ \theta_{11} \end{bmatrix} \\
& - [\theta_7 \quad \theta_{10} \quad \theta_{12}] (\sigma_V)^2 \mathbf{B}_p^{\text{abc}} (\mathbf{B}_p^{\text{abc}})^T \begin{bmatrix} \theta_{10} \\ \theta_8 \\ \theta_{11} \end{bmatrix} \tag{C.32}
\end{aligned}$$

$$\begin{aligned}
\Rightarrow R(1,2) = & (\sigma_C)^2 [\theta_1 \quad \theta_4 \quad \theta_6 \quad \theta_7 \quad \theta_{10} \quad \theta_{12}] \begin{bmatrix} \theta_4 \\ \theta_2 \\ \theta_5 \\ \theta_{10} \\ \theta_8 \\ \theta_{11} \end{bmatrix} \\
& - (\sigma_V)^2 \left\{ \begin{array}{l} [\theta_1 \quad \theta_4 \quad \theta_6] \mathbf{B}_p^{\text{abc}} (\mathbf{B}_p^{\text{abc}})^T \begin{bmatrix} \theta_4 \\ \theta_2 \\ \theta_5 \end{bmatrix} + [\theta_7 \quad \theta_{10} \quad \theta_{12}] \\ \mathbf{B}_p^{\text{abc}} (\mathbf{B}_p^{\text{abc}})^T \begin{bmatrix} \theta_{10} \\ \theta_8 \\ \theta_{11} \end{bmatrix} \end{array} \right\} \tag{C.33}
\end{aligned}$$